Exploration of interaction between *Plasmodium falciparum* Hsp70-x (PfHsp70-x) and human Hsp70-Hsp90 organizing protein (human Hop)

A thesis submitted in fulfillment of the requirements for the degree of

MASTER OF SCIENCE IN BIOCHEMISTRY

SCHOOL OF MATHEMATICS AND NATURAL SCIENCES

UNIVERSITY OF VENDA

by

BLESSING MABATE

11613080

Supervisor: Prof. A. Shonhai

Co-supervisor: Dr. T. Zininga

February 2017

ABSTRACT

Malaria is a disease that claims about half a million lives annually, mainly children. There are 5 *Plasmodium* species that cause malaria; namely, *P. falciparum*, *P. ovale*, *P. malariae*, *P. knowlesi* and *P. vivax*. *P. falciparum* is the most virulent of them all. The parasite upregulates some heat shock proteins (Hsps) in response to stress it encounters during its life cycle. These Hsps play a major role in proteostasis. The drug resistance of *P. falciparum* to traditionally used remedies has led to a need for the development of novel drugs. Hsps have been implicated as antimalarial drug targets. Hsps act as molecular chaperones and some make complexes, which are important in facilitating protein folding. As an example, heat shock protein 70 (Hsp70) and heat shock protein 90 (Hsp90) form a functional complex through an adaptor protein, Hsp70-Hsp90 organizing protein (Hop). *P. falciparum* expresses six Hsp70s that are localized in different subcellular compartments. Amongst them, *P. falciparum* Hsp70-x (PfHsp70-x), is exported to the erythrocyte where it is implicated in host cell remodeling. PfHsp70-x possesses an ATPase domain, substrate binding domain and a C-terminal subdomain. PfHsp70-x possesses an EEVN motif on its C-terminus which is implicated in interactions with co-chaperones amongst them, Hop. Although some of the chaperone functions of PfHsp70-x have been reported, its interaction with human chaperones has not been investigated. The availability of PfHsp70-x in the infected erythrocyte cytosol presents a possibility that this protein may functionally cooperate with human Hsp90 via human Hop (human Hop). This hypothesis that PfHsp70-x interacts with human chaperones is strengthened by the absence of Hsp90 and Hop of parasite origin in the infected erythrocytes. The main aim of this study was to explore the chaperone activity of PfHsp70-x and its functional co-operation with human Hop. Recombinant PfHsp70-x (full length and EEVN deletion mutant) proteins were expressed in *E. coli* XL1 Blue cells and purified using nickel affinity chromatography. PfHsp70-x was found to be structurally comprised of mostly alpha helices and demonstrated heat stability based on circular dichroism (CD) spectrometry studies. It was established that the EEVN motif may be important for the ATPase activity of PfHsp70-x. However, it was established that the EEVN motif was not important in regulating the holdase chaperone (protein aggregation suppression) function of PfHsp70-x. Furthermore, PfHsp70-x and its mutant preferentially bound to asparagine-rich peptides. Parasite proteins have high asparagine repeat regions as compared to human proteins. In addition, preference for asparagine-rich proteins

could signify that PfHsp70-x is biased towards binding proteins of parasitic origin. Surface plasmon resonance (SPR) analysis suggested that PfHsp70-x interacts with human Hop with relatively higher affinity compared to its EEVN minus derivative. In conclusion, the removal of the EEVN motif of PfHsp70-x does not affect the chaperone function of PfHsp70-x. However, the EEVN motif is essential for the interaction of PfHsp70-x with human Hop.

Keywords: Functional cooperation, PfHsp70-x, heat shock proteins, human chaperones, human Hop

DECLARATION

I Blessing Mabate, the undersigned, declare that this thesis submitted to the University of Venda for a Master's degree in Biochemistry under the Department of Biochemistry in the School of Mathematics and Natural Sciences, herein submitted by me, is my original work with the exception of citations and that this work has not been submitted to any other university in partial or entirely for the award of any degree.

Candidate signature…….. Date……

DEDICATION

I dedicate this thesis to God Almighty and to my family, particularly my mother and my son Junior Ropafadzo Mabate.

ACKNOWLEDGEMENTS

I thank the Lord Almighty for giving me the opportunity of doing this study and seeing me through it. I would like to express my gratitude to my supervisor Prof. Addmore Shonhai for his persistent guidance, mentorship, and patience.

I also wish to acknowledge my co-supervisor Dr. Tawanda Zininga for his mentorship, guidance, and patience in transferring skills. I have learned humility from him.

I would like to give my special gratitude to Mr. Stanely Makumire for his time in teaching me most of the techniques that I acquired during this study.

I would also express my sincere gratitude to Dr. Adelle Burger for her support.

I would like to extend acknowledgments to

- The University of Venda Research Committee for the research grant
- NRF (South Africa) for the student scholarship during this study period
- The University of Venda work study program for tuition and accommodation funding

I would also like to express my gratitude to the ProBioM research team (University of Venda) for their support.

I would also like to give special thanks to our lab technicians; namely, Mr. C. Ndou and Miss D Mmboyi for their support.

Finally, I would like to thank the Biochemistry Department singling specifically Miss B.J Mafoko and Mr. L Mathomu for the moral support they provided.

TABLE OF CONTENTS

LIST OF ABBREVIATIONS

CD	Circular dichroism
ER	Endoplasmic reticulum
HPD	Histidine-proline-asparagine
Hsp	Heat shock protein
Hop	Hsp70-Hsp90 organizing protein
IPTG	Isopropyl B-D-1 thiogalactopyranoside
kDa	kilo Dalton
mRNA	messenger Ribonucleic acid
NEF	Nucleotide exchange factor
PfHsp70-x	*Plasmodium falciparum* heat shock protein70-x
PfHsp70-x_T	*Plasmodium falciparum* heat shock protein70-x truncated version
PfEMP1	*Plasmodium falciparum* erythrocyte membrane protein 1
PEXEL	*Plasmodium* export element
PTEX	*Plasmodium* translocon of exported proteins
PV	Parasitophorous vacuole
PVM	Parasitophorous vacuole membrane
RBC	Red blood cell
RESA	Ring-infected erythrocyte antigen
SBD	Substrate binding domain
SDS-PAGE	Sodium dodecyl sulfate polyacrylamide gel electrophoresis
SPR	Surface plasmon resonance
UV	Ultraviolet

LIST OF FIGURES

LIST OF TABLES

CHAPTER 1: LITERATURE REVIEW

1.1 Epidemiology of malaria

Malaria is an infectious disease caused by parasitic protozoans of the genus *Plasmodium*. Members of the genus that infect humans comprise of the following species: *P. falciparum, P. ovale, P. malariae, P. vivax,* and *P. knowlesi*. *P. falciparum* is the most virulent of all the species that cause malaria. Malaria persists as a major cause of morbidity and death around the world (WHO, 2016). There are about 304 million malaria cases reported annually and most occur in Africa (WHO, 2016). Malaria is endemic in over 100 nations situated in continents including Africa, Asia, Middle East, the South Pacific and the Latin America (CDC, 2016). *P. falciparum* malaria claims about 424 700 lives yearly and 90 % of these deaths occur in Africa (WHO, 2016). The mortality rate is highest among children. Pregnant women are vulnerable to *P. falciparum* infections because the parasite has the propensity to attach to the placenta (WHO, 2016). Malaria in pregnant women caused by *P. falciparum* remains undetected and untreated as it rarely results in fever and this fact makes it dangerous.

In the past years, the *P. falciparum* parasite has become resistant to the traditionally used drugs. The World Health Organization (WHO) recommends artemisinin-based combination therapy as the first line to treat malaria. However, threatening the efforts to eliminate this disease is the remarkable capacity of *P. falciparum* in developing drug resistance (Fançony *et al*., 2016).

1.2 Life cycle and pathogenesis of *P. falciparum*

The *P. falciparum* parasite has a complex life cycle which occurs in two separate hosts namely, the mosquito and the human (Fig 1.1). The first stage is initiated by injection of sporozoites into humans during the mosquito's blood meal. The sporozoites in the circulatory system migrate to the liver to invade hepatocytes. (Bozdech *et al*., 2003). This stage marks the beginning of the exo-erythrocytic cycles (Fig 1.1). In the hepatocytes, the parasite multiplies asexually by cell division

without cytokinesis resulting in the formation of schizoints. Schizoints rupture to release merozoites into the bloodstream where they infect erythrocytes (Morrissette and Sibley, 2002).

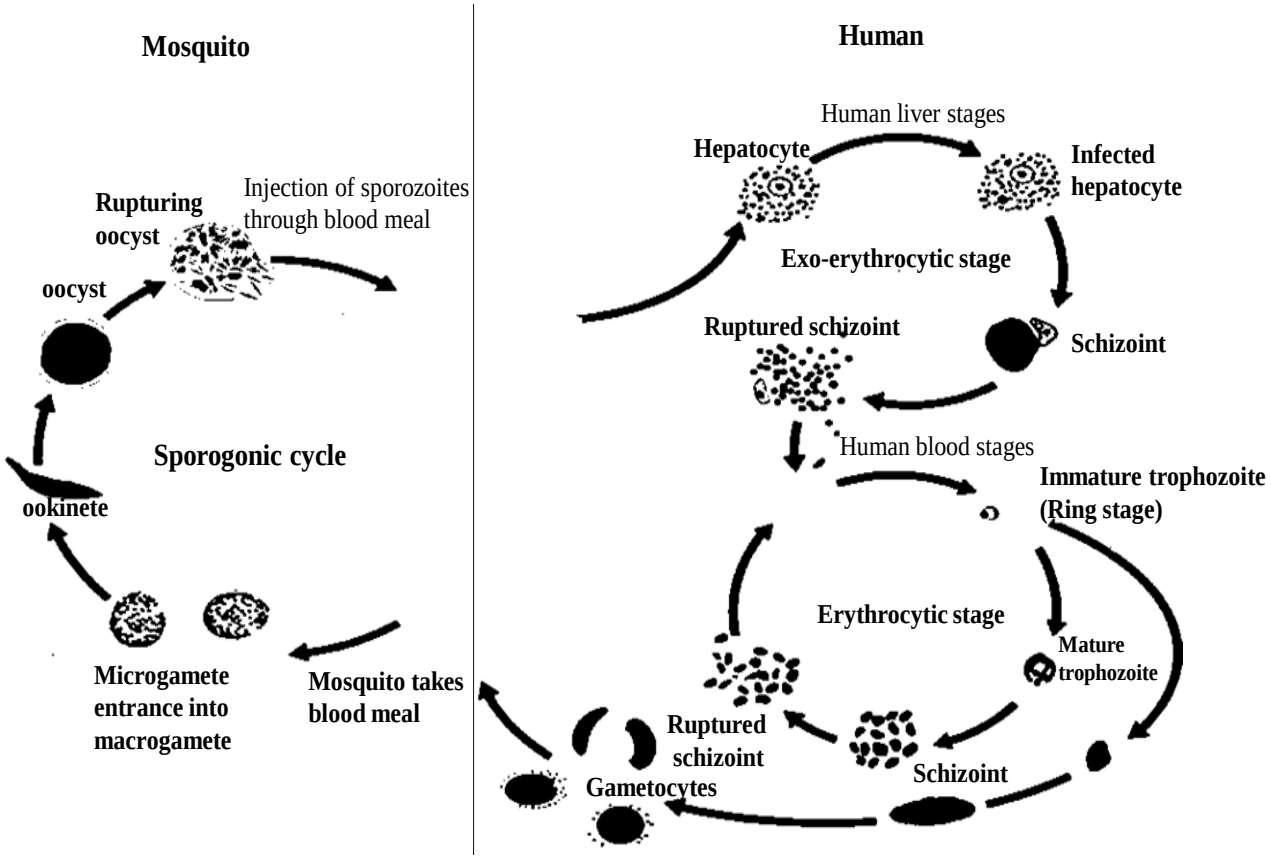

Fig 1.1: Life cycle of *P. falciparum*
The cycle involves 3 separate stages. The first stage occurs in the mosquito and is referred to the sporogonic cycle (mosquito stages). The second stage occurs in the liver of the human host and is known as the-exoerythrocytic stage. The third stage occurs in the red blood cells and is referred to as the erythrocytic stage and is responsible for pathology and fever; adapted from Center of disease control and prevention (2012).

The invasion of erythrocytes by merozoites marks the beginning of the erythrocytic cycle (Fig 1.1). After invading erythrocytes, merozoites undergo a trophic phase period where they form immature trophozoites referred to as ring forms because of their morphology. The trophozoite stage represents a phase of nourishment and multiplication in the erythrocyte (Cowman and Crab, 2002). The trophozoite differentiates into schizoints which rupture to release merozoites into the human bloodstream to invade uninfected erythrocytes (Fig 1.1). Some of the merozoites develop

into sexual forms through gametogenesis to form gametocytes. The female gametes are called macrogametes and the male gametes called microgametes (Fujioka and Aikawa, 2002).

The sporogonic cycle starts when a mosquito ingests gametocytes from an infected human during a blood meal (Fig 1.1). Microgametes which are flagellated fertilize the macrogametes generating zygotes (Billker *et al*., 1997). The zygotes develop and differentiate into motile ookinetes. The ookinetes develop to form oocysts. The oocysts rupture leading to numerous sporozoites being formed and these migrate and invade the salivary gland of the mosquito (Crompton *et al*., 2010). Inoculation of the sporozoites into a new human host endlessly continues the life cycle of the *P. falciparum* parasite. The unfavorable environmental changes including temperature spikes and change of host cause stress for the *P. falciparum* during its life cycle. As part of its survival tactics, the parasite upregulates heat shock proteins (Hsps) whose primary function is to augment proteostasis against cellular stress.

1.3 Heat shock proteins as molecular chaperones

Molecular chaperones are a group of proteins that facilitate the folding or unfolding of other proteins in order so they to attain the conformational structures necessary for their functions (Kim *et al*., 2013). Molecular chaperones also facilitate degradation of misfolded proteins that are beyond repair (Mayer and Bukau, 2005). Molecular chaperones are responsible for regulating protein conformational state, holding proteins in a primed state for processes such as post-translational modification or ligand binding (Kim *et al.*, 2013). Molecular chaperones also facilitate protein trafficking across membranes (Bukau *et al*., 2006).

Hsps are upregulated in response to stress although some of them are constitutively expressed (Laplante *et al*., 1998). Constitutively expressed Hsps are given a specific name ‘heat shock cognate’ (Hsc) (Hartl and Hayer- Hartl, 2002). Hscs play a housekeeping role as they are required for the maintenance of basic cellular functions (Ingolia and Craig, 1982). Hsps are highly conserved and found in most celled organisms (Li and Srivastava, 2004). They are classified based on their functions. Hsps that fold substrates to their native structure are called foldases, those that

unfold aggregated substrates are called unfoldases and those hold the substrate in a folding-competent state are called holdases (Saibil, 2013). Hsps can also be classified according to their molecular weight in kilo Daltons (kDa). Hsps are a diverse group and can be divided into several families which include small heat shock proteins (sHsp), Hsp40s, Hsp70s, and Hsp90s (Lindquist and Craig, 1988).

1.4 Major types of heat shock proteins from *P. falciparum*

1.4.1 Heat shock protein 40 (Hsp40)

Hsp40 (also called DnaJ in *E. coli*) family is made up of several unique proteins characterized by the presence of a highly conserved J domain (Laufen *et al*., 1999; Hennessy *et al*., 2005). The J domain has about 70 amino acid residues. The structure of J domains is generally conserved across all Hsp40 families. There is variation in the distribution of Hsp40s in different organisms. Hsp40s are generally fewer in prokaryotes but on the other hand, several isoforms exist in eukaryotes with at least 51 found in *P. falciparum* (Kampinga *et al*., 2009; Njunge *et al*., 2013).

Hsp40s are categorized into type I, II, III and IV according to their structure and functions (Fig 1.2: Cheetham and Caplan, 1998; Botha *et al*., 2011). Hsp40s can be classified structurally based on the presence of four typical domains: a J-domain characterized by a conserved tripeptide of His, Pro and Asp (HPD), glycine–phenylalanine (GF) rich region, zinc finger domain and the C-terminal. Type I has all four canonical domains as they occur in *E. coli* DnaJ (Fig 1.2).The type I group is unique from all the other types of Hsp40s because they possess a cysteine-rich zinc finger domain next to the G/F region (Kampinga and Craig, 2010). Type II contains all domains except the zinc finger domain. Of these four, type III and type IV are unique as the J domains are located anywhere along their structure (Fig 1.2).

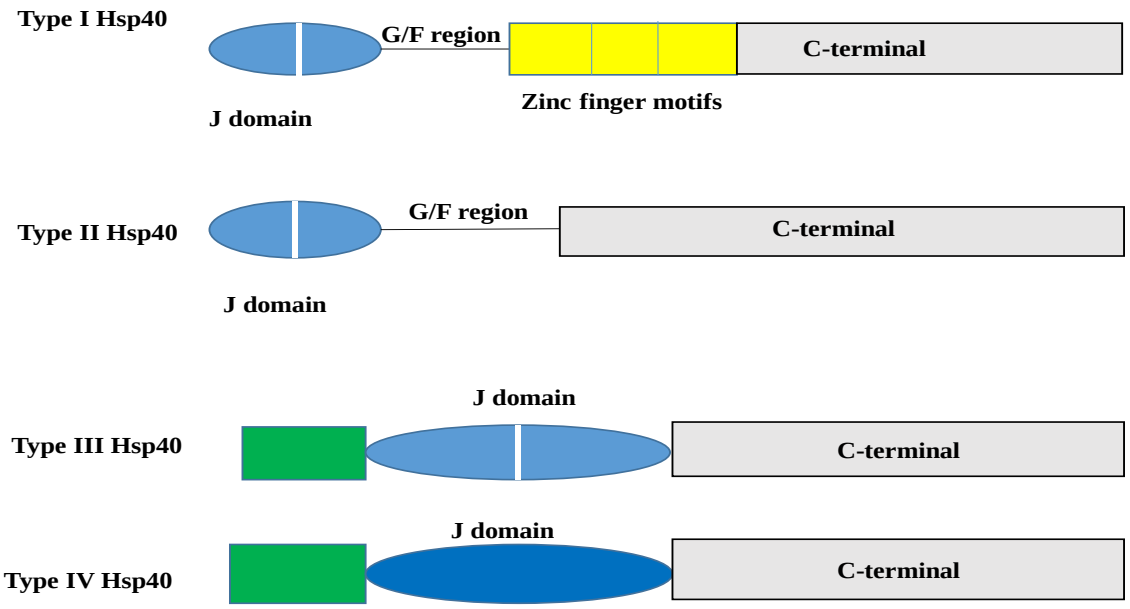

Fig 1.2 Types of Hsp40s
All Hsp40s characterized by the presence of a canonical J- domain. Type I and II contain G/F linker regions and type I contains zinc finger motifs which are distinct to the type I Hsp40. Hsp40s contain a C terminal important for substrate binding. Type III Hsp40s lack both G/F and zinc-finger domains and are poorly conserved. The type IV Hsp40 are similar the type III Hsp40 protein with their J like-domain towards C-terminal. The white line represents the conserved HPD motif; adapted from Botha *et al* (2007).

Type III Hsp40 lack a G/F linker and zinc finger domains (Fig 1.2). Type III Hsp40s contain a J domain with the HPD motif but lack the G/F region and the zinc finger motif (Fig 1.2; Botha *et al*.,2007). They are the most poorly conserved of all the Hsp40 proteins and vary greatly in terms of their size, sequence, and structure. (Nicoll *et al*., 2007). Type IV is similar to Type III in lacking a G/F linker region but constitutes a group of proteins easily noticed by the absence of a His-Pro-Asp (HPD) motif in their J domain (Kampinga and Craig, 2010).

Functionally, Hsp40s have the ability to bind to substrates through the zinc finger motif and peptide binding domain (Fig 1.2; Botha *et al*., 2007, 2011). Type I and II Hsp40s are also independent chaperones as they suppress heat-induced aggregation of substrates (Fan *et al*., 2003). Type I and II Hsp40s associate with Hsp70s (Section 1.4.2) to activate its ATPase activity (Njunge *et al*., 2015). The association of type I and II Hsp40s with Hsp70s firstly involves substrate recruitment and secondly Hsp70 ATPase activation. The association of Hsp40s and Hsp70s is mediated

through the J domains of the Hsp40s (Bascos and Landry, 2015). Type III Hsp40s have a different role altogether as they recruit Hsp70s to specific sites in the cell for the latter to facilitate substrate folding (Walsh *et al*., 2004).

P. falciparum possesses more than 51 genes encoding for Hsp40 like proteins that have been identified (Njunge *et al*., 2013). A type IV Hsp40 like protein named 'ring-infected erythrocyte surface antigen (RESA) (Favaloro *et al*., 1986) expressed during merozoite development plays a significant role in fortifying heat resistance of the parasite (Silva *et al*., 2005) as well as cytoadherence of erythrocytes (Goel *et al*., 2014). *P. falciparum* exhibits a unique profile of Hsp40s which probably accounts for its virulence compared to other less virulent *Plasmodium* species (Botha *et al*., 2007). The Hsp40 family in *P. falciparum* are one of the main groups of chaperones exported to the cytosol of the infected erythrocytes. The exported parasite Hsp40s are speculated to function as co-chaperones of Hsp70s to facilitate folding of other proteins in the parasite-infected erythrocyte. In general, Hsp40s have a role of targeting protein substrates to Hsp70s and secondly stabilizing the Hsp70 in the substrate-bound form (Craig *et al*., 2006).

1.4.2 Heat shock protein 70

Heat shock protein 70 (Hsp70) also referred to as DnaK in *E. coli* is one of the most important Hsp families (Lindquist and Craig, 1988). Hsp70s have a molecular weight of approximately 70 kDa. Hsp70s are highly conserved molecular chaperones (Kampinga *et al.*, 2009). Hsp70s have several functions including folding of nascent proteins (Szabo *et al*., 1994), the formation of multiprotein complexes (Song *et al.*, 2005) and protein translocation (Mayer, 2010). Some of the Hsp70 family members are stress induced. Hsp70s are also capable of suppressing protein aggregation and can refold misfolded peptides (Mayer, 2013). The Hsp70s consist of two distinct domains namely, a 45 kDa ATPase domain and a 25 kDa C-terminal substrate binding domain (SBD) (Swain *et al*., 2007) (Fig 1.3). The two Hsp70 domains are connected by a highly conserved short linker segment (Mayer *et al*., 2000). The linker motif in canonical (DnaK like) Hsp70s is composed of DVLLLDV residues. Mutations on the linker segment cause functional impairment of the Hsp70 (Vogel *et al*., 2006). The linker is important for inter-domain communication (Zhuravleva and Gierasch, 2011). Hsp70 binds to short hydrophobic peptides in cooperation with co-chaperones such as Hsp40 to facilitate refolding or degradation of its substrates (Zhang *et al*., 2014).

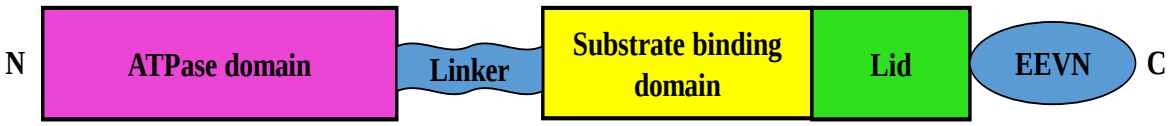

Fig 1.3 Structure and domain organization of Hsp70s
The Hsp70 protein consists of the ATPase domain, the substrate binding domain can interact and transiently associate with short peptide segments of folding intermediates and a C-terminal lid rich in alpha helical structure and acts as a 'lid' for the substrate binding pocket. The C-terminal contains an EEVN motif. Adapted from Ratheesh *et al* (2012).

The ATPase domain has a hydrophilic crevice which binds specifically to ATP. The ATPase domain of Hsp70 has modest ATPase activity on its own and it interacts with co-chaperones such as Hsp40s and nucleotide exchange factors (NEFs) which improve the efficiency of the Hsp70s (Lui *et al*., 2010). Hsp40s in synergy with bound substrate increase ATP hydrolysis by up to a 1000-fold compared to the basal Hsp70 activity (Craig *et* al., 2006) and the NEFs facilitates the replacement of ADP with ATP resulting in substrate release from the Hsp70 (Kabani, 2009). NEFs in prokaryotes and eukaryotes are structurally distinct but have a common role (Raviol *et al*., 2006). The common NEF for Hsp70s in prokaryotes is Grop-like gene E (Grp E) (Packshchies *et al*., 1997). The common NEFs in eukaryotes are Hsp110 (Dragovic *et al*., 2006), Bcl2-associated athanagene-1 (Bag-1) (Bimston *et al*., 2009) and heat shock protein binding protein (HspBP1) (Patury *et al*., 2009).

The Hsp70 SBD has a unique layered twisted β-sandwich that possesses a cleft where the hydrophobic patches on the substrates are bound (Kityk *et al*., 2012). The Hsp70 SBD also has a α-helical lid which has an unstructured stretch of approximately 30 residues (Flaherty, 1990). This α-helical lid temporarily binds linear peptide segments as intermediates of the folding process (Mayer *et al*., 2001). X-ray crystallographic experiments showed that the open conformation of the β-sandwich domain and the α-helical domain are anchored at different sites in the ATPase domain (Zhang *et al*., 2014). Furthermore, the association of these domains is controlled by allostery and substrate binding. The other part is the C-terminal subdomain that acts as a ‘lid’ for the substrate binding pocket (Mayer *et al*., 2000).

1.4.2.1 The Hsp70 functional cycle

The Hsp70 functional cycle is driven by ATP hydrolysis (Fig 1.4). Substrate binding is regulated by the switch between ATP and ADP bound conformations of the Hsp70 (Fig 1.4; Buchberger *et al*., 1995). When bound to ATP, Hsp70 is in an open conformation with a low substrate affinity. Hydrolysis of ATP is stimulated by Hsp40s co-chaperone in synergy with substrate binding. The hydrolysis of ATP results in a closed conformation with a high substrate affinity (Fig 1.4). These events are activated by interdomain communication betweeen the ATPase and substrate binding domains of Hsp70s (Fig 1.3).

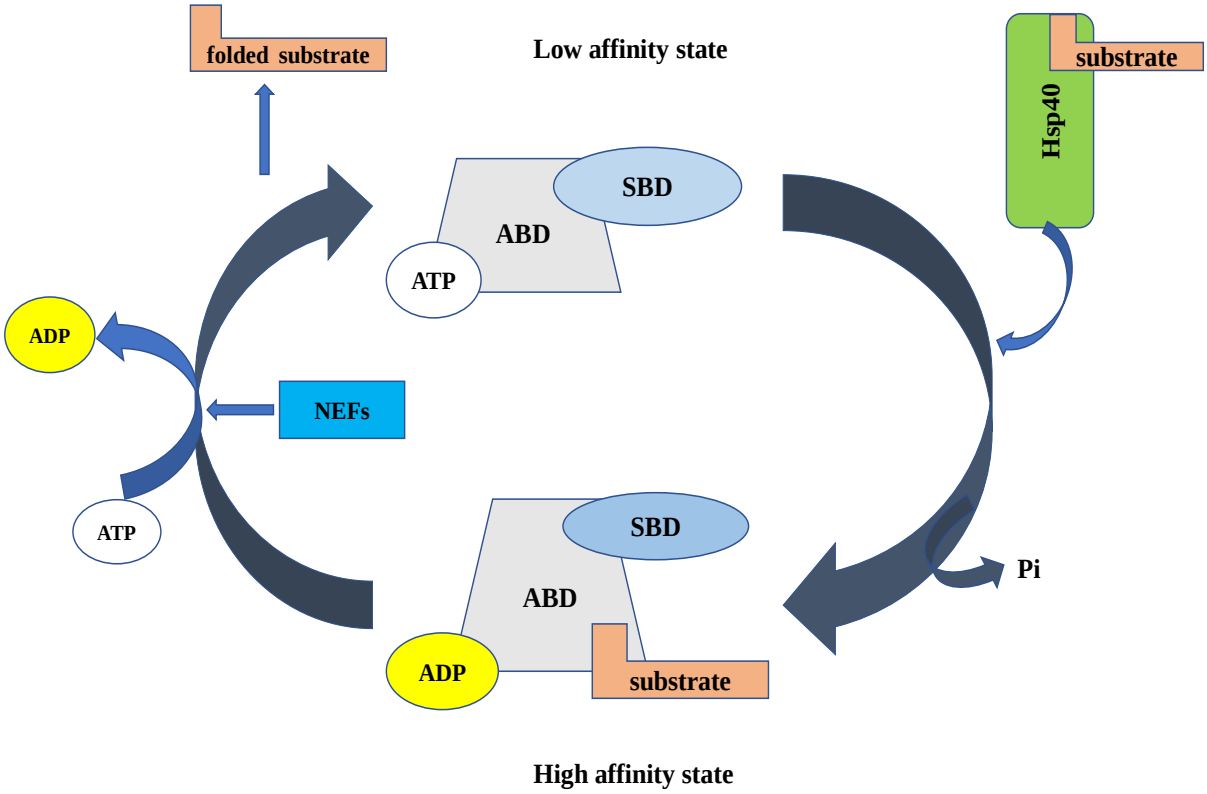

Fig 1.4 Hsp70 chaperone cycle
Chaperone-mediated folding by the Hsp70-Hsp40 chaperone complex. ATP hydrolysis and nucleotide exchange regulate the Hsp70 folding cycle of substrate binding and subsequent folding. Substrates are recruited by Hsp40 and they activate the hydrolysis of ATP which then translates to ADP-bound state with the high-affinity substrate. At this stage, the substrate refolds after which the NEFs facilitate the exchange of ADP for ATP resulting in folded substrate release; adapted from Hartl *et al* (2011).

The Hsp70 cycle is regulated by two co-chaperones, namely Hsp40 and a NEF. Nucleotide exchange by Hsp70 is a slow process, therefore, this increases the dwell time of the substrate which is necessary for protein folding. After successful folding of the substrate has occurred NEFs exchange ADP for ATP which subsequently leads to the release of folded proteins (Fig 1.4).

1.4.2.2 Heat shock protein 70s from *P. falciparum*

The *P. falciparum* genome encodes for six Hsp70s localized in different cellular compartments (Table 1.1; Shonhai *et al*., 2007). Compartmentalization facilitates specialized functions of the proteins. PfHsp70-1 is a well characterized canonical Hsp70 that facilitates protein quality control and is crucial for the development of malaria parasites during their life cycle (Matambo *et al*., 2004; Shonhai *et al*., 2008). PfHsp70-2 is known as the ER homolog, while PfHsp70-3 is the mitochondrial Hsp70 homolog (Shonhai *et al*., 2007; Shonhai, 2014). PfHsp70-y (Table 1.1) belongs to the Hsp110 group. The Hsp110 are known to be holdases as they are capable of holding client proteins in a competent folding manner under thermal stress (Goeckeler *et al*., 2002). The Hsp110s are thought to pass their substrates to capable chaperones such as Hsp70s for refolding (Goecker *et al*., 2002). PfHsp70-y is likely to serve as a NEF for the ER-localized PfHsp70-2 (Shonhai, 2014). Another *P. falciparum* Hsp70 homolog is PfHsp70-z which belongs to the Hsp110 family of proteins. PfHsp70-z is a holdase chaperone as it can suppress the heat-induced aggregation of malate and luciferase in vitro (Zininga *et al*., 2016). In addition, PfHsp70-z is also implicated in suppressing aggregation of asparagine-rich proteins (Muralidharan *et al*., 2012) which make up at least 25 % of the *P. falciparum* proteome (Singh *et al*., 2004b).

The pairwise sequence identity analysis within the Hsp70s show the highest percentage identity of 73 % between PfHsp70-1 and PfHsp70 (Section 1.8). PfHsp70-x shares 54 % identity with PfHsp70-2, PfHsp70-2 shares 46 % identity with PfHsp70-3 and the rest show low percentage identity between them (Shonhai *et al*., 2007). The divergence between *P. falciparum* Hsp70s suggests specialized roles for the chaperones.

Table 1.1. *Plasmodium falciparum* Hsp70 chaperone family

Protein	Size in kDa	Functions	Localization	References
PfHsp70-1 (PF3D7_0818900)	73. 9	Protein folding	cytosol and nucleus	(Shonhai *et al.*, 2007; 2014)
PfHsp70-2 (PF3D7_0917900)	72. 4	Import of protein into the ER Protein folding and quality control in the ER	ER	(Sharma, 1992; Nyalwidhe and Lingelbach, 2006).
PfHsp70-3 (PF3D7_1134000)	73. 3	Import of proteins into mitochondrial matrix	Mitochondria	(Sargeant *et al.*, 2006; Shonhai *et al.*, 2007; 2014).
PfHsp70-x (PF3D7_0831700)	76	Implicated in folding of *P. falciparum* proteins exported to the infected erythrocytes	erythrocyte cytosol, PV	(Shonhai *et al.*, 2007; Külzer *et al.*, 2012; Grover *et al.*, 2013)
PfHsp70-y (PF3D7_1344200)	108.2	Proposed NEF for PfHsp70-2	ER	(Sargeant *et al.*, 2006).
PfHsp70-z (PF3D7_0708800)	100	Possible NEF of PfHsp70-1. Implicated in parasite proteostasis	Cytosol	(Shonhai *et al.*, 2007; Muralidharan *et al.*, 2012; Zininga *et al.*, 2015)

PlasmoDB accession numbers are in brackets under the protein names. (ER): endoplasmic reticulum, NEF: nucleotide exchange factor, PV: parasitophorous vacuole; adapted from Shonhai *et al* (2007).

1.4.3 Heat shock protein 90

Heat shock protein 90 (Hsp90) is a molecular chaperone which is essential in eukaryotes (Li and Buchner, 2013). Hsp90s associate dynamically with many co-chaperones which regulate its mode of action in many ways including recruitment of client proteins and regulation of its ATPase

activity (Ratzke *et al*., 2010). Hsp90 facilitates final maturation of a selected group of proteins (Nathan *et al*., 1997). Examples of these proteins include protein kinases, transcription factors such as p53 and steroid hormone receptors (SHRs) (Zhao *et al*., 2005; McClellan *et al*., 2007;).

1.4.3.1 Structure of Hsp90

Hsp90 possesses an N-terminal ATP binding domain (N-domain) followed by a charged linker region of variable length, a middle domain (M-domain) which contains sites where co- chaperones and client proteins bind (Retzlaff *et al*., 2010; Street *et al*., 2011) and a C-terminal dimerization domain (Krukeberg *et al*., 2011). The C-terminal end of the Hsp90 has a conserved EEVD motif that acts as a binding site for the interactions with co-chaperones (Fig 1.5; Scheufler *et al*., 2000).

Fig 1.5 General structural organization of the Hsp90
This structure begins with the ATP binding domain also known as the N domain then followed by the M domain and lastly the C-terminal which is known as the dimerization domain; adapted from Ali *et al* (2006).

P. falciparum Hsp90 (PfHsp90) (Plasmo DB: Accession number PF3D7_0708400) shares functional similarities with the mammalian homolog. PfHsp90 has a higher ATPase activity compared to its homologs which have low basal ATPase activity (Pallavi *et al*., 2010). The ATPase activity of PfHsp90 makes the protein to have a higher substrate turnover compared to its human homolog (Krukenberg *et al*., 2011). PfHsp90 was shown to co-localize with PfHop (Section 1.5) in the cytosol of 3D7 strains of *P. falciparum* parasites (Gitau *et al*., 2012). PfHsp90 is essential for parasite survival as it is overexpressed in response to stress (Pallavi et al., 2010) therefore is considered a druggable candidate (Zininga and Shonhai, 2014).

1.5 Hsp70 Hsp90 organizing protein (Hop)

1.5.1 Structure and function of Hop

Hsp70-Hsp90 organizing protein (Hop) (also called STI) is one of the most ubiquitous co-chaperones of Hsp90 (Johnson and Brown, 2009). The Hop protein was first identified by Nicolet and Craig in 1989 and was named Stress-inducible gene (*STI*) after heat shock in yeast. Hop is made up of three tetratricopeptide repeat (TPR) domains and two domains rich in aspartate and proline (DP domains) (Allan and Ratajezak, 2011). The DP domains have an α-helical structure and are located on the C-terminals of the TPR1 domain and the TPR2B domain (Allan and Ratajezak, 2011). The DP domains are important structural elements for Hop function (Nelson *et al*., 2003). A TPR motif is a protein to protein interaction site involved in diverse cellular processes. TPR domains are formed by an array of two antiparallel α-helices (the TPR motif), which makes a right-handed helical structure with a channel which is amphipathic and is the main site of protein interactions (Allan and Ratajezak, 2011). Hop is an abundant and highly conserved protein in most organisms (Beraldo *et al*., 2013). Hop is a largely cytosolic protein but can also be found in the nucleus (Hajj *et al*., 2013).

Hop is an important co-chaperone as it connects and regulates Hsp90 and Hsp70 chaperone machinery (Johnson and Brown, 2009). The mechanism of action of Hop has been proposed to occur in a couple of pathways. The first model postulates that Hsp70 binds to substrate first, interacts with Hop and lastly passes the substrate to Hsp90 (Li *et al*., 2013; Röhl *et al*., 2015). The second mechanism of Hsp70-Hop-Hsp90 functional complex is thought to occur through the multiple TPR domain that Hop possesses which interact with the C-terminal EEVD motif which is found on both Hsp70 and Hsp90 (Gitau *et al*., 2012; Schmid *et al.,* 2012). The Hsp70 substrate complex binds to Hop TPR1 domain first, then Hsp90 docks onto the TPR2A domain which causes conformational changes on the TPR2B domain which subsequently increases its affinity for Hsp70 (Röhl *et al*., 2015). This results in the Hsp70 substrate complex initially bound on the TPR1 domain shifting and binding to the TPR2B domain (Röhl *et al*., 2015). Finally, the substrate is passed to Hsp90 for further folding. A study by Zininga and colleagues also found that PfHsp70-1 binds both TPR1 and TPR2B domains supporting that Hsp70 binds to the TPR2B domain of

Hop. Another function of Hop is to stabilize the Hsp90 dimer and induce conformational changes which inhibit ATPase activity of the chaperone (Siligardi *et al*., 2004; Schmid *et al*., 2012).

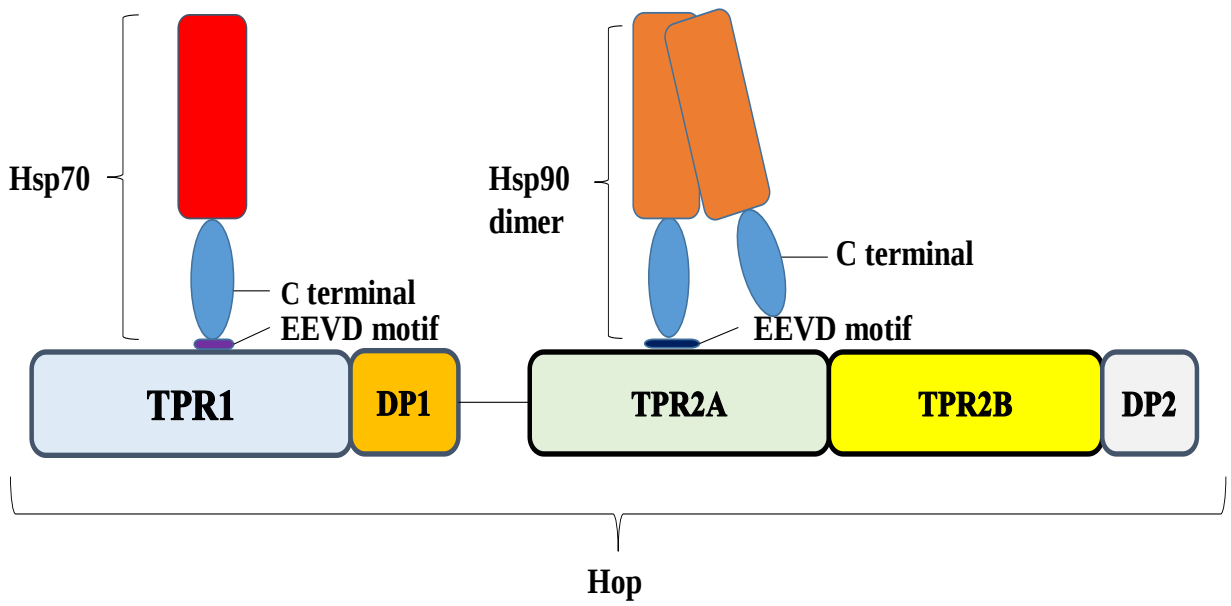

Fig 1.6 Structure and domain organization of Hop
TPR1: tetratricopeptide repeat domain 1; DP1: aspartate-proline motif domain 1; TPR2A, B: tetratricopeptide repeat domains 2A and B; DP2: aspartate-proline motif domain 2. The figure also shows the regions where Hsp70 and Hsp90 bind. The Hsp70 binds first to the TPR1 domain then Hsp90 binds to TPR2A domain increasing the affinity of TPR2B for Hsp70 which subsequently moves and binds to TPR2B before substrate release to Hsp90; adapted from Onuoha *et al* (2008).

It has been suggested that Hop possesses independent ATPase activity (Yamamoto *et al*., 2014). Its affinity for ATP is comparable to that of Hsp90 and Hsp70 but the hydrolysis of the nucleotide occurs at a much slower rate. The ATPase activity of Hop is associated with the N-terminal regions (TPR1, DP1, and TPR2A domains) of the protein (Yamamoto *et al*., 2014). The domains which show ATPase activity are those involved in binding both Hsp70 and Hsp90 and therefore it is reasonable that the ATP-induced conformational changes may be involved in the transfer of client protein between Hsp70 and Hsp90 (Röhl *et al*., 2015).

P. falciparum Hop (PfHop) has conserved TPR1 and TPR2A (Fig1.6) which are known to associate with PfHsp70-1 and PfHsp90 respectively (Gitau *et al*., 2012; Zininga *et al*., 2015). PfHop colocalizes with the parasite cytosol chaperones, PfHsp70-1 and PfHsp90 at the blood

stages of the malaria parasite. The association of PfHsp70-1 and PfHsp90 via PfHop may be important for facilitating the folding of select malarial proteins.

1.6 Heat shock proteins as antimalarial drug targets

P. falciparum drug resistance to traditional drugs has led to a need for novel approaches to eliminating this parasite. The ability of the parasite to acclimatize under drug selection pressure could be facilitated by Hsps whose primary function is to refold proteins (Reviewed in Shonhai, 2010; Shonhai *et al*., 2011; Zininga and Shonhai, 2014). As sentinels in protein folding, Hsps may be potential drug targets (Whitesell and Lindquist, 2005). The high conservation of Hsps among some organisms is a drawback to their prospects as drug targets. Despite this drawback, some Hsps have shown great potential and have entered clinical trials for cancer treatment (Murphy, 2013).

Hsps have features that make them ideal as druggable targets (Zininga and Shonhai, 2014). Most Hsps are regulated by nucleotides (Zininga and Shonhai, 2014). As an example, the potential druggable Hsps are Hsp70s and Hsp90s, of which these are ATPases. Most inhibitors used are ATP analogs and compounds which inhibit their ATPase activity (Banumathy *et al*., 2003). The ATPase activity of Hsp70s and Hsp90s vary between organisms (Vali *et al*., 2010). The ATPase activity of tumor cells is known to increase about 10-fold compared to normal cells (Vali *et al*., 2010). Therefore, ATP analogs may be used to inhibit these Hsps which may reduce disease progression. Hsps also exhibit structurally divergent SBDs. Some proline-rich antibacterial peptides target the SBD of bacterial Hsp70 but not human Hsp70 (Vali *et al*., 2010). Hsp70 also show distinct association rates with NEFs due to the sequence diverging motifs that associate with the NEFs (Mayer *et al*., 2001). Consequently, nucleotide exchange of Hsp70 could be targeted in potential drug design.

Co-chaperones have a role in delivering substrates to Hsp70s and modulating the ATPase activity of Hsp70s. The distribution of these co-chaperones varies between humans and parasites. It has been reported that *P. falciparum* has a bigger complement of co-chaperones compared to humans (Burger *et al*., 2014). To justify the targeting of the co-chaperones as drug targets, some compounds are known to selectively target the interaction of Hsp40 with Hsp70 in malaria

parasites but with limited cytotoxicity to humans (Cockburn *et al*., 2011). Inhibition of one isoform of a protein could lead to the upregulation of another with a compensatory role. For instance, it was demonstrated that the inhibition of Hsc70 or stressed induced Hsp70 did not stop the growth of tumor cells but when both isoforms were inhibited a reduction of tumor growth was observed. Therefore, it is important to target Hsp isoforms that are essential. In addition, PfHop is fairly divergent from human Hop. PfHop is known to act as a module that brings PfHsp70-1 and PfHsp90 together to form a functional complex (Zininga *et al*., 2015b). Thus, PfHop also presents a potential antimalarial drug target (Gitau *et al*., 2012; Zininga *et al*., 2015b). PfHop could be a druggable candidate as it divergent from the human Hop homolog.

1.7 Protein Export

P. falciparum parasite exports over 400 hundred proteins into the erythrocytes that they infect (Hiller *et al*., 2004). These proteins have various roles including facilitating the uptake of nutrients from the blood plasma, promote cytoadherence to the blood vessels and remodel the infected erythrocytes towards the parasites benefit (Goel *et al*., 2014). It has been reported that the *Plasmodium* translocon of exported proteins (PTEX) facilitates the movement of these exported proteins across the membrane of the vacuole that demarcates the parasite from the cytosol of the infected erythrocyte (de Koning *et al*., 2009). The PTEX has a putative pore-forming component exported protein 2 (EXP2) which forms a membrane-spanning channel. Heat shock protein 101 (HSP101), a member of Clp/Hsp100 family of ATPases is a component of the PTEX complex. HSP101 unfolds proteins so they can be competent for export across the parasitophorous vacuole membrane (PVM) (de Koning *et al*., 2009). The erythrocyte being a cell without a nucleus could present a difficult environment for the parasite. The erythrocyte cytosol has a limited number of substances which could be utilized by the parasite as a source of nutrition. For the purposes of host cell remodeling the parasite exports proteins like *P. falciparum* erythrocyte membrane protein 1 (PfEMP1). PfEMP1 is the major virulence factor of the *P. falciparum* parasite (Senczuk *et al*., 2001). The parasite also exports some proteins to facilitate the trafficking of other exported proteins, for example, PfPTPI (PfEMP1 trafficking protein 1). PfPTP1 is needed for trafficking of PfEMP1 (Rug *et al*., 2014).

Exported proteins are classified into two major groups. One of the classes contains a plasmodium export element (PEXEL) motif also known as a host-targeting (HT) sequence which is 5 amino acids long (Hiller *et al*., 2004; Marti *et al*., 2004). For functionality, this motif should be about 20 amino acids downstream of signal peptide which directs entry into the ER (Hiller *et al*., 2004). The other group of the exported proteins is known as the PEXEL negative exported (PNEPs). The PNEPS possess a hydrophobic region that facilitates entrance into the secretory pathway (Heiber *et al*., 2013). The PEXEL motif functions through cleavage by an ER resident protease Plasmepsin V which cleaves the substrate at the third and fourth residues of the motif (Tarr and Osborne 2015).

1.7.1 The protein export pathway

The export of proteins can be grouped into two main stages: traveling within the parasite as well as a movement into the host. The initial phase involves the entry of the protein into the ER usually directed by ER retention signals or through a classical secretory mechanism (Deponte *et al*., 2012). During this initial phase, the protein travels across the parasites secretory system. At the ER, the PEXEL motif takes effect but its mechanism of action is not clear. Considering some studies done on PEXEL like sequences in other organisms such as *Cryptosporidium parvum* and *Babesia bovis* evidence was provided that these motifs have a role in the timed secretion of proteins to the infected erythrocytes (Pelle *et* al., 2015). Therefore, it is possible that the PEXEL like motif has a role in revealing the unique transport signals in secretory trafficking pathways of apicomplexan parasites (Speilmann and Gilberger, 2015).

The export of proteins involves a number of steps (Fig 1.7). The exported proteins are secreted into the parasitophorous vacuole (PV), a compartment made of plasma membrane containing cytoplasm and the parasite. The membrane enclosing the PV is called the parasitophorous vacuolar membrane (PVM). According to de Koning-Ward and colleagues, (2009), there is a protein-conducting channel at the PVM, named the translocon for exported proteins (PTEX) (Fig 1.7). The PTEX is essential for the passage of most known types of exported proteins into the host cell. PTEX is essential for most types of proteins shuttled to the host (Beck *et* al., 2014) and this could give the complex a regulatory role. It has been shown that transcriptional downregulation of the PTEX component abrogates the shuttling of both major classes of the exportome (Beck *et al*.,

2014). PTEX has been found to be made up of five proteins and one of the proteins namely EXP2 forms a pore through which the unfolded proteins pass through with the help of the chaperone HSP101, which has a role in unfolding the protein before it enters the pore (Beck *et al*., 2014). Experimental data through transcriptional repression has shown that suppression of either HSP101 or PTEX prevents the export of two broad classes of parasite proteins (de Koning., *et al*., 2009).

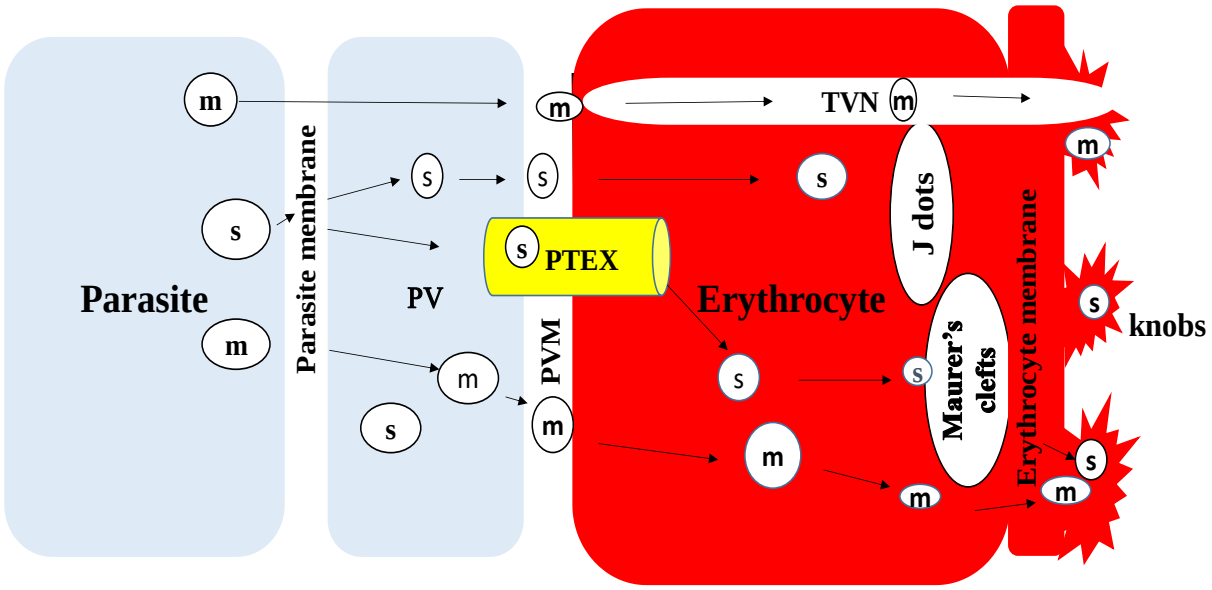

Fig 1.7 Alternative export routes of parasite proteins
(S) represents soluble proteins and (m) membrane proteins, PTEX- Plasmodium translocon of exported proteins, PV- Parasitophorous vacuole, TVN- tubular vascular network. S- represent the routes that soluble proteins might take to reach the erythrocyte membrane, m- represent the route that membrane proteins traveling all the way to the cell surface of the erythrocyte through vesicular pathways through the Maurer's clefts. Alternatively, the membrane proteins can move through the tubular vascular network; adapted from Botha *et al* (2007).

The next stage of protein export involves the movement of soluble proteins to the erythrocyte cytosol where their refolding may be facilitated by other molecular chaperones. Membrane proteins are also transported to the plasma membrane of the erythrocyte through extensions which develop and remain attached to the PV to form the tubulovesicular network (TVN) (Deponte *et al*., 2012). Some of the exported proteins possess multiple interaction domains that may lead to the protein interlinking with many structures in the erythrocyte cytosol, which may be the reason why infected erythrocytes are rigid. Among other proteins *P. falciparum* knob associated histidine

rich protein (KAHRP) attach to the Maurer's clefts where they can be modified for their fate in knob formation on the periphery of the infected erythrocytes (Fig 1.7; Rug *et al*., 2014).

1.8 PfHsp70-x, a special exported protein

P. falciparum Hsp70-x (PfHsp70-x) (PlasmoDB: Accession number PF3D7_0831700) is part of the *P. falciparum* exportome. PfHsp70-x has an EEVN motif similar to the EEVD motif possessed by PfHsp70-1 (Fig 1.3). PfHsp70-x is localized in the erythrocyte cytosol and co-localize within an extra parasitic structure in the infected erythrocyte called J Dots (Külzer *et al*., 2012). PfHsp70-x partially associates with Maurer's clefts as it colocalizes with MAHRP1, a Maurer's cleft marker which suggests that PfHsp70-x may be involved in parasite protein sorting and export (Grover *et al*., 2103). A study by Daniyan and colleagues (2016) confirmed that a malarial Hsp40 (PFA0660w) which specifically and directly binds to PfHsp70-x as a co-chaperone. This strongly implies PfHsp70-x has a major role in chaperoning other proteins in the host's erythrocytes.

The presence of PfHsp70-x exclusively to *P. falciparum* species suggests a possible role of this protein in the pathogenesis of parasite making the species most virulent (Cockburn *et al*., 2014). PfHsp70-x has an N-terminal signal peptide of the size (24 amino acids) which potentially directs the protein to the endoplasmic reticulum (ER). The absence of the ER retention sequence suggests that the chaperone passes through the ER before being exported (Rhiel *et al*., 2016). Interestingly, PfHsp70-x does not contain the PEXEL (pentapeptide) motif of which most exported proteins (Hiller *et al*., 2004). Grover and colleagues, (2013) suggested that PfHsp70-x may follow an unusual route for its exportation to the host erythrocytes' cytoplasm.

1.9 Problem statement and motivation

Human chaperones have since been reported to associate with parasite proteins in the host infected erythrocytes (Banumathy *et al*., 2002). This association is important in the pathogenicity and infectivity of *P. falciparum* (Külzer *et al*., 2010). Moreover, *P. falciparum* virulence is demonstrated by the parasites' ability to export proteins to erythrocytes causing them to adhere to the vascular membrane (Shonhai *et al*., 2011). Detergent solubilization experiments have shown that in uninfected erythrocytes human chaperones are soluble. In infected erythrocytes, the human chaperones are detected in knob enriched fractions as insoluble cross-linked to virulence proteins suggesting that the host chaperone system is diverted functionally during knob formation (Banumathy *et al*., 2002). It is known that Hsp70s, Hop and Hsp90 are able to form a complex (Hsp70-Hop-Hsp90) through a series of steps which is important in protein folding (Hernández *et al.*, 2002; Zininga *et al*., 2015). The availability of PfHsp70-x in the infected erythrocytes poses a possibility that this protein may functionally cooperate with human Hsp90 via human Hop (human Hop) as the parasite does not export its Hop or Hsp90 proteins. It is likely that the interaction of PfHsp70-x with human Hop and hHsp90 could facilitate folding of select proteins implicated in host immune evasion. The absence of PfHsp70-x in other less virulent *Plasmodium* species suggests a possible role of this protein in *P. falciparum* pathogenesis. Therefore, this study investigated the possible interaction of PfHsp70-x with human Hop. Furthermore, it is known that *P. falciparum* proteins are rich in asparagine repeat regions as compared to human proteins (Muralidharan *et al* 2012). For this reason, the current study investigated binding affinity of PfHsp70-x to asparagine rich peptides. The binding affinity to asparagine-rich proteins could indicate that PfHsp70-x preferentially binds to the *P. falciparum* proteins resident in the infected erythrocytes.

1.10 Hypothesis

Exported PfHsp70-x functionally cooperates with human Hsp90 through human Hop. This partnership facilitates folding of malarial proteins exported to the host erythrocytes.

1.11 Main Objective

To investigate the functional interaction of exported protein PfHsp70-x with human Hop and human Hsp90 *in vitro.*

1.11.1 Specific Objectives

1. To express and purify PfHsp70-x and human Hop from *E. coli* XL1 Blue cells and *E. coli* JM109 cells
2. To determine the secondary structure and the heat stability of PfHsp70-x using circular dichroism (CD) spectrometry
3. To investigate the effect of the EEVN motif on ATP binding and basal ATPase activity of PfHsp70-x
4. To investigate the effect of the EEVN motif on the chaperone activity of PfHsp70-x
5. To investigate the physical association of PfHsp70-x and human Hop using slot blot and SPR analyses

CHAPTER 2: MATERIALS AND METHODS

2.0 Materials

The plasmids used this study are listed in Table 2.1. The plasmid constructs were made by Genscript (USA) (Table 2.1). The pQE30/PfHsp70-x plasmid was used to express the wild type PfHsp70-x. The PfHsp70-x insert was cloned between *Bam*HI and *Hind*III restriction sites. The pQE30/PfHsp70-x_T plasmid was used to express the mutant type of PfHsp70-x lacking the EEVN motif. Similarly, the PfHsp70-x_T insert was cloned between *Bam*HI and *Hind*III restriction sites The pQE30/human Hop plasmid was utilized to express human Hop (human Hop) recombinant protein. The human Hop insert was also cloned between *Bam*HI and *Hind*III restriction sites. The recombinant proteins were expressed attached to an N-terminal polyhistidine tag. Anti-PfHsp70-x antibodies were used to detect PfHsp70-x and PfHsp70-x_T. Anti-His antibodies were used to confirm PfHsp70-x, PfHsp70-x_T and human Hop. Anti-DnaK antibodies were used to identify and confirm the presence of DnaK. The other reagents used in this study are listed in (Appendix A).

Table 2.1 Plasmid constructs and strains used to express the recombinant proteins

Cell lines	**Description**	**Supplier/Reference**
E. coli JM109	e14$^-$ (McrA$^-$) recA1 endA1 *gyr*A96 thi-1 hsdR17 (rK$^-$ mK$^+$) A1 Δ(*lac*-proAB) (F´ traD36 proAB *lac*I^{q}ZΔM15).	Thermofisher Scientific, USA
E. coli XL1 Blue	*rec*A1 *end*A1 *gyr*A96 *thi*1 *hsd*R17 supE44 *rel*A1*lac* (F´proAB *lac*IqZM15 Tn10 (Tetr)	Bullock *et al*., (1987)
Plasmids	**Description**	**Supplier**
pQE30/PfHsp70-x	pQE30 encoding PfHsp70-x, Amp^R	Genscript, USA
pQE30/PfHsp70-x_T	pQE30 encoding PfHsp70-x_T, Amp^R	Genscript, USA
pQE30-human Hop	pQE30 encoding human Hop, Amp^R	Genscript, USA

2.1 Confirmation of constructs

Plasmid constructs expressing PfHsp70-x, PfHsp70-x_T and human Hop were purified by using the Zymo Research Plasmid Miniprep™ kit (Epigenetics, U.S. A) following manufacturer's instructions (Appendix B1). The restriction enzymes, *Hind*III and *Bam*HI (Thermo Scientific, U.S.A) were used to digest the plasmid DNA. The products of restriction digest were analyzed using 0.8 % agarose gel electrophoresis (Appendix B2). Sequencing was further conducted to confirm the plasmids.

2.2 Expression of recombinant proteins

Chemically made competent *E. coli* cells (Table 2.1) were transformed with the respective plasmid DNA (Table 2.1). A single colony containing the plasmid was inoculated into 50 ml 2 X YT (1.6 % (w/v) tryptone, 1.0 % (w/v) yeast, 1.5 % (w/v) agar, 0.5 % (w/v) NaCl) broth containing 100 µg/ml of ampicillin. The inoculum was incubated overnight at 37 ºC with gentle shaking. Proceeding overnight incubation 1: 10 dilution of the overnight culture was transferred into fresh 2 X YT broth and was incubated at 37 ºC until mid-log phase (OD_{600} 0.5–0.6). Protein expression was initiated with the addition of 1 mM isopropyl-β-D-1-thiogalactopyranoside (IPTG, Sigma) and thereafter the culture was incubated at 37 ºC for 24 hours with gentle shaking. Post-induction samples were collected at hourly intervals. After 24 hours, the cells were harvested by centrifugation at 5000 g for 20 minutes at 4 °C. The pellet fraction was suspended in lysis buffer (100 mM Tris–HC1, pH 7.4, 300 mM NaCl, 10 mM Imidazole, 1 mM phenylmethylsulfonyl fluoride (PMSF) and 1 mg/ml lysozyme). The cells were incubated at room temperature for 45 minutes preceding storage of the cell lysates at -80 °C. Protein expression was confirmed by analyzing the samples using 12 % sodium dodecyl sulfate-polyacrylamide gel electrophoresis (SDS-PAGE) and visualized by Coomassie blue (Appendix B3). Western blotting was conducted to confirm the expressed recombinant proteins (Appendix B4). The antibodies used were mouse monoclonal anti-His_6-horseradish peroxide conjugated antibodies (α-His) [1: 2000 dilution] (Sigma-Aldrich, U.S.A). Rabbit raised anti-PfHsp70-x (α-PfHsp70-x) [1: 2000 dilution] was used as a primary antibody for binding both full-length and truncated PfHsp70-x. Goat raised anti-rabbit horseradish peroxidase conjugated antibodies (1: 5000 dilution) were utilized as secondary antibodies. Visualization of

the Western blot was done using the chemiluminescent substrate (ECL) (Thermo scientific, USA) as per manufacturer's instructions and the images were captured using ChemiDoc Imaging system (Bio-Rad, USA).

2.3 Purification of recombinant proteins

Cell lysates from -80 ℃ storage were thawed on ice and polyethyleneimine (PEI) 0.1 % (v/v) was added to the lysate. The utilization of PEI was to solubilize insoluble proteins and precipitate nucleic acids which may be linked to the protein, separating the target protein in the supernatant (Shonhai *et al*., 2008; Zininga *et al*., 2015). Lysates were centrifuged at 5000 g for 20 minutes at 4 ℃. The supernatant was isolated and the pellet was re-suspended in 10 ml of lysis buffer and centrifugation repeated as before. The supernatant was loaded onto a HisPur™ Nickel-charged nitrilotriacetic acid (Ni-NTA) (ThermoScientific) immobilized metal affinity chromatography column (IMAC). Washing was conducted with 2 bed volumes of wash buffer 1 (100 mM Tris pH 7.5; 300 mM NaCl, 25 mM imidazole, 1 mM PMSF and 5 mM ATP) and wash buffer 2 (100 mM Tris pH 7.5; 300 mM NaCl, 80 mM imidazole, 1 mM PMSF and 5 mM ATP). ATP was added to the wash buffers to eliminate possible contaminating *E. coli* Hsp70 (DnaK). The proteins were subsequently eluted using elution buffer 1 (100 mM Tris pH 7.5; 300 mM NaCl, and 250 mM imidazole) and elution buffer 2 (100 mM Tris pH 7.5; 300 mM NaCl, and 500 mM imidazole, 1 mM PMSF). The samples collected were then analyzed using 12 % SDS-PAGE (Appendix B4) and Western blotting (Appendix B5). The antibodies used for Western blotting are described in (Section 2.0).

The purified recombinant proteins were dialyzed using ThermoScientific™ SnakeSkin™ dialysis tubing. The tubing was equilibrated for 15 minutes in dialysis buffer 1 (150 mM NaCl, 10 mM imidazole, 10 mM Tris, 10 % glycerol (v/v), pH 7.5, 1 mM PMSF). The sample was dialyzed for 8 hours in dialysis 1 and then stored for 6 hours in dialysis buffer 2 (150 mM NaCl, 10 mM Tris, pH 7.5, 1 mM PMSF). Recombinant proteins were concentrated by polyethylene glycol (PEG) for 30 minutes. Protein concentrations were determined by Bradford's assay using bovine serum

albumin as a standard (Appendix B6). The Christoph-Leidig (http://christophleidig.de/tprot.html; Appendix B7) tool was also used to confirm recombinant protein concentrations.

2.4 Investigation of the secondary structure and the heat stability of PfHsp70-x using CD spectrometry

CD spectroscopy was carried out to establish the secondary structure and heat stability of PfHsp70-x. The secondary structure of recombinant PfHsp70-x was analyzed using Far-UV circular dichroism (CD). The procedure was performed as previously described (Zininga *et al*., 2015). Briefly, 0.2 µM PfHsp70-x recombinant protein was suspended in 20 mM Tris-HCl pH 7.4, 100 mM sodium fluoride buffer. The analysis was conducted using the J-1500 CD spectrometer (JASCO Ltd, UK) equipped with a Peltier temperature controller at 19 ℃, using a 0.1 cm path-length quartz cuvette (Hellma). The machine was set to automatically subtract buffer background signal and the averaged CD signals were converted to mean residue ellipticity [θ] (mdeg.cm^{2}dmol^1).

$$[\theta] = (100 \times \theta_\lambda)/Cnl \quad \text{.....Equation 1}$$

The variables in the equation are as follows,
θ is measured ellipticity in millidegree
n is the number of residues
l is the path length (cm)
C is the molarity of the recombinant protein in mM.

The data was analyzed by the Dichroweb online server (Whitmore and Wallace, 2008) using the CDSSTR program. This program de-convolutes the conformation of the proteins into fractions of beta sheets, alpha helices and random coils (Zininga *et al*., 2015a).

The thermal stability of the recombinant protein was determined by fixing the wavelength at 222 nm and subjecting the protein to stepwise increase in temperature as described by Zininga and colleagues (2015). The temperature was raised from 19 ℃ to 95 ℃ at a rate of 0.5 ℃ per minute.

The folded state of the PfHsp70-x protein at any given temperature was calculated as described by Misra and Ramachandran (2009). The equation is as follows:

$$([\theta]^t - [\theta]^h)/ ([\theta]^l - [\theta]^h) \quad \text{.....Equation 2}$$

where $[\theta]^t$ is the molar ellipticity at any given temperature, $[\theta]^h$ molar ellipticity at the highest temperature, and $[\theta]^l$ molar ellipticity at the lowest temperature.

2.5.1 ATP-binding assay for PfHsp70-x / PfHsp70-x$_T$ using SPR

The nucleotide binding affinity of PfHsp70-x and PfHsp70-x$_T$ was conducted using surface plasmon resonance (SPR) as previously described (Zininga *et al*., 2015). The assay was conducted at 25 ºC using filter sterilized and degassed PBS-Tween running buffer (10 mM Na_2HPO_4, 1.46 mM KH_2PO_4, 137 mM NaCl, 3 mM KCl, 0.005 % (v/v) Tween 20 and 20 mM EDTA; pH 7.4). Conditioning of the chip was done by a buffer containing (0.5 % (w/v) SDS, 50 mM NaOH and 100 mM HCl). Prior immobilization of the recombinant proteins the ProteOn HTE sensor chips were activated using 20 mM 1-ethyl-3-(3-dimethylaminopropyl) carbodiimide hydrochloride (EDC) and 5 mM N-hydroxy sulfasuccinamide. The recombinant PfHsp70-x (1 µg/ml) and its truncated version were immobilized onto respective ProteOn HTE sensor chips as the ligands. Varying concentrations of the analyte (ATP) were injected at a flow rate 100 µl/min and association and dissociation was allowed to occur in a period of 10 minutes. The resulting association and dissociation data was analyzed using BiaEvaluation and ProteOn Manager™ software version 3.1.0.6.

2.5.2 Investigating the basal ATPase activity of PfHsp70-x

The ability of PfHsp70-x and PfHsp70-x$_T$ to hydrolyse ATP was investigated by conducting an ATPase assay**.** The ATPase activity of PfHsp70-x and PfHsp70-x$_T$ were determined as previously described with minor modifications (Matambo *et al*., 2004). The ATPase activity of the PfHsp70-x/ PfHsp70-x$_T$ was determined by quantifying the amount of inorganic phosphate released. In brief, 1 µM PfHsp70-x was incubated for 5 minutes in the assay buffer (100 mM KCl, 2 mM

$MgCl_2$, 0.5 Mm DTT, 10 mM HEPES-KOH pH 7.5). The reaction was initiated by addition of ATP of concentration range (0 to 1 mM) and subsequent incubation at 37 °C for 2 hours. The addition of 10 % (w/v) SDS was done to stop the reaction, followed by addition of 1.25 % (w/v) ammonium molybdate in 6.5 % H_2SO_4 In order to quantitate the amount of inorganic phosphate released, 9 % ascorbic acid (w/v) was added for color development. The reaction mixture was incubated at room temperature for 30 minutes. After the incubation, absorbance was read at 660 nm using a SpectraMax M3 spectrometer (Molecular Devices, U.S.A). The reaction mixture without the protein was used as a non-enzymatic control and all the absorbances were standardized to spontaneous hydrolysis of ATP. Extrapolation of absorbance values was done against a standard calibration curve using Na_2HPO_4 as standard (Appendix B6). The ATPase activity of PfHsp70-x was expressed as nmol Pi released/min/mg of recombinant protein. Michaelis–Menten plots using GraphPad Prism 6.05 software were generated to determine V_{max} and K_m. At least three independent purification batches of recombinant protein were used in different experiments.

2.6.1 Exploring the capability of PfHsp70-x and PfHsp70-x$_T$ to suppress the heat-induced aggregation of luciferase

The chaperone function of recombinant PfHsp70-x was investigated by its ability to suppress the heat-induced aggregation of model substrate luciferase from *Photinus pyralis* (Sigma-Aldrich). The experiment was conducted as previously described with minor modifications (Zininga *et al*., 2016). The assay was conducted by adding 0.6 µM luciferase and 0.2 µM recombinant chaperone in assay buffer (25 mM HEPES-KOH, pH 7.5, 5 mM Mg $(OA_C,)_2$, 5 mM, $NaOA_C$, 50 mM KCl, 5 mM β-mercaptoethanol) heated to 48 °C for 90 minutes. The concentration of the required levels of PfHsp70-1 and PfHsp70-z was previously optimized by titration (Zininga *et al*., 2016). Therefore, the same chaperone concentration was used in this assay. The resulting luciferase aggregation was monitored at 340 nm using SpectraMax M3 spectrometer (Molecular Devices, U.S.A). The assay was repeated using 0.6 µM Bovine serum albumin (BSA) as a control.

2.6.2 Analysis of the capability of PfHsp70-x and PfHsp70-x$_T$ to suppress the aggregation of malate dehydrogenase (MDH)

The chaperone function of PfHsp70-x and PfHsp70-x$_T$ was investigated by monitoring the suppression of a heat-induced aggregation model protein, malate dehydrogenase (MDH) from the *porcine* heart (Sigma-Aldrich). The procedure followed was adapted from previously described protocols (Shonhai *et al.,* 2008; Makumire *et al.,* 2014; Zininga *et al*., 2016) with minor modifications. In short, the chaperone function of PfHsp70-x in suppressing the thermally induced aggregation of MDH was monitored spectrophotometrically. MDH (0.6 µM final concentration) was added to the pre-heated buffer (50 mM Tris, pH 7.4, 100 mM NaCl) at 48 °C and the temperature was maintained at 48 °C for 90 minutes during which the light scatter due to protein aggregates was monitored at 340 nm. This assay was performed using SpectraMax M3 spectrometer (Molecular Devices, U.S.A). The assay was repeated in the presence of PfHsp70-x/ PfHsp70-x$_T$ at a final concentration of 0.6 µM. BSA was used as a control in this assay. The data were analyzed through GaphPad Prism 6.05 software.

2.6.3 Analysis of binding affinities of PfHsp70-x and PfHsp70-x$_T$ for peptides

The association of PfHsp70-x and PfHsp70-x$_T$ with specific peptides was investigated using SPR analysis as described in (Section 2.7.1). Briefly, PfHsp70-x and PfHsp70-x$_T$ were immobilized onto respective ProteOn HTE sensor chips as ligands. The ligands used were peptides. Peptide 1 was modified by substituting valine and leucine residues for asparagine to make peptide 2. Peptide 3 was also modified to make peptide 4 by substituting leucine for asparagine. Peptide 1 (GFT**VVL**MYRF), peptide 2 (GFT**NNN**MYRF), peptide 3 (NR**LL**TG) and peptide 4 (NR**NN**TG) at varying concentrations (125 nM, 250 nM, 500 nM, 750 nM, 1000 nM and 2000 nM) were passed over the immobilized ligands. The analytes were injected at a flow rate of 50 µl/ min and association and dissociation were allowed to occur for 10 minutes. Analysis of association and dissociation data was conducted using BiaEvaluation and ProteOn Manager™ software version 3.1.0.6. The assay was repeated in the presence of 5 mM ADP/ ATP.

2.7 Determination of the physical association between PfHsp70-x and human Hop

Slot blot and surface plasmon resonance (SPR) were used to investigate interaction between the PfHsp70-x and human Hop.

2.7.1 Determination the physical interaction between PfHsp70-x and human Hop by slot blot analysis

To confirm the specificity of the PfHsp70-x antibody, bovine serum albumin (BSA) the negative control, PfHsp70-x the positive control and human Hop were immobilized in varying amounts (2 µg, 4 µg and 16 µg) onto the nitrocellulose membrane using Bio-Dot ^{TM}SF apparatus as previously described by (Zininga *et al*., 2016). Western blotting using α-PfHsp70-x [1: 2000] (Genscript, USA) as primary antibodies and using goat raised α-rabbit IgG secondary HRP-conjugated antibody [1: 4000] (Sigma-Aldrich, USA) was conducted. To determine the physical interaction between PfHsp70-x and human Hop of the bait protein (human Hop), the prey protein (PfHsp70-x) and BSA negative control were spotted onto the nitrocellulose membrane. The membranes were thereafter blocked with 5 % (w/v) fat-free milk for 1 hour. The membranes were overlaid with PfHsp70-x (10 µg/ml) final concentration in 5 % (w/v) fat-free milk. The overlay process was repeated in the presence of 5 mM ADP/ATP with the concentration of the nucleotides constant in the following steps of the protocol. Subsequently, overnight incubation of the overlaid blots on ice was carried out. The membranes were washed three times for 10 minutes with TBST after overnight incubation. The prey proteins were detected by Western blotting. Visualization of the Western blot was done as previously described in section 2.3.

2.7.2 SPR analysis of interaction between PfHsp70-x and human Hop

SPR analysis was conducted to determine the direct interaction kinetics the of the recombinant PfHsp70-x and human Hop protein as described by Zininga and colleagues (2015). The interaction between the truncated PfHsp70-x_T and human Hop was also investigated. Briefly, the assay was conducted at 25 ºC using filter sterilized and degassed PBS-Tween running buffer (8 mM Na_2HPO_4, 1.46 mM KH_2PO_4, 137 mM NaCl, 3 mM KCl, 0.005 % (v/v) Tween 20 and 20 mM

EDTA; pH 7.4). The ProteOn HTE sensor chips were activated using 20 mM 1-ethyl-3-(3-dimethylaminopropyl) carbodiimide hydrochloride (EDC) and 5 mM N-hydroxy sulfasuccinamide. Conditioning of the chip was done by a buffer containing (0.5 % (w/v) SDS, 50 mM NaOH and 100mM HCl). The recombinant PfHsp70-x (1 µg/ml) and its truncated version were immobilized onto respective ProteOn HTE sensor chips as ligands. The human Hop recombinant protein at varying concentrations (125 nM, 250 nM, 500 nM, 1000 nM and 2000 nM) was then passed over the immobilized PfHsp70-x as ligands. The process was repeated with human Hop immobilized while varying concentrations of the PfHsp70-x and PfHsp70-x_T were passed over the human Hop. The analytes were injected at flow rate 50 µl/min and association and dissociation occurred in a period of 10 minutes. The resulting association and dissociation data were analyzed using the ProteOn Manager™ software version 3.1.0.6. The assay was then repeated in the presence of 5 mM ADP/ATP.

CHAPTER 3: RESULTS

3.1.1. Confirmation of the integrity of the pQE30/PfHsp70-x construct

The integrity of the pQE30/PfHsp70-x was verified by sequencing and restriction diagnostic digest using restriction enzymes, *Bam*HI and *Hind*III (Fig 3.1A, B). Single digestion by either *Bam*HI or *Hind*III produced a linearized plasmid of size 5465 bp (Fig 3.1B). Double digestion using both restriction enzymes resulted in two fragments of 3425 and 2040 bp corresponding to the pQE30 expression vector and *PfHsp70-x* insert (Fig 3.1B). The predicted fragment sizes are shown in the plasmid map (Fig 3.1A) and correspond to the fragments generated by restriction digestion (Fig 3.1B).

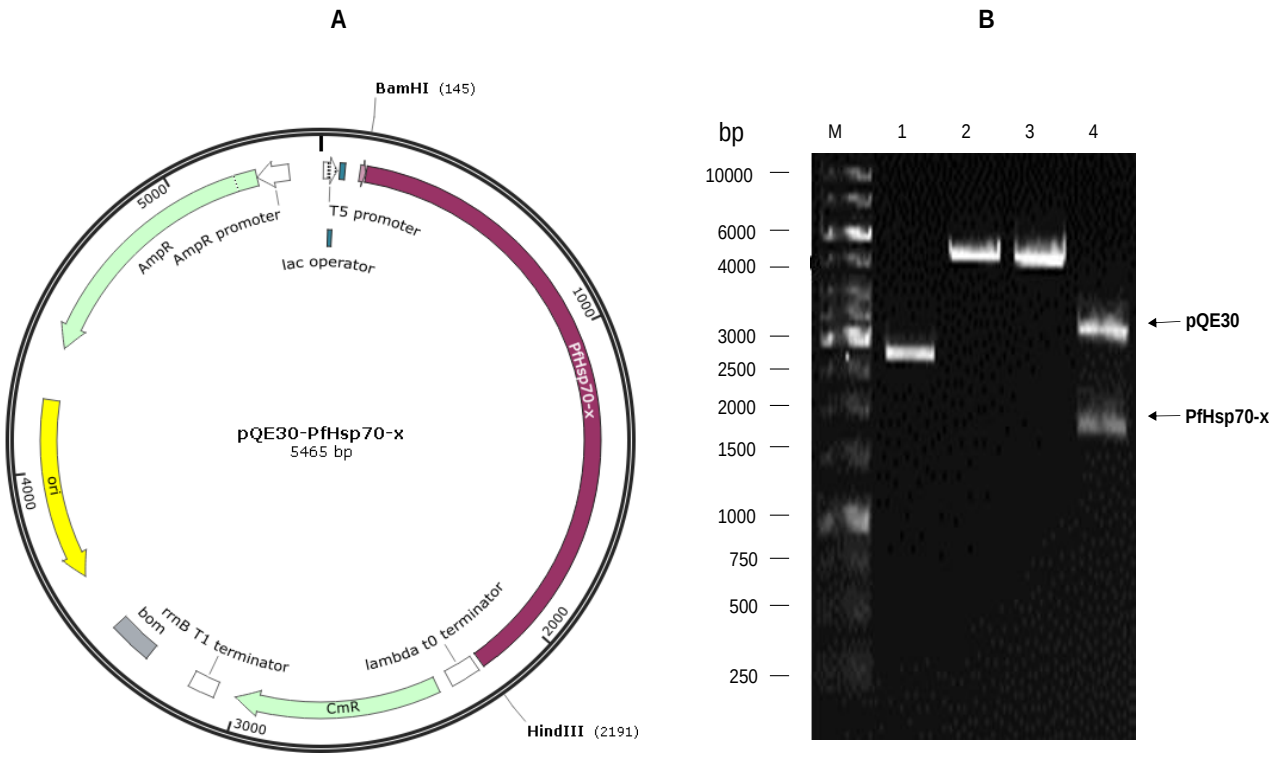

Fig 3.1 Restriction analysis of pQE30/PfHsp70-x DNA plasmid
(**A**) Plasmid map of pQE30/PfHsp70-x showing the *Bam*HI and *Hind*III restriction sites. (**B**) Agarose gel electrophoresis of pQE30/PfHsp70-x: lane M, DNA molecular weight marker in bp; lane 1, undigested pQE30/PfHsp70-x plasmid; lane 2, pQE30/PfHsp70-x digested with *Bam*HI; lane 3, pQE30/PfHsp70-x digested with *Hind*III; lane 4, pQE30/PfHsp70-x digested with both *Bam*HI and *Hind*III.

3.1.2. Confirmation of the integrity of the pQE30/PfHsp70-x_T construct

The integrity of the pQE30/ PfHsp70-x_T was confirmed by sequencing and restriction diagnostic digest using restriction enzymes *Bam*HI and *Hind*III (Fig 3.2A, B). Single digestion by either *Bam*HI or *Hind*III produced a linearized plasmid of size 5454 bp (Fig 3.2B). Digestion using both restriction enzymes resulted in two distinct fragments of the respective sizes 3425 and 2029 bp (Fig 3.2B). The resulting fragment sizes correspond with the vector and insert respectively. The sizes of fragments also compliment the respective plasmid map (Fig 3.2A).

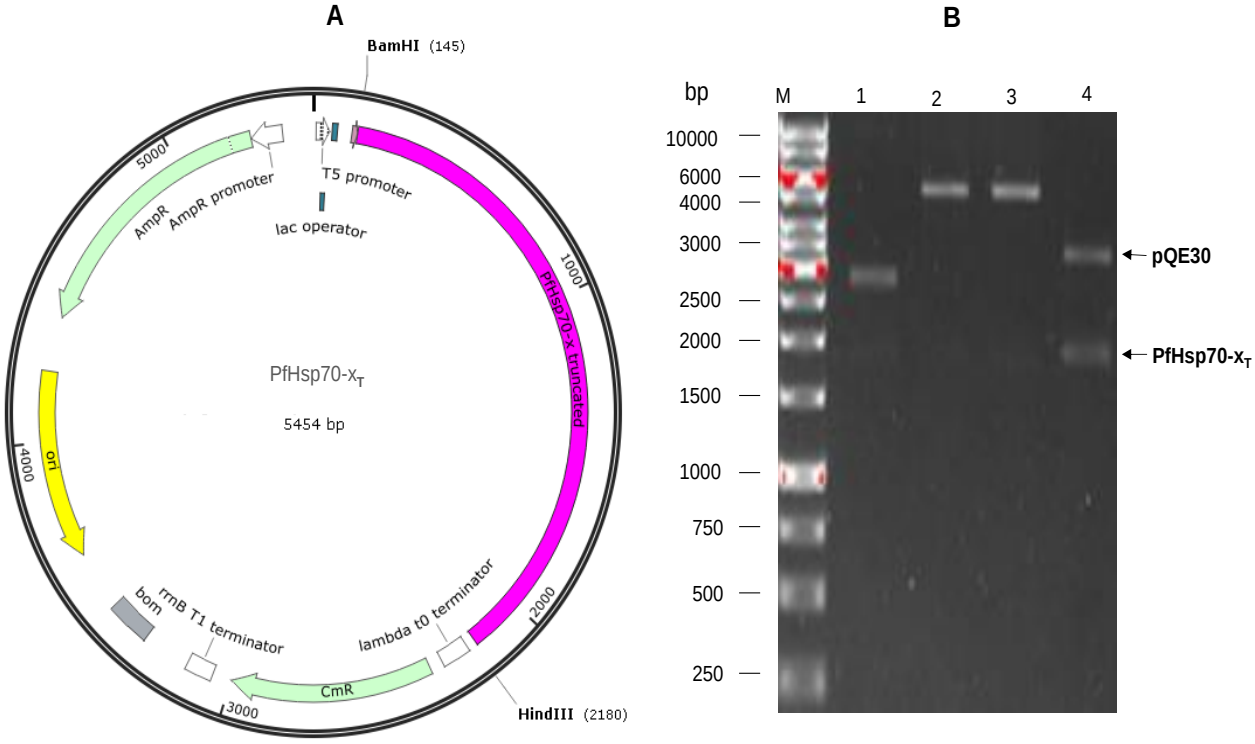

Fig 3.2 Restriction analysis of pQE30/PfHsp70-x_T DNA plasmid
(**A**) Plasmid map of pQE30/PfHsp70-x_T showing the *Bam*HI and *Hind*III restriction sites. (**B**) Agarose gel electrophoresis of pQE30/PfHsp70-x_T: lane M, DNA molecular weight marker in bp; lane 1, undigested pQE30/PfHsp70-x_T plasmid; lane 2, pQE30/PfHsp70-x_T digested with *Bam*HI; lane 3, pQE30/PfHsp70-x_T digested with *Hind*III; lane 4, pQE30/PfHsp70-x_T digested with both *Bam*HI and *Hind*III.

3.1.3. Confirmation of the integrity of the pQE30/human Hop plasmid

The pQE30/human Hop plasmid was verified by sequencing and restriction digestion to confirm the identity of the expression plasmid (Fig 3.3A, B). The restriction enzymes used in this restriction digest are *Bam*HI and *Hind*III. The single digest with either of the restriction enzymes resulted in a linearized band at approximately 5068 bp corresponding to the size of the plasmid. Double digestion with *Bam*HI and *Hind*III produced two distinct bands. The larger band is approximately 3424 bp which corresponds to the size of the pQE30 vector. The smaller fragment of approximate size 1644 bp corresponds to the human Hop insert (Fig 3.3B). The products of restriction digestion compliment the sizes shown in the pQE30/human Hop plasmid map (Fig 3.3A).

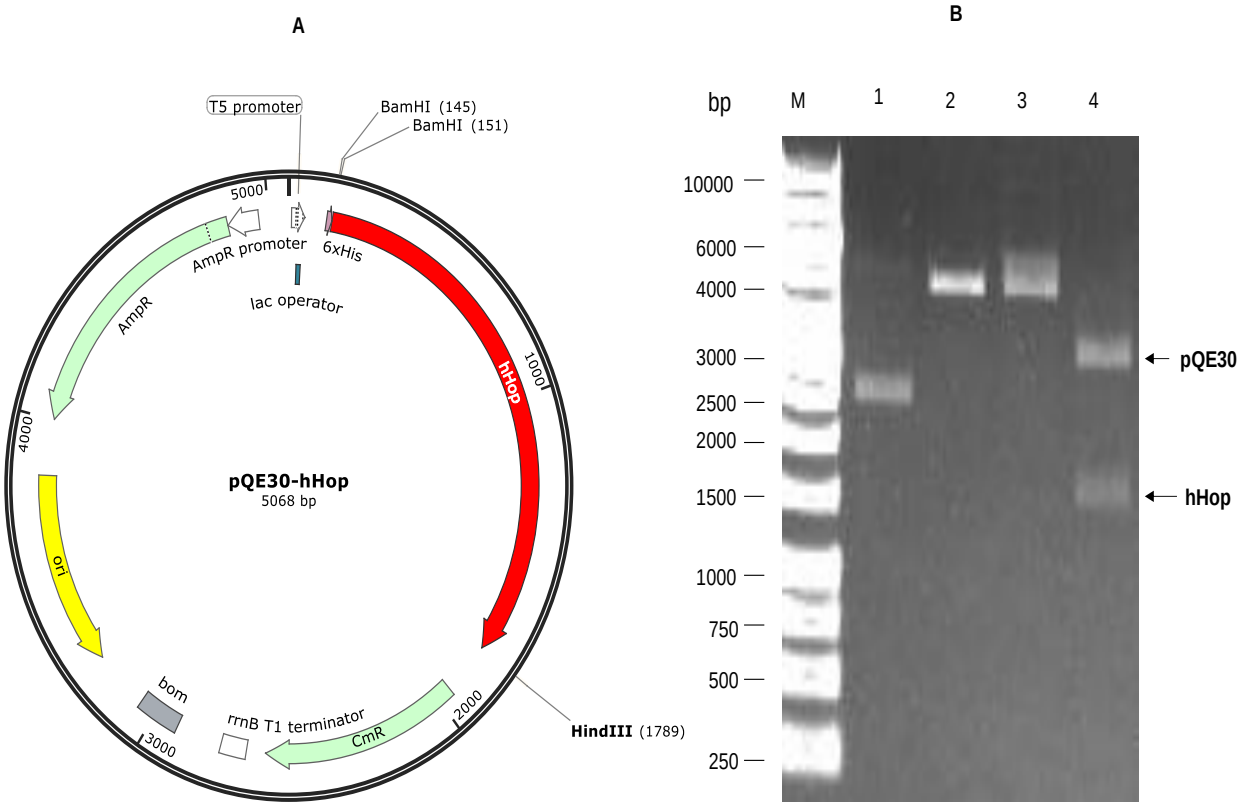

Fig 3.3 Restriction analysis of pQE30/PfHsp70-x$_T$ DNA plasmid
(**A**) Plasmid map of pQE30/human Hop showing the *Bam*HI and *Hind*III restriction sites. (**B**) Agarose gel electrophoresis of pQE30/human Hop: lane M, DNA molecular weight marker in bp; lane 1, undigested pQE30/human Hop plasmid; lane 2, pQE30/human Hop digested with *Bam*HI; lane 3, pQE30/human Hop digested with *Hind*III; lane 4, pQE30/human Hop digested with both *Bam*HI and *Hind*III.

3.2.1. Expression of PfHsp70-x

PfHsp70-x was successfully expressed in *E. coli* XL1 Blue and resolved at approximately 76 kDa on the SDS-PAGE (Fig 3.4). The recombinant protein was His-tagged and therefore its expression was confirmed by Western blotting using α-His antibodies and α-PfHsp70-x antibodies respectively (Fig 3.4). As expected, the PfHsp70-x species were not present in the total cell extracts transformed with the pQE30 plasmid which served as a negative control (Fig 3.4; lane C). Leaky expression was observed as the PfHsp70-x expression occurred before induction (Fig 3.4; lane 0) but was not toxic to the cells. Expression levels of the recombinant protein post induction appeared constant from 1 hour to 6 hours but more protein was produced after 24 hours (Fig 3.4; lane 24).

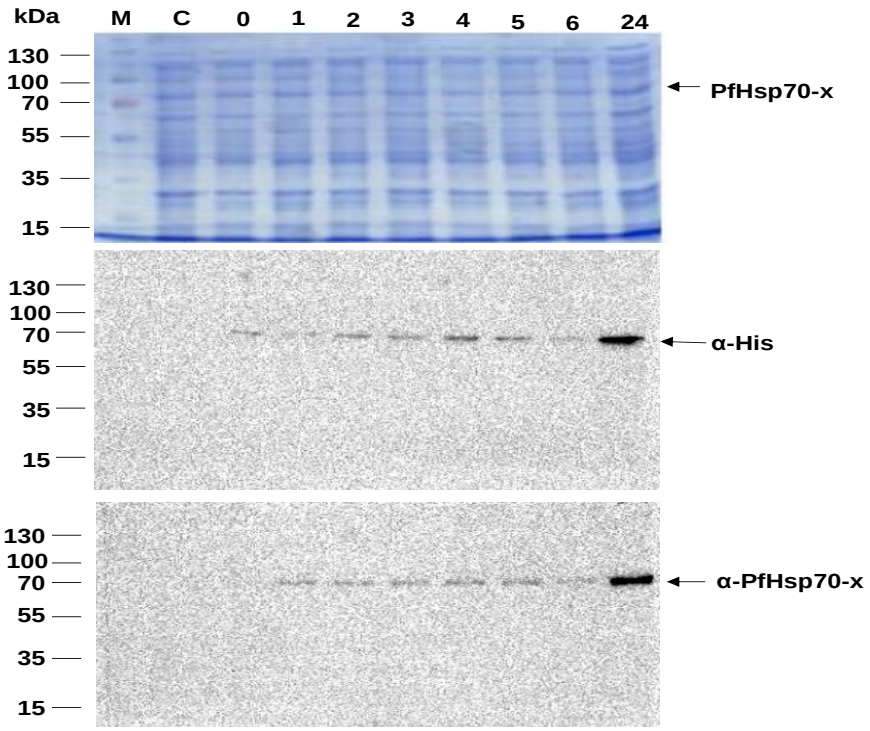

Fig 3.4 Analysis of the expression of PfHsp70-x in *E. coli* XL1 Blue
Coomassie blue stained SDS-PAGE analysis (Upper panel) and Western analysis using α-His and α-PfHsp70-x antibodies for the expression of PfHsp70-x in *E. coli* XL1 Blue cells. Samples of *E. coli* XL1 Blue cells transformed with pQE30/PfHsp70-x plasmid taken at different time intervals. Lane C, represents the total extract of cells transformed with pQE30 plasmid after IPTG induction; Lane 0, represents total extract of cells transformed with pQE30/PfHsp70-x plasmid prior to IPTG induction; lane 1-6 and 24, represent hourly samples of cells transformed with pQE30/PfHsp70-x plasmid post induction.

3.2.2 Expression of PfHsp70-x_T

The PfHsp70-x_T species was not present in the total cell extracts transformed with the pQE30 plasmid which was the negative control (Fig 3.5; lane C). Leaky expression was observed (Fig 3.5; lane 0). PfHsp70-x was successfully expressed in *E. coli* XL1 Blue and resolved at approximately 76 kDa on the SDS-PAGE (Fig 3.5). The recombinant protein was His-tagged and therefore its expression was confirmed by Western blotting using α-His antibodies and α PfHsp70-x antibodies (Fig 3.5). Post-induction protein expression was observed from the first hour until the sixth hour. Protein expression occurred at a constant level after induction but was higher in the 24th hour (Fig 3.5; lane 24).

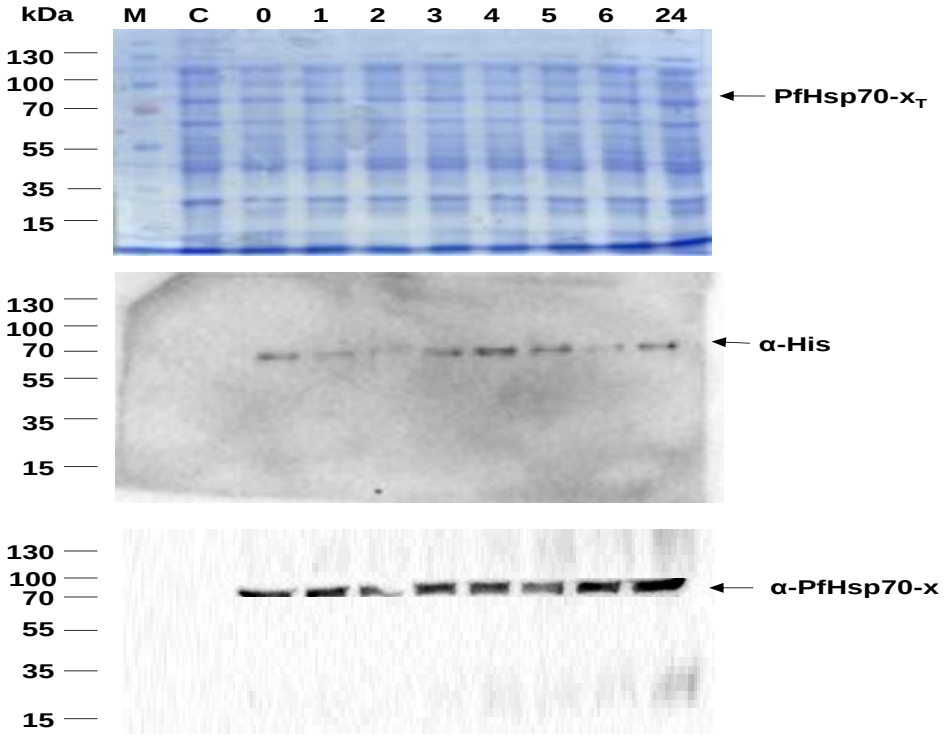

Fig 3.5 Analysis of the expression of PfHsp70-x_T in *E. coli* XL1 Blue cells
Coomassie blue stained SDS-PAGE analysis (Upper panel) and Western analysis using α-His and α-PfHsp70-x antibodies for the expression of PfHsp70-x in *E. coli* XL1 Blue cells. Samples of *E. coli* XL1 Blue cells transformed with pQE30/PfHsp70-x_T plasmid taken at different time intervals. Lane C, represents the total extract of cells transformed with pQE30 plasmid after IPTG induction; Lane 0, represents total extract of cells transformed with pQE30/PfHsp70-x_T plasmid prior to IPTG induction; lane 1-6 and 24, represent hourly samples of cells transformed with pQE30/PfHsp70-x_T plasmid post induction.

3.2.3 Expression of human Hop recombinant protein

There was no recombinant protein production in the control with the cell extracts transformed with the pQE30 plasmid (Fig 3.6; lower panel, lane C). Leaky expression occurred as the recombinant proteins was produced before induction with IPTG although this did not result in cytotoxicity (Fig 3.6; lane 0). The human Hop recombinant protein was successfully expressed as distinct bands are observed at approximately 66 kDa (Fig 3.6). Western blotting using α-His antibodies was used to identify the human Hop recombinant protein (Fig 3.6; lower panel). Expression of human Hop increased post induction from 1-4 hours (Fig 3.6; lane 1-4).

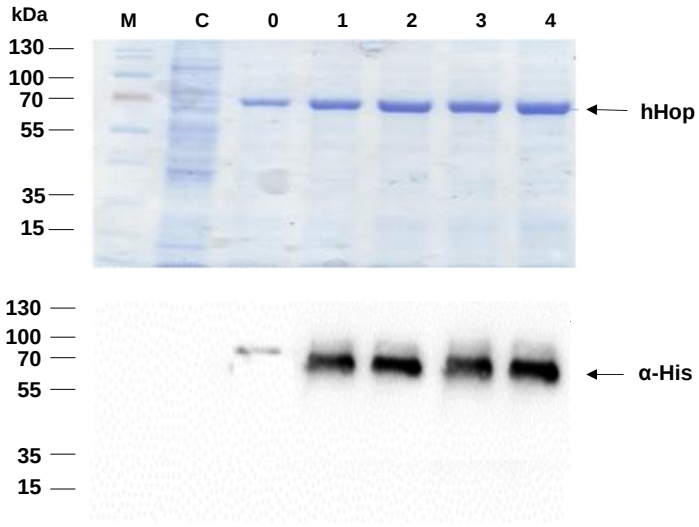

Fig 3.6 Analysis of the expression of human Hop in *E. coli* JM109
Coomassie blue stained SDS-PAGE analysis (Upper panel) and Western analysis (lower panel) using α-His for the expression of human Hop in *E. coli* JM109 cells. Samples of *E. coli* JM109 cells transformed with pQE30/human Hop plasmid taken at different time intervals. Lane C, represents the total extract of cells transformed with pQE30 plasmid after IPTG induction; Lane 0, represents total extract of cells transformed with pQE30/human Hop plasmid prior to IPTG induction; lane 1-4, represent hourly samples of cells transformed with pQE30/human Hop plasmid after induction.

3.3.1. Purification of PfHsp70-x

Affinity chromatography allows isolation of target proteins from complex biological mixtures. Sepharose nickel affinity chromatography was used to purify the recombinant proteins. The PfHsp70-x recombinant protein was successfully purified natively and analyzed by 12 % SDS-PAGE with subsequent confirmation using Western blotting (Fig 3.7). Some of the recombinant

protein was in the pellet insoluble fraction and a part of it was detected in the supernatant soluble fraction. There was no protein detected in the flow through (Fig 3.7; lane FT) and some protein was lost during washing (Fig 3.7; lane W2). This species in the washes was detected by α-PfHsp70-x and not α-His because the His tag on the species may have detached. Although some protein was lost during the washing step most was eluted successfully. Furthermore, DnaK was not detected in the elutions by Western blotting suggesting the eluted proteins were not DnaK contaminated.

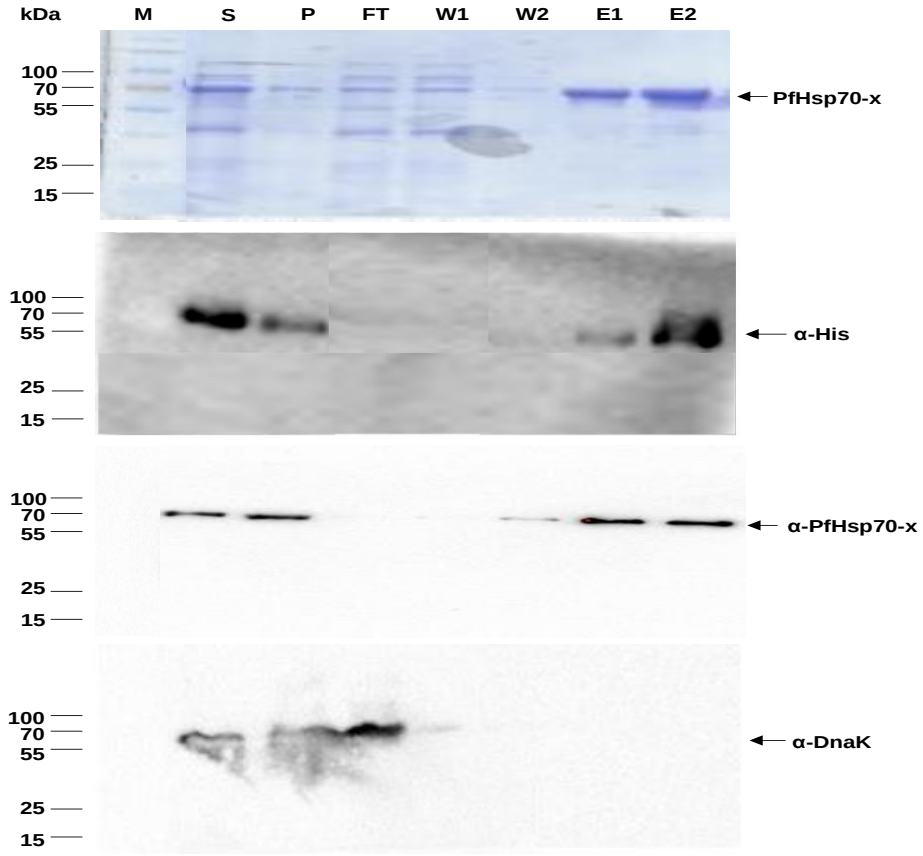

Fig 3.7 Purification of PfHsp70-x
Coomassie blue stained SDS-PAGE analysis (upper panel) and Western analysis (lower panels) of PfHsp70-x expressed from *E. coli* XL1 Blue using α-His, α–PfHsp70-x and α-DnaK antibodies respectively. Lane M represents the molecular weight marker in kDa, S-supernatant fraction, P-pellet fraction, FT-flow through, W1-wash 1, W2-wash 2, E1-elution 1 and E2 –elution 2.

3.3.2 Purification of PfHsp70-x$_T$

Solubility study data showed that less PfHsp70-x$_T$ protein occurred in the soluble fraction than in the insoluble fraction according to the α-PfHsp70-x Western blot (Fig 3.8; lane S, P) respectively. The recombinant protein was purified in native form throughout the procedures. The protein bound to the beads successfully as no protein was detected in the flow through (Fig 3.8; lane FT). No detectable PfHsp70-x$_T$ was lost during the washing steps (Fig 3.8; lane W1, W2), therefore, the recombinant protein was eluted successfully. The eluted protein was free of DnaK contamination (Fig 3.8).

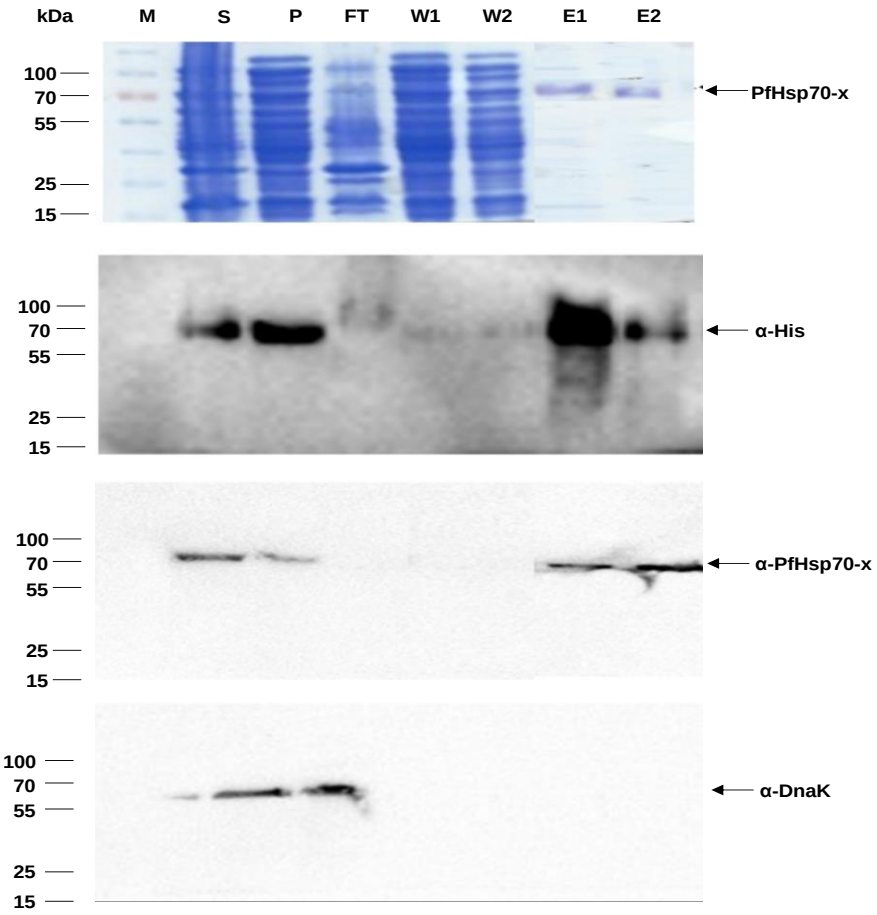

Fig 3.8 Purification of PfHsp70-x$_T$
Coomassie blue stained SDS-PAGE analysis (upper panel) and Western analysis (lower panels) of PfHsp70-x expressed from *E. coli* XL1 Blue using α-His and α–PfHsp70-x antibodies respectively. Lane M represents the molecular weight marker in kDa, S-supernatant fraction, P-pellet fraction, FT-flow through, W1-wash 1, W2-wash 2, E1-elution 1 and E2 –elution 2.

3.3.3 Purification of human Hop

The human Hop recombinant protein was successfully purified natively from the soluble fraction as most of the protein was detected from this source. The purification was confirmed by 12 % SDS-PAGE with subsequent confirmation using Western blotting (Fig 3.9). Western blotting was done using α-His antibodies and α-DnaK antibodies. Some of the recombinant protein did not bind to the beads and hence was detected in the flow through. Some protein was lost during the washing step although most of the protein was eluted successfully (Fig 3.9). The elutions were free of DnaK contamination as no DnaK was detected by Western blotting in these fractions as shown in (Fig 3.9)

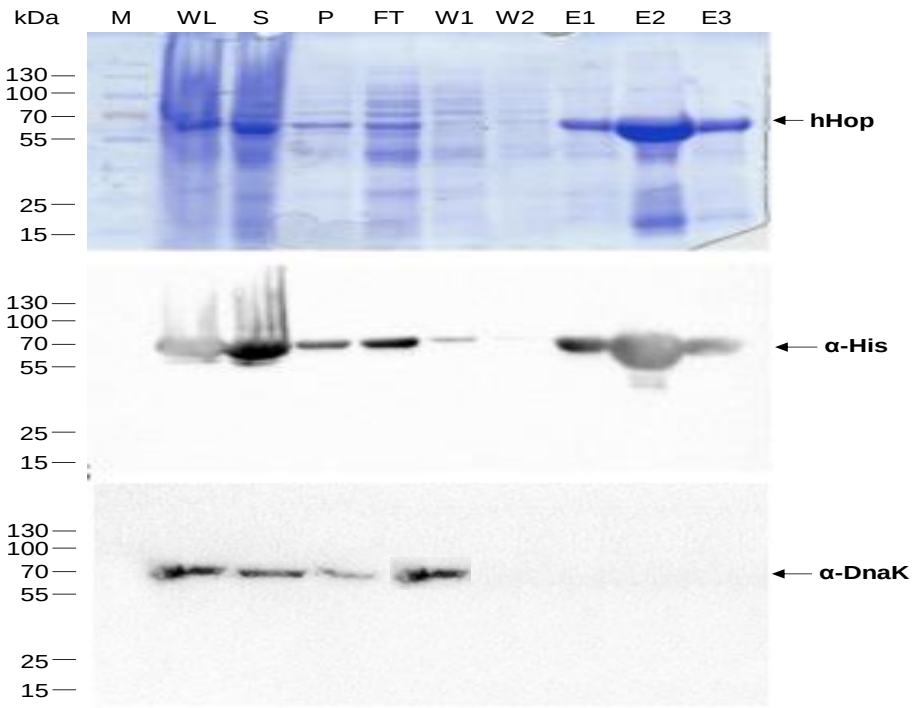

Fig 3.9 Purification of human Hop
Coomassie blue stained SDS-PAGE analysis (upper panel) and Western analysis (lower panels) of human Hop from *E. coli* JM109 cells using α-His antibodies. Lane M represents the molecular weight marker in kDa, WL-whole lysate,S-supernatant fraction, P-pellet fraction, FT-flow through, W1-wash 1, W2-wash 2, E1-elution 1, E2 –elution 2 and E3- elution 3.

3.4. Secondary structure analysis of PfHsp70-x

The secondary structure and thermal stability of PfHsp70-x recombinant protein were investigated by circular dichroism (CD) spectroscopy. The experimental CD spectra were attained using DICHROWEB with CDSSTR as the reference database (Fig 3.10A) (Sreerama and Woody, 2000; Whitmore and Wallace, 2008). The far-UV spectra exhibited two negative troughs at 209 nm and 221 nm representing the predominately alpha helical character of the recombinant protein (Fig 3.10A). The secondary structure of the protein was constituted by 51 % alpha helices, 17 % beta sheets and 37 % random coils. The recombinant protein was exposed to different temperatures ranging from 19 ^{o}C to 95 ^{o}C at the wavelength 221 nm. PfHsp70-x was found to be a heat stable protein as 50 % of the protein was still folded at 70 ^{o}C (Fig 3.10B).

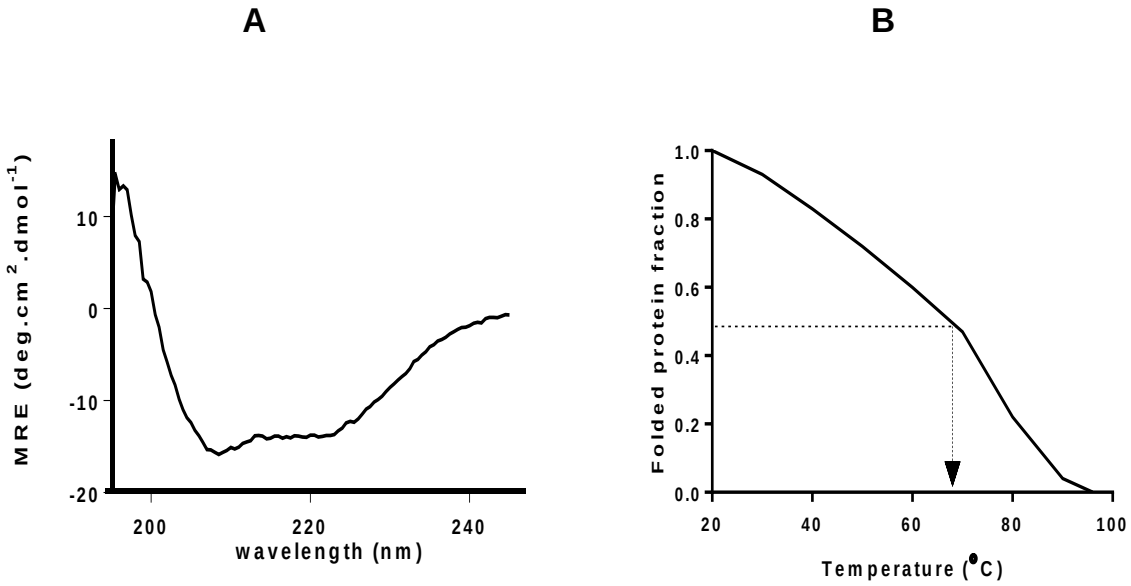

Fig 3.10 PfHsp70-x is predominantly alpha-helical and thermally stable
A. The UV spectra of recombinant PfHsp70-x protein. The CD spectrum of PfHsp70-x was presented as molar residue ellipticity (MRE). PfHsp70-x displays an alpha-helical conformation due to the negative troughs observed at 209 nm and 221 nm. **B**. The UV spectra of the folded fraction of the recombinant protein PfHsp70-x with varying temperature exposure. Readings were taken at 221 nm. About 50 % of the PfHsp70-x was still folded at approximately 70 °C

3.5.1 ATP equilibrium binding of PfHsp70-x and PfHsp70-x_T

PfHsp70-x and PfHsp70-x_T ATP binding affinities were determined using SPR analysis (Fig 3.11). The ATP affinity of the recombinant proteins was analyzed by equilibrium analysis (Fig 3.11). The equilibrium analysis was conducted on the SPR sensorgrams at steady state varying ATP concentrations as analyte on the recombinant proteins which were ligands. No response units were observed when BSA was used as control ligand, therefore, as expected BSA did not bind to the nucleotides. PfHsp70-x_T showed hundredfold lower ATP binding affinity compared to PfHsp70-x (Table 3.1).

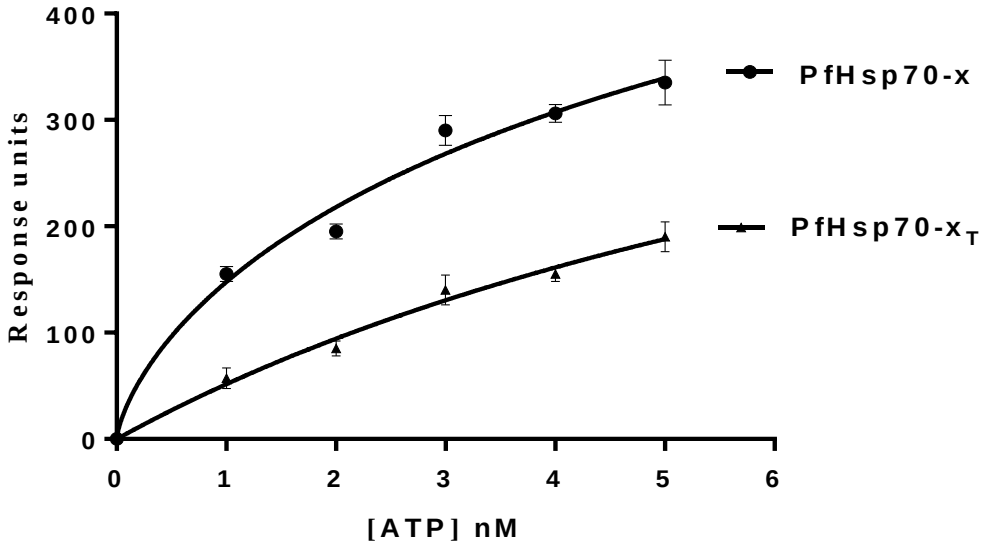

Fig 3.11 Equilibrium analysis of ATP-binding by PfHsp70-x and PfHsp70-x_T.
The data represents the equilibrium analysis of ATP-binding constants for both proteins. The equilibrium constant K_D was obtained for PfHsp70-x and PfHsp70-x_T. The analysis was conducted by plotting total response units from the association curves of PfHsp70-x and PfHsp70-x_T against ATP concentration. The standard deviations of at least three independent assays are shown.

Table 3.1: Comparative affinities of PfHsp70-x and PfHsp70-x_T for ATP binding

Ligand	ATP analyte
	K_D in µM (+/- std deviations)
PfHsp70-x	0.11 (+/- 0.03)
PfHsp70-x_T	11.2 (+/- 1.76)

Legend: Standard deviation shown are for at least three independent assays

3.5.2 PfHsp70-x exhibits basal ATPase activity

The ATPase activity of PfHsp70-x and PfHsp70-x_T were determined using a colorimetric assay (Zininga *et al.*, 2015). The concentrations of ATP were varied from 0 µM to 1000 µM. The Michaelis-Menten plots for PfHsp70-x and PfHsp70-x_T were determined for at least three independent batches of the recombinant proteins (Fig 3.12). Both PfHsp70-x and PfHsp70-x_T possess intrinsic ATPase activity (Fig 3.12). The determined K_m values are higher in PfHsp70-x_T suggesting that the recombinant protein has a lower affinity for ATP (Table 3.2). PfHsp70-x_T needs a higher concentration of ATP to reach V_{max} as compared to the PfHsp70-x recombinant protein. The V_{max} was calculated as 14.73 and 12.7 nmol/min/mg for PfHsp70-x and PfHsp70-x_T respectively (Table 3.2). The data suggest that the removal of the EEVN motif reduces the affinity of PfHsp70-x for ATP.

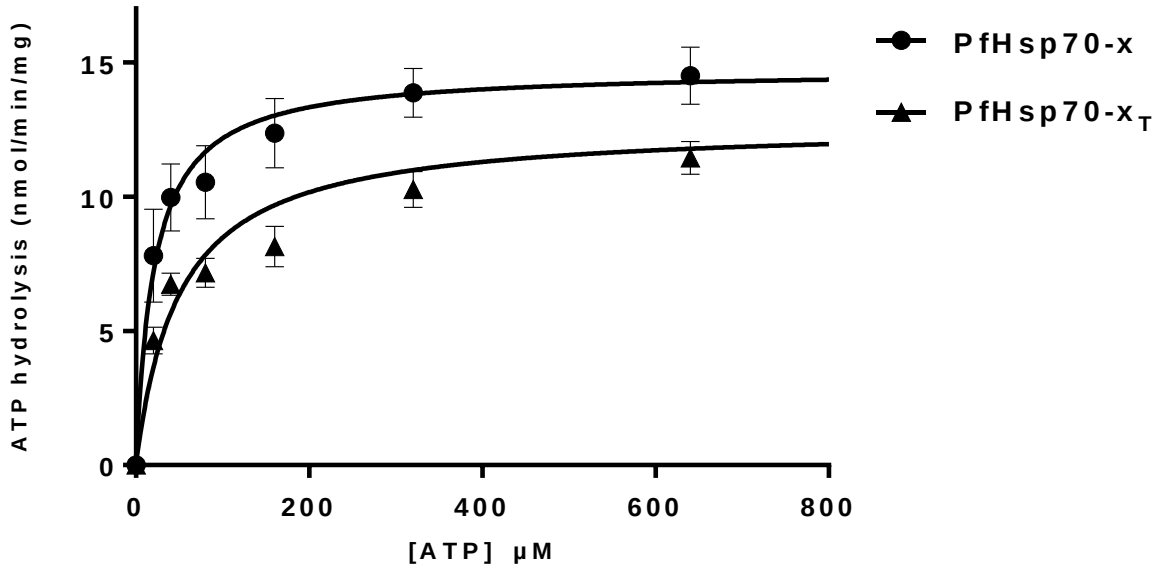

Fig 3.12. Analysis of the basal ATPase activity of PfHsp70-x
The inorganic phosphate released was monitored by direct calorimetry at 595 nm wavelength. The graphs show the basal ATPase activities of PfHsp70-x and PfHsp70-x_T expressed as mean (+/-) standard deviation. Error bars are indicated on each curve indicates statistical significance at $p < 0.05$ relative to basal ATPase value for respective chaperone using unpaired t-test.

Table 3.2: ATPase kinetics of PfHsp70-x

Protein	V_{max} (nmol/min/mg)	K_m (µM)	Reference
PfHsp70-x	14.70 (+/- 0.42)	21.4 (+/- 3.40)	This study
PfHsp70-x_T	12.70 (+/- 0.52)	50.0 (+/- 8.80)	This study
PfHsp70-x	17.20 (+/- 0.61)	393.0 (+/- 93.00)	(Cockburn *et al* 2014**)**
PfHsp70-x	12.80 (+/- 0.13)	ND	(Daniyan *et al* 2016)

Table legends: V_{max} – is the maximum rate of the catalysis reaction; K_m - is the substrate concentration at which the reaction rate is at half-maximum. ND, not determined. Standard deviations shown represent at least three independent assessment made using separate protein purification batches.

3.6.1. PfHsp70-x and PfHsp70-x_T suppressed heat-induced aggregation of luciferase and malate dehydrogenase (MDH)

The ability of PfHsp70-x to suppress heat-induced aggregation of model substrates luciferase and MDH were investigated by observing the change in turbidity of the respective reaction mixtures at 340 nm. Luciferase and MDH were observed to aggregate at 48 °C in the absence of chaperones (Appendix C1). The aggregation percentage was expressed relative to the aggregation of luciferase and MDH without the chaperone added. BSA was used as a negative control and its addition to the reaction mixture did not suppress the aggregation of luciferase and MDH. The heat stability of PfHsp70-x and PfHsp70-x_T was determined (Appendix C4). Both PfHsp70-x and PfHsp70-x_T protein displayed stability at 48 °C. The relative heat stability of both PfHsp70-x and PfHsp70-xT were comparable to one another (Appendix C5).

PfHsp70-x and PfHsp70-x_T displayed the capability to suppress the aggregation of luciferase and MDH in a concentration-dependent fashion (Fig 3.13A; B). The effect of nucleotides on the ability of PfHsp70-x and PfHsp70-x_T to suppress the aggregation of luciferase and MDH respectively was also investigated (Fig 3.13C; D). According to this data set, the presence of ADP showed no significant effect on the chaperoning ability of both PfHsp70-x and PfHsp70-x_T. However, the addition of ATP in the reaction mixture drastically increases the aggregation percentage of luciferase and MDH (Fig 3.13C; D, $p < 0.05$). The data suggests that removal of the EEVN motif had no effect on the chaperone activity of PfHsp70-x.

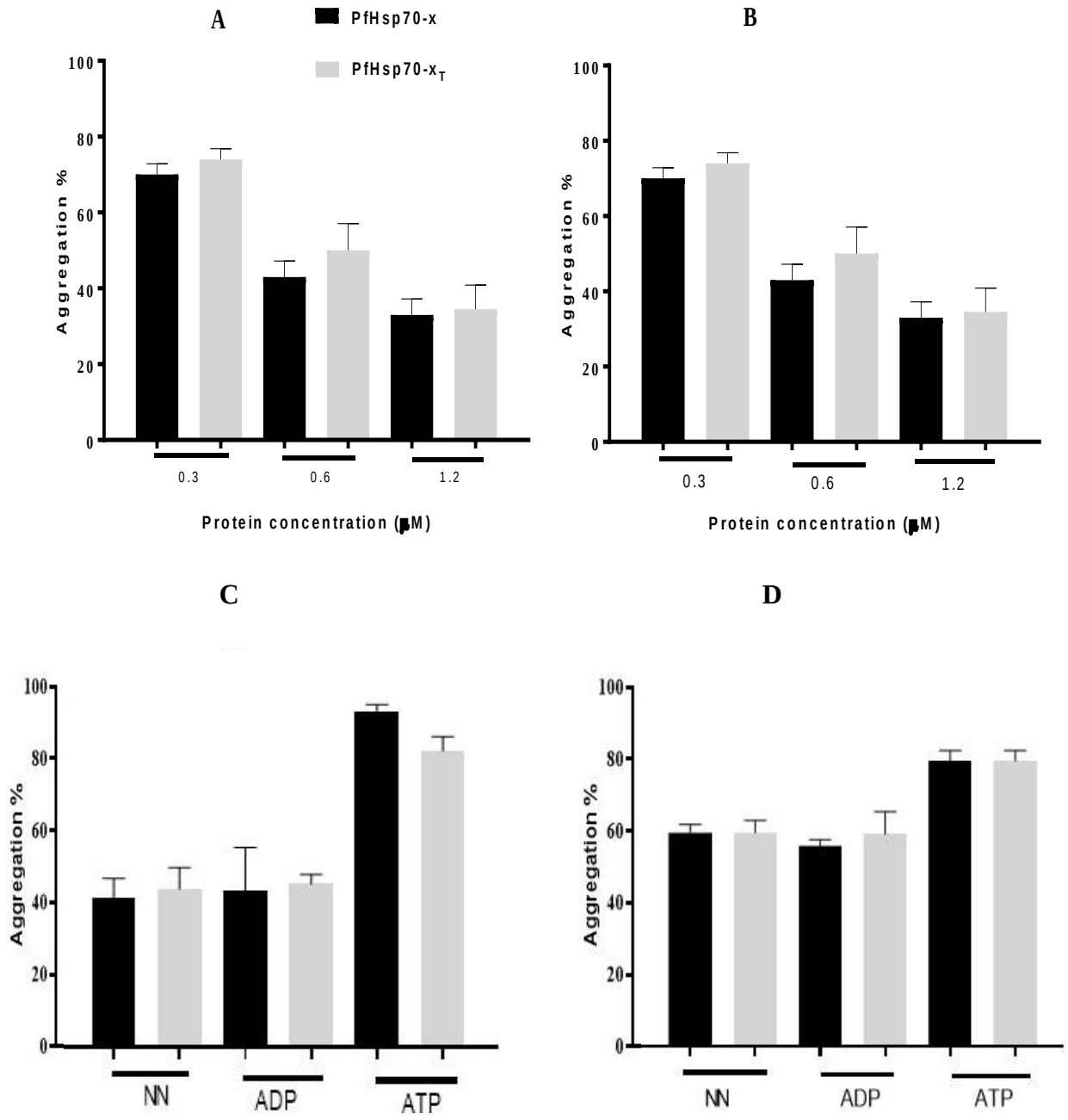

Fig 3.13 PfHsp70-x suppresses heat-induced aggregation of luciferase and malate dehydrogenase
The heat-induced aggregation of model substrates luciferase and MDH were monitored *in vitro* at a temperature of 50 °C at 340 nm. Both PfHsp70x and PfHsp70-x$_T$ showed concentration-dependent aggregation suppression of both luciferase and MDH (**A**, **B**). There was no significant difference in the aggregation suppression of PfHsp70-x and PfHsp70-x$_T$. The addition of 5 µM of ATP in the reaction mixture reduced the ability of the chaperones to suppress the heat-induced aggregation of model substrates. The addition of 5 µM ADP did not significantly change the ability of chaperones in suppression (**C**, **D**, $p < 0.05$). Standard deviations as shown by error bars were obtained from three independent replicate assays.

3.6.2. PfHsp70-x and PfHsp70-x_T associate with asparagine-rich peptides

The interaction of the PfHsp70-x/ PfHsp70-x_T and various peptides was further investigated by SPR analysis. The amino acid sequence of the peptides is shown (Table 3.3). The PfHsp70-x (Fig 3.14A) and PfHsp70-x_T (Fig 3.14B) had low-affinity kinetics for peptide 1 but a higher affinity for peptide 2 (Fig 3.14A, B). The association constants and dissociation constants are comparable in the presence of or absence of nucleotides although dissociation constants increase with the addition of ATP (Table 3.3). There was no significant difference in the K_D values of either PfHsp70-x or PfHsp70-x_T for peptide 2 (Table 3.3) and this shows the truncation of PfHsp70-x did not affect its chaperone activity of PfHsp70-x ($p < 0.05$).

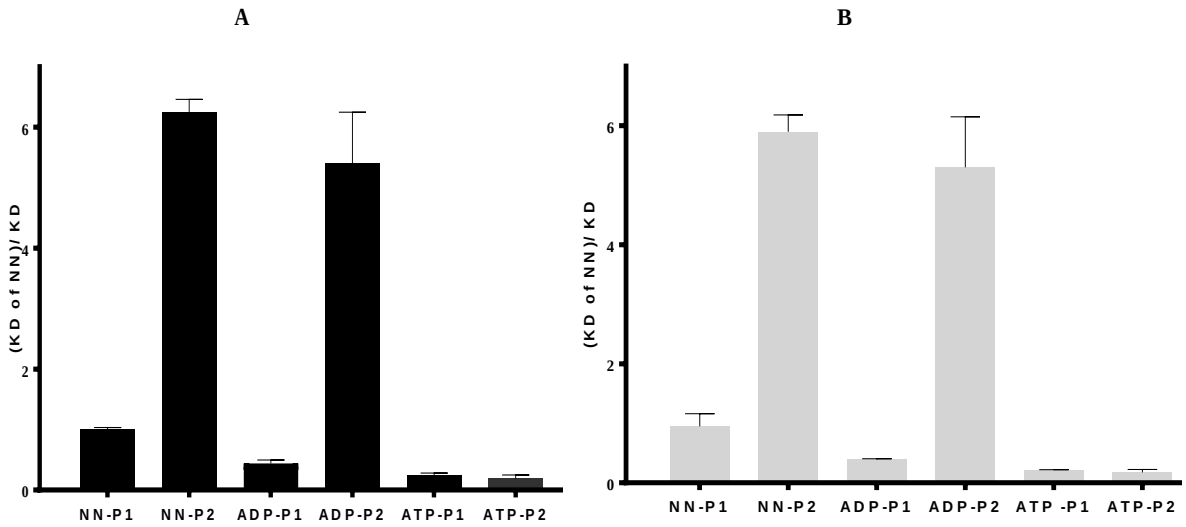

Fig 3.14 PfHsp70-x and PfHsp70-x_T associate with asparagine-rich peptides
A Relative affinity of PfHsp70-x for peptide 1 and peptide 2 in the presence of nucleotides. **B**: Relative affinity of PfHsp70-x_T for peptide 1 and peptide 2 in the presence of nucleotides. NN represents data obtained in the absence of nucleotides, the columns labeled ADP and ATP show the reactions into which a final concentration of 5 mM respective nucleotides was added. The relative affinities were normalized to PfHsp70-x full-length interaction with peptide 1 in the absence of nucleotides (NN). The error bars show the standard deviation about the mean. All comparison data was subjected to t-tests ($p < 0.05$).

The addition of ATP reduced the affinity kinetics of the chaperones to the peptides (Fig 3.14A, B). The addition of ADP, however, resulted in comparable affinity deduced in the nucleotide-free reaction (Table 3.3). This effect of nucleotides on these associations agrees with the phenomenon that Hsp70 release substrates when it is bound to ATP and binds to substrate with higher affinity in the ADP-bound state (Shonhai *et al*., 2008).

Table 3.3. Interaction kinetics of PfHsp70-x and peptide 1 and peptide 2

Ligand	Analyte	*ka* (1/ Ms)	*kd* (1/s)	K_D (M)	$\chi 2$
PfHsp70-x	Peptide 1 GFT**VVL**MYRF	4.03 (+/- 0.19) e^{2}	1.03 (+/- 0.40) e^{-5}	1.09 (+/- 0.10) e^{-7}	0.812
	Peptide 1 + ADP	3.53 (+/- 0.18) e^{2}	1.00 (+/- 0.14) e^{-5}	2.85 (+/- 0.20) e^{-7}	2.18
	Peptide 1 + ATP	1.11 (+/- 0.20) e^{2}	1.17 (+/- 0.44) e^{-4}	1.90 (+/- 0.12) e^{-6}	4.12
PfHsp70-x_T	Peptide 1 GFT**VVL**MYRF	2.48 (+/- 0.40) e^{1}	2.52 (+/- 0.34) e^{-6}	2.99 (+/- 0.10) e^{-7}	0.68
	Peptide 1 + ADP	1.14 (+/- 0.19) e^{2}	1.01 (+/- 0.22) e^{-5}	1.76 (+/-0.11) e^{-7}	2.36
	Peptide 1 + ATP	1.02 (+/- 0.16) e^{2}	1.01 (+/- 0.23) e^{-4}	1.10 (+/- 0.20) e^{-6}	5.91
PfHsp70-x	Peptide 2 GFT**NNN**MYRF	9.03 (+/- 0.34) e^{2}	1.28 (+/- 0.2) e^{-7}	2.40 (+/- 0.15) e^{-9}	0.89
	Peptide 2 + ADP	4.60 (+/- 0.15) e^{2}	1.01(+/- 0.23) e^{-7}	6.25 (+/- 0.80) e^{-9}	4.21
	Peptide 2 + ATP	2.54 (+/- 0.13) e^{2}	1.01 (+/- 0.11) e^{-5}	3.97 (+/-0.15) e^{-7}	2.58
PfHsp70-x_T	Peptide 2 GFT**NNN**MYRF	3.60 (+/- 0.34) e^{2}	1.01(+/- 0.14) e^{-7}	2.20 (+/-0.12) e^{-9}	1.37
	Peptide 2 + ADP	5.32 (+/- 0.45) e^{2}	1.01 (+/- 0.40) e^{-7}	1.40 (+/- 0.15) e^{-9}	3.10
	Peptide 2 + ATP	8.57 (+/- 0.14) e^{2}	1.00 (+/- 0.20) e^{-5}	5.17 (+/- 0.16) e^{-7}	1.87

The table shows the binding kinetics parameters of PfHsp70-x with peptide 1 and peptide 2. The association rate constant is represented by (*ka*), dissociation rate constants (*kd*), and the equilibrium constant which denotes the affinity represented by (K_D). PfHsp70-x was made the ligand and the peptides the analytes respectively. The ligand was the immobilized protein on the HTE chip surface, and the analyte was the respective peptide injected at a flow rate of 100 µl/min.

PfHsp70-x and PfHsp70-x_T have a low affinity for peptide 3 (amino acid sequence NR**LL**TG) but high affinities for peptide 4 (NR**NN**TG) (Fig 3.15A, B). There is no significant difference in the affinity for peptide 3 by PfHsp70-x and PfHsp70-x_T. Furthermore, there is no significant difference in affinity for peptide 4 by PfHsp70x and PfHsp70-x_T, suggesting that the EEVN motif does not regulate peptide binding (Fig 3.15A, B) (Table 3.3). The addition of ATP significantly reduced the affinity of the chaperones to the peptides (Fig 3.15A, B). This was expected as binding of ATP to

Hsp70s cause them to release substrates (Kabani, 2009). The reaction where ADP was added had comparable affinities in magnitude with the nucleotide-free reaction (Table 3.4).

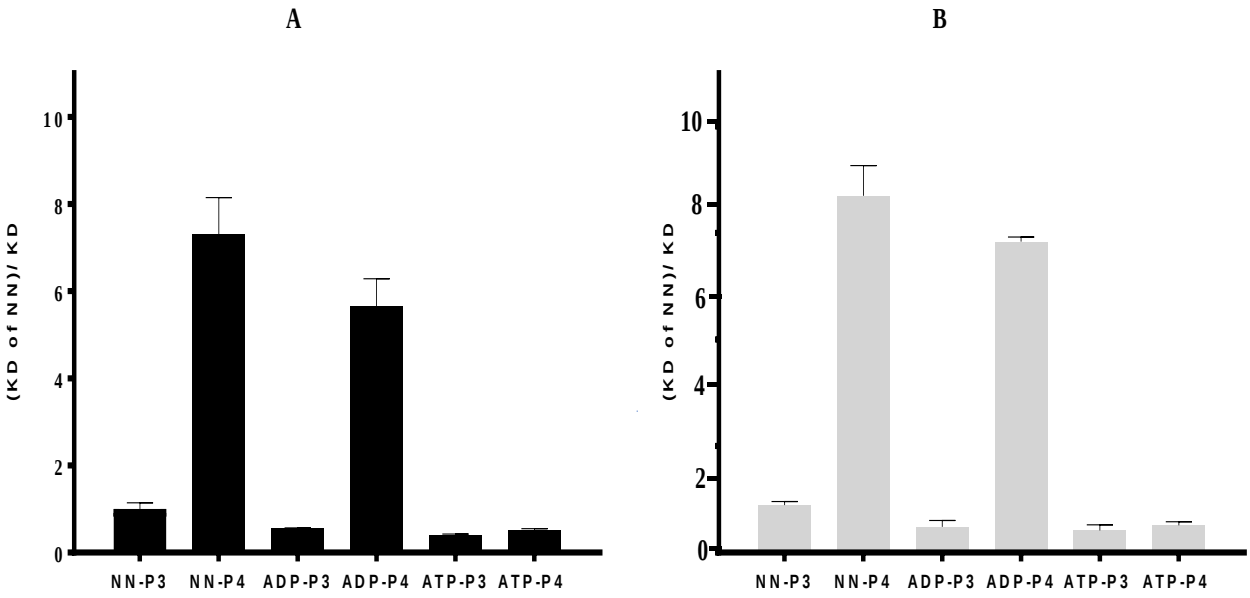

Fig 3.15 PfHsp70-x and PfHsp70-x_T associate with asparagine-rich peptides
(A) Relative affinity of PfHsp70-x for peptide 3 and peptide 4 in the presence of nucleotides. **(B):** Relative affinity of PfHsp70-x_T for peptide 3 and peptide 4 in the presence of nucleotides. NN represents the reaction with no nucleotides added, the columns labeled ADP and ATP show the reactions where a final concentration of 5 mM respective nucleotides was added. The relative affinities were normalized to PfHsp70-x full-length interaction with peptide 3 in the absence of nucleotides (NN). The error bars show the standard deviation about the mean. In general addition of nucleotides diminished the association of PfHsp70-x with the peptides. All comparison data were subjected to t-tests ($p< 0.05$).

Furthermore, the k_a values in the presence of nucleotides and absence of nucleotides are comparable in the association of either PfHsp70-x or PfHsp70-x_T with peptide 3 and 4 (Table 3.4). The dissociation of the formed complexes (k_d) was not affected by the addition of ADP in the reaction mixture. The dissociation of complexes was greater in the reactions where ATP was added (Table 3.4).

Table 3.4. Interaction kinetics of PfHsp70-x and peptide 3 and peptide 4

Ligand	Analyte	k_a (1/ Ms)	k_d (1/s)	K_D (M)	$\chi 2$
PfHsp70-x	Peptide 3 NR**LL**TG	3.86 (+/- 0.20)	9.97 (+/- 0.41) e^{-6}	2.50 (+/- 0.34) e^{-7}	0.98
	Peptide 3 + ADP	1.62 (+/- 0. 22)	1.01 (+/- 0.28) e^{-5}	6.20 (+/- 0.12) e^{-7}	4.38
	Peptide 3 + ATP	1.21 (+/- 0.23)	1.01 (+/- 0.13) e^{-5}	1.70 (+/- 0.30) e^{-6}	2.10
PfHsp70-x_T	Peptide 3 NR**LL**TG	3.15 (+/- 0.31)	8.67 (+/- 0.42) e^{-6}	2.80 (+/- 0.14) e^{-7}	0.24
	Peptide 3 + ADP	6.0 (+/- 0.51)	1.00 (+/- 0.21) e^{-5}	1.70 (+/- 0.34) e^{-7}	3.21
	Peptide 3 + ATP	3.18 (+/- 0.42) e^{1}	1.61(+/- 0.36) e^{-4}	1.80 (+/- 0.23) e^{-6}	2.37
PfHsp70-x	Peptide 4- NR**NN**TG	2.43 (+/- 0.45)	9.49 (+/- 0.27) e^{-9}	6.91 (+/- 0.43) e^{-11}	1.31
	Peptide 4+ADP	2.55 (+/- 0.23)	1.03 (+/- 0.41) e^{-9}	4.31 (+/- 0.30) e^{-11}	3.98
	Peptide 4+ATP	7.33 (+/- 0.22)	1.01 (+/- 0.31) e^{-6}	1.37 (+/- 0.20) e^{-7}	4.10
PfHsp70-x_T	Peptide 4- NR**NN**TG	3.52 (+/- 0.18)	2.79 (+/- 0.19) e^{-9}	7.92 (+/- 0.50) e^{-10}	1.56
	Peptide 4+ADP	5.96 (+/-0.1)	1.01 (+/- 0.31) e^{-9}	1.69 (+/- 0.30) e^{-10}	2.10
	Peptide 4-ATP	9.37 (+/-0.17)	1.01 (+/- 0.21) e^{-5}	1.07 (+/- 0.20) e^{-7}	3.91

The table shows the binding kinetics parameters of PfHsp70-x with peptide 3 and peptide 4. The association rate constant is represented by (*ka*), dissociation rate constants (*kd*), and the equilibrium constant which denotes the affinity represented by (K_D). PfHsp70-x was made the ligand and the peptides the analytes respectively. The ligand was the immobilized protein on the HTE chip surface, and the analyte was the respective peptide injected at a flow rate of 50 µl/min. The data is presented with plus/ minus standard deviations.

3.7. Slot blot based data for PfHsp70-x and human Hop association

The direct interaction of PfHsp70-x and human Hop was validated using the recombinant forms of the proteins. Immobilization of the recombinant proteins and controls were done onto a nitrocellulose membrane using the slot blotting technique (Zininga *et al*., 2016). The bait protein (human Hop), negative control (BSA), and PfHsp70-x recombinant proteins were immobilized onto a nitrocellulose membrane. Immunoblotting was done using α-PfHsp70-x antibodies and this was done to confirm the specificity of the antibody. The antibodies were specific for PfHsp70-x and there was no cross-reactivity with either BSA or human Hop protein (Fig 3.15A, B).

Furthermore, to ascertain the transfer of recombinant proteins onto the blot Western analysis was conducted using α-His antibodies. Both PfHsp70-x and human Hop were detected as these recombinant proteins were His-tagged (Fig 3.15C, D). The association of the recombinant proteins was investigated by overlaying the membrane with the prey protein (PfHsp70-x/PfHsp70-x_T). Afterward, Western blotting utilizing α-PfHsp70-x antibodies was conducted to detect if the PfHsp70-x/ PfHsp70-x_T bound to the immobilized human Hop. The band intensity was low on the blots overlaid with PfHsp70-x but slightly increased as the amount of human Hop immobilized on the membrane was also increased which suggest a concentration-dependent association. This suggests that PfHsp70-x interacted with human Hop. However, association between human Hop and PfHsp70-x_T was not observed (Fig 3.15E). The data showed that human Hop interacts with full-length PfHsp70-x and that the EEVN motif is essential for this association.

The assay was repeated in the presence nucleotides (ATP/ADP). The addition of ADP appeared to have increased the association of human Hop and PfHsp70-x but the addition of ATP abrogated the interaction (Fig 3.15E, F). The effect of the nucleotides on these associations was expected as it has been established that PfHsp70-1 and PfHop association is enhanced by ADP but abrogated by the presence of ATP (Zininga *et al*., 2015b).

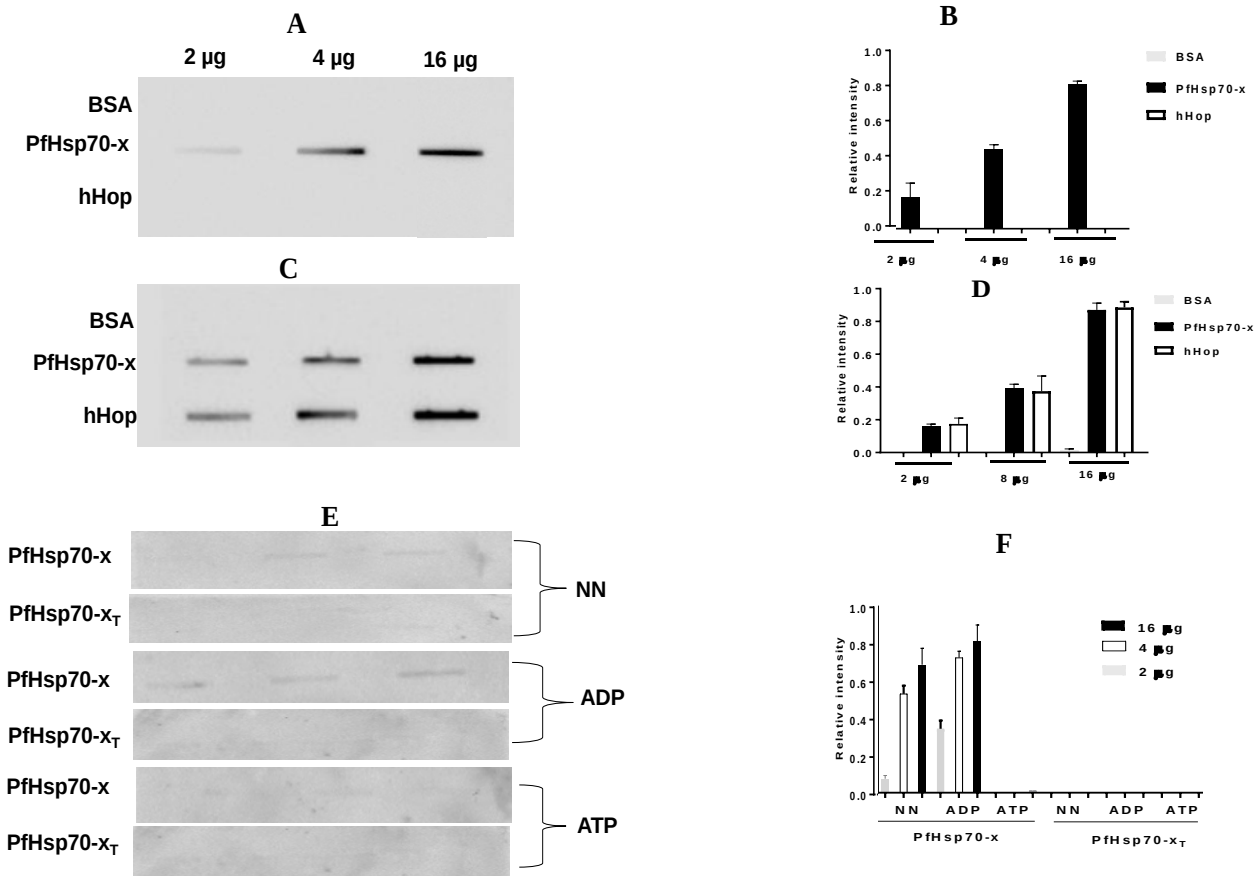

Fig 3.15 PfHsp70-x interacts with human Hop
A: α PfHsp70-x is specific to PfHsp70-x. **B**: Densitometric analysis of blot A. **C**: Analysis of the interaction of PfHsp70-x and human Hop. Immobilized human Hop was overlaid by PfHsp70-x/ PfHsp70-x_T. PfHsp70-x showed association with human Hop although PfHsp70-x_T did not. The experiment was repeated in the presence of 5 mM ADP and 5 mM ATP, no interactions were observed for PfHsp70-x_T and human Hop. The addition of ADP enhanced the interaction in the blot overlaid by PfHsp70-x and ATP abrogated these interactions. **D**: accompanying densitometric analysis of blots in **C**.

3.8. Confirmation of the interaction between PfHsp70-x and human Hop by SPR analysis

To further validate the association of PfHsp70-x/PfHsp70-x_T and human Hop, interaction kinetics and affinity analysis were conducted using SPR. PfHsp70-x associated with human Hop in a concentration-dependent fashion (Fig 3.16). BSA was used as a control and showed no association when it was injected over immobilized PfHsp70-x/PfHsp70-x_T.

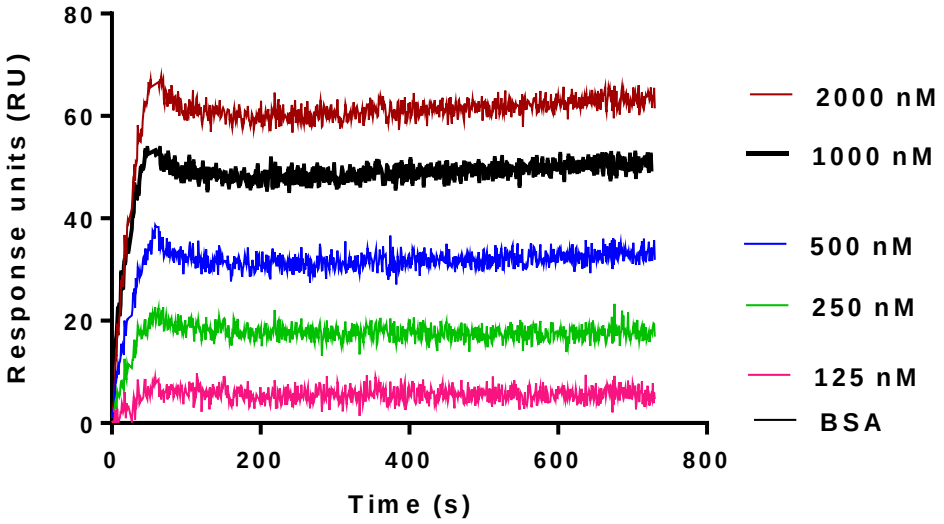

Fig 3.16 Representative SPR sensorgrams
The SPR sensorgrams showing a concentration-dependent association between PfHsp70-x immobilized on the chip and different ligands such as human Hop as well as peptides introduced in solution. The assay was performed in the absence of nucleotides then repeated in the presence of nucleotides namely ATP and ADP.

The SPR kinetics data was generated by analyzing the SPR sensorgrams (Table 3.5). The kinetics data for the associations were monitored for the association and the dissociation phases and hence association and dissociation constants were determined, respectively. Furthermore, the equilibrium constant (binding affinity) was also determined. The k_a shown describes the rate of complex formation between the ligand and analyte per second, k_d describes the stability of the complex thus formed and hence the fraction of the complex that decays in a second. In addition, K_D describes the ratio of the k_d/k_a. The association between PfHsp70-x/ PfHsp70-x_T and human Hop was comparable as it was in the same order of magnitude in the presence or absence of nucleotides (Table 3.5). The dissociation constant (k_d) between PfHsp70-x and human Hop was comparable in the absence of nucleotides and when ADP was added although it increased by 10-fold magnitude when ATP was added (Table 3.5). The rate of association was higher for PfHsp70-x than PfHsp70-x_T but dissociation was higher for PfHsp70-x_T compared to PfHsp70-x (Table 3.5). These factors explain the higher affinity that PfHsp70-x has for human Hop compared to PfHsp70-x_T.

Table 3.5 Interaction kinetics of PfHsp70-x and human Hop

Ligand	Analyte	*ka* (1/Ms)	*kd* (1/s)	K_D (M)	X^2
PfHsp70-x	human Hop-	4.30 (+/- 0.40) e^3	2.30 (+/- 0.35) e^{-5}	3.01 (+/- 0.15) e^{-8}	1.1
	human Hop +ADP	3.30 (+/- 0.12) e^3	3.70 (+/- 0.43) e^{-5}	2.31 (+/- 0.25) e^{-8}	1.31
	human Hop +ATP	3.47 (+/- 0.40) e^3	4.40 (+/- 0.36) e^{-4}	3.80 (+/- 0.35) e^{-7}	1.5
PfHsp70-x_T	human Hop-	2.47 (+/- 0.14) e^1	1.01 (+/- 0.22) e^{-5}	2.10 (+/- 0.12) e^{-6}	3.92
	human Hop+ADP	4.26 (+/- 0.54) e^1	2.10 (+/- 0.24) e^{-5}	1.66 (+/- 0.05) e^{-6}	1.09
	human Hop +ATP	5.41 (+/- 0.10) e^1	3.20 (+/- 0.14) e^{-4}	4.10 (+/- 0.13) e^{-5}	3.2

Table legends: ***ka*** is the association rate constant, ***kd*** dissociation rate constant, K_D equilibrium constant, X^2 is the chi-squared value correlation for SPR sensorgram fitting to the Langmuir model. Data is presented as mean plus/minus standard deviation.

PfHsp70-x associated with human Hop with relatively higher affinity as compared with PfHsp70-x_T (Fig 3.17). The association of PfHsp70-x with human Hop is in the nanomolar range suggesting a more stable interaction compared to the association of PfHsp70-x_T and human Hop which is in the micromolar range (Table 3.5). The binding affinity data showed that ATP abrogated the interaction of PfHsp70-x and human Hop while the addition of ADP is comparable to the K_D deduced in the nucleotide-free reaction (Table 3.5).

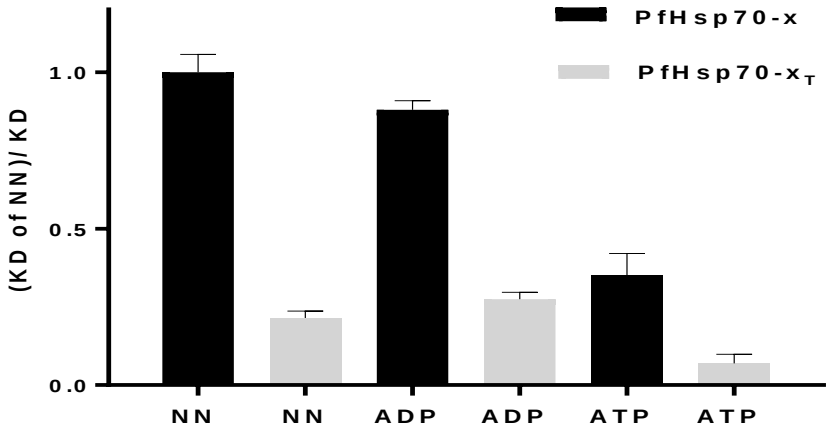

Fig 3.17 PfHsp70-x exhibits a higher affinity for human Hop than PfHsp70-x_T
NN represents the reaction with no nucleotides added, the columns labeled ADP and ATP show the reactions where a final concentration of 5 mM respective nucleotide was added. The error bars represent the standard deviation about the mean. PfHsp70-x associated with human Hop with higher affinity than PfHsp70-x_T in the absence or presence of nucleotides ($p< 0.05$) There was no significant difference in the association of PfHsp70-x with human Hop in the presence of ADP and in the nucleotide-free reaction (t-test at $p< 0.05$).

CHAPTER 4: DISCUSSION AND CONCLUDING REMARKS

P. falciparum is the most virulent of the species causing human malaria and has become increasingly resistant to traditionally used drugs. This warrants a need to develop novel strategies to control this parasite. Hsps form functional networks which are implicated in the development of parasite drug resistance. PfHsp70-x is exported to the cytosol of the parasite-infected erythrocyte. PfHsp70-x interacts with PFA066w an exported type II Hsp40 as a co-chaperone for the refolding of unfolded exported proteins in the infected erythrocyte cytosol (Daniyan *et al*., 2016). In addition, PfHsp70-x colocalizes in the parasite infected erythrocyte with human Hsp90 and human Hop. For this reason, PfHsp70-x could associate and cooperate with human Hsp90 via a human Hop mediated partnership. Therefore, the current study sought to establish if PfHsp70-x potentially interacts with human Hop.

In this study two bacterial strains; namely, *E. coli* JM109 and *E. coli* XL1 Blue cells were used to express human Hop and PfHsp70-x, respectively. The PfHsp70-x recombinant protein was successfully expressed (Fig 3.4). PfHsp70-x_T was successfully expressed as a species of approximately 76 kDa (Fig 3.5) although leaky expression was observed as the production of the recombinant proteins started before induction with IPTG. The leaky expression is caused by promoters, which are not tightly regulated, especially *lac* promoters (Rosano and Ceccarelli, 2014). The human Hop recombinant protein was also successfully expressed as a species of approximately 70 kDa although leaky expression also occurred (Fig 3.6). The leaky expression could result in toxicity to cells although this effect did not occur in all the expressions conducted.

The PfHsp70-x and PfHsp70-x_T recombinant proteins were purified from soluble fractions (Fig 3.7, 8). The protein yield of PfHsp70-x and PfHsp70-x_T was approximately 1 mg of protein per liter of culture. A study by Cockburn and colleagues, (2014) produced PfHsp70-x between 4-8 mg per liter of the culture. The relatively lower yields of proteins could have occurred because some of the protein aggregated (Fig 3.7, 8) and some protein was lost in the washing steps (Fig 3.7). The difference in the protein yield produced could be attributed to the different expression systems used to express the protein in the respective studies. The current study expressed PfHsp70-x in *E. coli* XL1 Blue cells while Cockburn and colleagues expressed the recombinant protein in *E. coli*

M15[pRep4] cells. The pQE30/human Hop plasmid also resulted in successful purification with a high yield of the protein of at least 2 mg of protein per liter of culture. (Fig 3.9). Contamination by DnaK is a common problem in the purification of Hsp70s as the size of DnaK is similar to the Hsp70s (Rial and Ceccarelli, 2002). To avoid confounding results in this study, the washes done during purification of recombinant proteins (section 2.4) had 5 mM ATP to wash the DnaK from the column to reduce the chances of DnaK contamination in the elutions. The elutions were extensively dialyzed to eliminate the ATP after purifications. Furthermore, the recombinant proteins were immunoblotted with α-DnaK antibody and no contamination was found (Fig 3.7, 8, 9).

This study also sought to investigate the secondary structure and thermal stability of PfHsp70-x. The far-UV spectra exhibited a positive peak centered at 194 nm and two troughs at 209 and 221 nm, respectively (Fig 3.10A). This spectrum represents the predominantly α-helical character of the recombinant protein. The protein displayed thermal stability as 50 % of the recombinant protein remained folded when it was heated to approximately 70 ℃ (Fig 3.10B). PfHsp70-z is more heat stable than PfHsp70-x as 50 % of the recombinant protein was folded at 80 ℃ (Zininga *et al*., 2015a). This is the first study to report on the heat stability of PfHsp70-x. Its thermal stability demonstrates its characteristic of being an independent chaperone. Heat shock proteins maintain other proteins in a competent folding state during stress and hence should be thermally stable themselves (Shonhai *et al*., 2007).

Equilibrium state ATP binding studies by SPR revealed that PfHsp70-x protein had a higher affinity for ATP than PfHsp70-x_T (Fig 3.11) (Table 3.1). This implies that the EEVN motif of PfHsp70-x could enhance the affinity of PfHsp70-x for ATP. Some studies suggested that ATP binding is important for chaperone activity (Shaner *et al*., 2004; Hrizo *et al*., 2007). Therefore PfHsp70-x is capable of binding and hydrolyzing ATP which suggests that the recombinant protein could be an independent chaperone. The basal ATPase activity was also investigated. This assay demonstrated that PfHsp70-x hydrolyses ATP faster than PfHsp70-x_T (Table 3.2). The basal ATPase activity of PfHsp70-x in this study concurs with the study done by Daniyan and colleagues, (2016) which showed comparable V_{max} values (Table 3.2).

The ability of PfHsp70-x and PfHsp70-x_T to suppress the heat-induced aggregation of model substrates was investigated. Both PfHsp70-x and PfHsp70-x_T were able to suppress the heat-induced aggregation of MDH and luciferase (Fig 3.13A, B). There was no significant difference in the aggregation suppression of luciferase and MDH by PfHsp70-x and PfHsp70-x_T in comparison (Fig 3.13A, B $p< 0.05$). The data suggests that the EEVN motif is not essential for the chaperone function of PfHsp70-x. The presence of ADP showed no effect on the chaperoning ability of both PfHsp70-x and PfHsp70-x_T. (Fig 3.13C, D). This was was expected as Shonhai and colleagues, (2008) reported that ADP did not affect the chaperone function of PfHsp70-1. The presence of ATP in the reaction mixture inhibits the association of the PfHsp70-x with the substrates making the latter available for heat-induced aggregation. The findings of this study were in line with those of Cockburn and colleagues (2014), which demonstrated the independent chaperoning ability of PfHsp70-x. The findings of this study also concur with a study by Zininga and colleagues (2016) which suggested dose response independent capabilities of PfHsp70-1 and PfHsp70-z in suppressing the heat-induced aggregation of MDH and luciferase.

The ability of PfHsp70-x binding to peptide substrates was further investigated by SPR analysis. It is known that asparagine repeat regions in *P. falciparum* proteins increase their natural tendency to aggregate (Mularidharan *et al*., 2012). Heat shock protein 70s as they are chaperones would associate with such proteins as substrates to prevent their aggregation. In this study, both PfHsp70-x and PfHsp70-x_T selectively associated with asparagine-rich peptides implying that the PfHsp70-x chaperone may bind preferentially to *P. falciparum* proteins within the erythrocyte cytosol. The presence of ADP did not affect these interactions (Fig 3.15; Table 3.3). The presence of ATP reduces the affinity of PfHsp70-x to the peptide substrates. This characteristic is expected as most Hsp70s have a low substrate affinity when bound to ATP. This study suggests that the EEVN motif is not a requirement for PfHsp70-x to bind to substrates.

The major focus of this study was to explore possible functional cooperation between PfHsp70-x and human Hop. This functional complex could be a potential drug target as it may be important for the refolding of exported *P. falciparum* proteins. The α-PfHsp70-x antibodies were specific only to the PfHsp70-x protein (Fig 3.15A). Slot blot data reveals that there was interaction between PfHsp70-x and human Hop but no interactions was established between PfHsp70-x_T and human

Hop (Fig 3.15C). Furthermore, these interactions were confirmed by SPR analysis. SPR data suggested that PfHsp70-x associated with human Hop with greater affinity which was in the nanomolar range as compared to the association between PfHsp70-x_T and human Hop which was in the micromolar range (Table 3.5). This study suggests that the EEVN motif could be necessary for the interaction as PfHsp70-x_T showed lower affinity for human Hop as compared to PfHsp70-x ($p< 0,05$). The addition of ADP does not affect the affinity of these proteins. The addition of ATP never-the-less abrogated these interactions (Fig 3.15). These findings concur with a study by Zininga and colleagues (2015) which reported that PfHop associated with PfHsp70-1 in a nucleotide-dependent fashion demonstrated by this study.

The prospects of PfHsp70-x associating with human Hsp90 via human Hop in the infected erythrocyte cytosol could be further investigated as the current study provided the first direct evidence of the physical association of PfHsp70-x and human Hop through slot blot and SPR technique. This study also provided evidence that removal of the EEVN motif of PfHsp70-x does not interfere with its chaperone function. However, the data confirms that the EEVN motif is important for the Hop-Hsp70 association. Colocalization studies could be conducted to establish interacting partners of both PfHsp70-x and human Hop within the erythrocyte which could be targeted for antimalarial drug design.

References

Ali, M. M, Roe, S. M, Vaughan, C. K, Meyer, P, Panaretou B, Piper, P. W. (2006) Crystal structure of an Hsp90-nucleotide-p23/Sba1 closed chaperone complex. *Nature*, 440: 1013-1017.

Allan, R. K, Ratajczak, T. (2011) Versatile TPR domains accommodate different modes of target and adaptation of chaperone function. *Cell Stress Chaperones,* 3: 28-36.

Banumathy, G, Singh, V, Pavithra, S. R, Tatu, U. (2002) Host chaperones are recruited in membrane-bound complexes by *Plasmodium falciparum. J Biol Chem,* 277: 3902–3912.

Banumathy, G, Singh, V, Pavithra, S. R, Tatu, U. (2003) Heat shock protein 90 function is essential for *Plasmodium falciparum* growth in human erythrocytes. *J Biol Chem,* 278: 18336- 18345.

Bascos, N. A. D and Landry, S. J. (2015) Structural rigidity regulates functional interactions in the Hsp40-Hsp70 molecular machine. *Biophys J,* 108: 210.

Beck, J. R, Muralidharan, V, Oksman, A, Goldberg, D. E. (2014) PTEX component HSP101 mediates export of diverse malaria effectors into host erythrocytes. *Nature,* 511: 592–595 55.

Billker, O, Shaw, M. K, Margos, G, Sinden, R. E. (1997) The roles of temperature, pH and mosquito factors as triggers of male and female gametogenesis of *Plasmodium berghei in vitro*. *Parasitol,* 115: 1-7.

Bimston, D, Song, J, Winchester, D, Takayama, S, Reed, J. C, Morimoto, R. I. (1998) BAG-1, a negative regulator of Hsp70 chaperone activity, uncouples nucleotide hydrolysis from substrate release. *EMBO J,* 17: 6871–6878.

Botha, M, Chiang, A. N, Needham, P. G, Stephens, L. L, Hoppe, H. C, Külzer, S, Przyborski, J. M, Lingelbach, K, Wipf, P, Brodsky, J. L, Shonhai, A, Blatch, G. L. (2011) *Plasmodium falciparum* encodes a single cytosolic type I Hsp40 that functionally interacts with Hsp70 and is upregulated by heat shock. *Cell Stress Chaperones,* 16: 389–401.

Botha, M, Pesce, E-R, Blatch, G. L. (2007) The Hsp40 proteins of *Plasmodium falciparum* and other apicomplexan: regulating chaperone power in the parasite and the host. *Int J Biochem,* 39: 1781–1803.

Bousema, T and Drakeley, C. (2011) Epidemiology and infectivity of *Plasmodium falciparum* and *Plasmodium vivax* gametocytes in relation to malaria control and elimination. *Clin Microbiol Rev,* 24: 377-410.

Bozdech, Z, Llinás, M, Pulliam, B. L, Wong, E. D, Zhu, DeRisi J. L. (2003) The transcriptome of the intraerythrocytic developmental cycle of *Plasmodium falciparum*. *PLoS Biol,* 1: 85-100.

Buchberger, A, Theyssen, H, Schröder, H, McCarty, J. S, Virgallita, G, Milkereit, P, Reinstein, J, Bukau, B. (1995) Nucleotide-induced conformational changes in the ATPase and substrate binding

domains of the DnaK chaperone provide evidence for interdomain communication. *J Biol Chem*, 270: 16903–16910.

Bukau, B, Weissman, J and Horwich, A. (2006) Molecular chaperones and protein quality control. *Cell*, 125: 443-449.

Centers for disease control and prevention (CDC). (2012) Division of parasitic diseases and malaria, Available from http://www.cdc.gov/malaria/about/biology. (Accessed 18 February 2015).

Centers for disease control and prevention (CDC). (2016) The impact of malaria, Available from https://www.cdc.gov/malaria/malaria_worldwide/impact.html. (Accessed 12 January 2016).

Cheetham, M. E, Caplan, A. J. (1998) Structure, function, and evolution of DnaJ: conservation and adaptation of chaperone function. *Cell Stress Chaperones*, 3: 28-36.

Cockburn, I. L, Boshoff, A, Pesce, E and Blatch, G. L (2014) Selective modulation of Plasmodial Hsp 70s by small molecules with anti-malarial activity. *Biol Chem*, 395: 1437-4315.

Cockburn, I. L, E-R. Pesce, J. M. Pryzborski, M. T. Davies-Coleman and P. G. K. Clark, P. G, Keyzers, R. A, Stephens, L. L, Blatch, G. L. (2011) Screening for small molecule modulators of Hsp70 chaperone activity using protein aggregation suppression assays: Inhibition of the plasmodial chaperone PfHsp70-1. *Biol Chem*, 392: 431-438.

Cowman, A. F and Crabb, B. S. (2002) The *Plasmodium falciparum* genome – a blue print for erythrocyte invasion. *Science*, 298: 126-128.

Craig, E. A, Haung, P, Aron, R, Andrew, A (2006) The diverse roles of J proteins, the obligate Hsp70 chaperone. *Rev Physiol Biochem Pharmacol*, 156: 1- 21.

Crompton, P. D, Pierce, S. K, Miller, L. H. (2010) Advances and challenges in malaria vaccine development. *J Clin Invest*, 120:l 4168-78.

Daniyan, M. O, Boshoff, A, Prinsloo, E, Pesce, E. R, Blatch, G. L. (2016) The Malarial Exported PFA0660w Is an Hsp40 Co-Chaperone of PfHsp70-x. *PLoS ONE*,11: e0148517.

de Koning-Ward, T. F, Gilson, P. R., Boddey, J. A, Rug, M, Smith, B. J, Papenfuss, A. T. (2009) A newly discovered protein export machine in malaria parasites. *Nature*, 459: 945–949.

Deponte, M, Hoppe, H, C, Lee, M. C, Maier, A. G, Richard, D, Rug, M. (2012) Where ever I may roam: protein and membrane trafficking in *Plasmodium. falciparum*-infected red blood cells. *Mol Biochem Parasitol*, *186*:95–116.

Dragovic, Z, Broadley, S. A, Shomura, Y, Bracher, A, Hartl, F. U. (2006) Molecular chaperones of the Hsp110 family act as nucleotide exchange factors of Hsp70s. *EMBO J*, 25: 2519-2528.

Fan, C.-Y, Lee, S, Cyr, D. M. (2003) Mechanisms for regulation of Hsp70 function by Hsp40. *Cell Stress Chaperones*, 8: 309–316.

Fançony, C, Brito, M, Gil, J. P. (2016) *Plasmodium falciparum* drug resistance in Angola. *Malar J*, 15: 74.

Favaloro, J. M, Coppel, R. L, Corcoran, L. M, Foote, S. J, Brown, G. V, Anders, R.F and Kemp D.J (1986) Structure of the RESA gene of *Plasmodium falciparum*. *Nucleic Acids Res*, 14: 8265–8277.

Flaherty, K. M, Deluca-Flaherty, C, McKay, D. B. (1990) Three-dimensional structure of the ATPase fragment of a 70K heat-shock cognate protein. *Nature*, 346: 623–628.

Fujioka, H, Aikawa, M. (2002). Structural and life cycle. In: *Malaria and parasite and disease*, functional specificity. *Nat Rev Mol Cell Biol*, 11: 579–592.

Gitau, G.W, Mandal, P, Blatch, G.L, Przyborski, J, Shonhai, A. (2012) Characterization of the *Plasmodium falciparum* Hsp70-Hsp90 organizing protein (PfHop). *Cell Stress Chap*, 17: 191-202.

Goel, S, Muthusamy, A, Miao, J, Cui, L, Salanti, A, Winzeler, E.A, Gowda, D.C. (2014) Targeted disruption of a ring-infected erythrocyte surface antigen (RESA)-like export protein gene in *Plasmodium falciparum* confers stable chondroitin 4-sulfate cytoadherence capacity. *J Biol Chem*, 289: 34408-21.

Grover, M, Chaubey, S, Ranade, S and Tatu U. (2013) Identification of an exported heat shock protein 70 in *Plasmodium falciparum*. *Parasite*, 20: 1123-1132.

Hajj, G, N. M, Arantes, C. P, Dias M. V. S. (2013) The unconventional secretion of stress-inducible protein 1 by a heterogeneous population of extracellular vesicles. *Cell Mol Life Sci*, 70: 3211–3227.

Hartl, F. U, Bracher, A and Hartl-Hayer, M. (2011) Molecular chaperones in protein folding and proteostasis. *Nature*, 475: 324- 332.

Hartl, F.U and Hayer-Hartl, M. (2002) Molecular chaperones in the cytosol: from nascent chain to folded protein. *Science*, 295: 1852-1858.

Heiber, A, Kruse, F, Pick, C, Grüring, C, Flemming, S. (2013) Identification of new PNEPs indicates a substantial non-PEXEL exportome and underpins common features in *Plasmodium falciparum* protein export. *PLOS Pathogens* 9: e1003546.

Hernández, M. P, Sullivan, W. P, and Toft, D. O. (2002) The assembly and intermolecular properties of the Hsp70–Hop–Hsp90 molecular chaperone complex. *J Biol Chem.* 277: 38294–38304.

Hennessy, F, Nicoll, W. S, Zimmermann, R, Cheetham, M. E, Blatch, G. L (2005) Not all J domains are created equal: implications for the specificity of Hsp40-Hsp70 interactions. *Protein Sci*, 14: 1697– 1709.

Hiller, N. L, Bhattacharjee, S, van Ooij, C, Liolios, K, Harrison, T, Lopez-Estrano, C, Haldar, K. (2004) A host-targeting signal in virulence proteins reveals a secretome in malarial infection. *Science*, 306: 1934–1937.

Hrizo, S.L, Gusarova, V, Habiel, D. M, Goeckeler, J. L, Fisher, E. A, Brodsky, J. L. (2007) The Hsp110 molecular chaperone stabilizes apolipoprotein B from endoplasmic reticulum-associated degradation (ERAD). *J Biol Chem*, 282: 32665-32675.

Ingolia, T. D, Craig, E. A. (1982) Four small Drosophila heat shock proteins are related to each other and to mammalian -crystallin. *Proc Natl Acad Sci*, 79: 2360-2364.

Johnson J, L, and Brown, C. (2009) Plasticity of the Hsp90 chaperone machine in divergent eukaryotic organisms. *Cell Stress Chaperones*, 14: 83–94.

Kabani, M. (2009) Structural and functional diversity among eukaryotic Hsp 70 nucleotide exchange factors. *Protein Pept Lett*, 16: 623-660.

Kabani, M., Martineau, C. N. (2008) Multiple Hsp70 isoforms in the eukaryotic cytosol: mere redundancy or functional specificity? *Curr Genomics*, 9: 338–248.

Kampinga, H. H, Hageman, J, Vos, M. J, Kubota, H, Tanguay, R. M, Bruford, E, Cheetham, M.E, Chen, B., Hightower, L. E. (2009) Guidelines for the nomenclature of the human heat shock proteins. *Cell Stress Chaperones*, 14: 105–111.

Kampinga, H. H, Craig, E. (2010). The Hsp70 chaperone machinery: J proteins as drivers of functional specificity. *Nat Rev Mol Cell Biol*, 11: 579–592.

Kim, Y. E, Hipp, M. S, Bracher, A, Haye-Hartl, M and Hartl, F. U. (2013) Molecular chaperone functions in protein folding and proteostasis. *Annu Rev Biochem*, 82: 323-355.

Kityk, R., Kopp, J., Sinning, I., Mayer, M. P. (2012) Structure and dynamics of the ATP-bound open conformation of Hsp70 chaperones. *Mol Cell*, 48: 863–874.

Krukenberg, K. A, Street, T. O, Lavery, L. A, Agard, D. A. (2011) Conformational dynamics of the molecular chaperone Hsp90. *Quart Rev Biophy*, 44: 229- 255.

Külzer, S, Rug, M, Brinkmann, K, Cannon, P, Cowman, A, Lingelbach, K. (2010) Parasite-encoded Hsp40 proteins define novel mobile structures in the cytosol of the *P. falciparum*-infected erythrocyte. *Cell Microbiol*, 12: 1398–1420.

Külzer, S., Charnaud, S., Dagan, T., Riedel, J., Mandal, P., Pesce, E. R. (2012) *Plasmodium falciparum*-encoded exported hsp70/hsp40 chaperone/co- chaperone complexes within the host erythrocyte. *Cell. Microbiol,* 10: 141784–1795.

Laplante, A, Moulin, V, Auger, F, Landry, J, Li, H, Morrow, G. (1998) Expression of heat shock proteins in mouse skin during wound healing. *J Histochem Cytochem,* 46: 1291- 1301.

Laufen, T, Mayer, M. P, Beisel, C, Klostermeier, D, Reinstein, J and Bukau, B. (1999) Mechanism of regulation of Hsp70 chaperones by DnaJ co-chaperones. *Proc Natl Acad Sci USA,* 96: 5452–5457.

Li, J and Buchner, J. (2013) Structure, Function and regulation of the Hsp90 machinery. *Biomed J,* 36: 106-117.

Li, Z and Srivasta K. (2004) Heat shock proteins. *Curr Protoc Immunol,* 10: 1002- 1011.

Lindquist, S. And Craig, E.A. (1988). The heat shock proteins. *Annual Review of Genetics*, 22: 631-677.

Maier, A.G, Rug, M, O'Neill, M.T, Brown, M, Chakravorty, S, Szestak, T. (2008) Exported proteins required for virulence and rigidity of *Plasmodium falciparum*-infected human erythrocytes. *Cell* 134**:** 48–61.

Makumire, S, Chakravadhanula, V. S. K, Köllische G, Redel, E, Shonhai, A. (2014) Immunomodulatory activity of zinc peroxide (ZnO2) and titanium dioxide (TiO_2) nanoparticles and their effects on DNA and protein integrity. *Toxicol Lett*, 227: 56–64.

Marti, M, Good, R. T, Rug, M, Knuepfer, E and Cowman A. F. (2004) Targeting malaria virulence and remodeling proteins to the host erythrocyte. *Science*, 306: 1930–1933.

Matambo, T. S, Odunuga, O. O, Boshoff, A, Blatch, G. L. (2004) Overproduction, purification, and characterization of the *Plasmodium falciparum* heat shock protein 70. *Protein Expr Purif*, 33: 214–222.

Mayer, M. P. (2013) Hsp70 chaperone dynamics and molecular mechanism. *Trends Biochem Sci*, 38: 507–514.

Mayer, M. P, Brehmer, D, Gassler, C. S. and Bukau, B. (2001) Hsp70 chaperone machines. *Adv Protein Chem*, 59: 1-44.

Mayer, M. P, Schröder, H, Rüdiger, S, Paal, K, Laufen, T, Bukau, B. (2000) Multistep mechanism of substrate binding determines chaperone activity of Hsp70. *Nat Struct Biol,* 7: 586-593.

Mayer, M. P. (2010) Gymnastics of molecular chaperones. *Mol Cell*, 39: 321–331.

Mayer, M. P and Bukau, B. (2005) Hsp70 chaperones: cellular functions and molecular mechanism. *Cell Mol Life Sci*, 62: 670-684.

McClellan, A.J, Xia, Y, Deutschbauer, A. M, Davis, R. W, Gerstein, M, Frydman, J. (2007) Diverse cellular functions of the Hsp90 molecular chaperone uncovered using systems approaches. *Cell*, 131: 121-35.

Misra, G, Ramachandran, R. (2009) Hsp70-1 from *Plasmodium falciparum*: protein stability, domain analysis, and chaperone activity. *Biophys Chem*, 142: 55-64.

Morrissette, N. S and Sibley, L. D. (2002) Cytoskeleton of apicomplexan parasites. Microbiology *Mol Biol Rev*, 66: 21-38.

Muralidharan, V, Oksman, A, Pal, P, Lindquist, S, Goldberg, D. E. (2012) *Plasmodium falciparum* heat shock protein 110 stabilizes the asparagine repeat-rich parasite proteome during malarial fevers. *Nat Commun*, 3:1310.

Murphy, M. E. (2013). The Hsp70 family and cancer. *Carcinogenesis*, 34: 1181–1188.

Nathan, D. F, Vos M. H, Lindquist, S. (1997) *In vivo* functions of the *saccharomyces cerevisiae* Hsp90 chaperone. *Proc Natl Acad Sci* 94: 12949-56.

Nicolet, C. M, Craig, E. A. (1989) Isolation and characterization of STI1, a stress-inducible gene from *Saccharomyces cerevisiae*. *Mol Cell Biol*, 9: 3638–3646.

Nicoll, W.S, Botha, M, McNamara, C, Schlange, M, Pesce, E-R, Boshoff, A, Ludewig, M. H, Zimmerman, R, Cheetham, M. E, Chapple, J. P. and Blatch, G. L. (2007) Cytosolic and ER J-domains of mammalian and parasitic origin can functionally interact with DnaK. *Int J Biochem and Cell Bio*, 39: 736-751.

Njunge, J. M, Ludewig, M. H, Boshoff, A, Pesce, E, Blatch, G. L. (2013) Hsp70s and J proteins of *Plasmodium* parasites infecting rodents and primates: structure, function, clinical relevance, and drug targets. *Curr Pharm Des*, 19: 387-403.

Njunge, J. M, Mandal, P, Przyborski, J. M, Boshoff, A, Pesce, E.-R, Blatch, G. L. (2015) PFB0595w is a *Plasmodium falciparum* J protein that co-localizes with PfHsp70-1 and can stimulate its in vitro ATP hydrolysis activity. *Int J Biochem Cell Biol*, 62: 47–53.

Nyalwidhe, J, Lingelbach, K. (2006) Proteases and chaperones are the most abundant proteins in the parasitophorous vacuole of *Plasmodium falciparum*-infected erythrocytes. *Proteomics*, 6: 1563-1573.

Onuoha, S. C, Coulstock, E. T, Grossmann, J. G and Jackson, S. E. (2008) Structural Studies on the Co-chaperone Hop and Its Complexes with Hsp90. *J Mol Biol*, 379: 732–744.

Packschies, L, Theyssen, H, Buchberger, A, Bukau, B, Goody, R. S, Reinstein, J. (1997) GrpE accelerates nucleotide exchange of the molecular chaperone DnaK with an associative displacement mechanism. *Biochemistry,* 36: 3417–3422.

Pallavi, R, Archarya, P, Chandran, S, Daily, J.P, Tatu, U. (2010) Chaperone expression profiles correlate with distinct physiological states of *Plasmodium falciparum* in malaria patients. *Malar J*, 9: 236.

Patury, S, Miyata, Y, Gestwicki, J. E. (2009) Pharmacological targeting of the Hsp70 Chaperone. *Curr Top Med Chem*, 9: 1337-1351.

Pelle, K.G, Jiang, K. H, Xiao, Y. P, Marti, M. (2015) Shared elements of host-targeting pathways among apicomplexan parasites of differing lifestyles. *Cell. Microbiol*, 17: 1618-1639.

Ratheesh, K. R, Nagarajan, N. S, Arunraj, S. P, Devanjan, Sinha, Vinoth, B. R, Vinoth, K. E and D'Silva, P. (2012) HSPIR: a manually annotated heat shock protein information resource. *Oxford journals*, 28: 2853-2855.

Ratzke, C, Mickler, M, Hellenkamp, B, Buchner, J, Hugel, T. (2010) Dynamics of heat shock protein 90 C-terminal dimerization is an important part of its conformational cycle. *Proc Natl Acad Sci* 107: 16101-16106.

Raviol, H, Sadlish, H, Rodriguez, F, Mayer, M. P, Bukau, B. (2006) Chaperone network in the yeast cytosol: Hsp110 is revealed as an Hsp70 nucleotide exchange factor. *EMBO J,* 25: 2510–2518.

Retzlaff, M, Hagn, F, Mitschke, L, Hessling, M. Gugel, F. Kessler, H, Richter, K. Buchner, J. (2010) Asymmetric activation of the hsp90 dimer by its co-chaperone aha1, *Mol Cell*, 37: 344–354.

Rhiel, M, Bittl1, V, Tribensky, A, Charnaud, S. C, Strecker, M, Müller, S, Lanzer, M, Sanchez, C, Külzer, S, Przyborski, J. M. (2016) Trafficking of the exported *P. falciparum* chaperone PfHsp70-x. *Scie rep*, 6: 36174.

Rial, D.V. and Ceccarelli, E. A. (2002) Removal of DnaK contamination during fusion protein purifications. *Prot Exp Puri*, *25*: 503-507.

Röhl, A, Wengler, D, Madl, T, Lagleder, S, Tippel, F, Herrmann, M, Hendrix, J, Richter, K, Hack, G, Schmid, A.B, Kessler, H, Lamb, D.C. Buchner, J. (2015) Hsp90 regulates the dynamics of its co-chaperone Sti1 and the transfer of Hsp70 between modules. *Nat Commun*, 6: 6655.

Rosano, G. L and Ceccarelli, F. A. (2014) Recombinant proteinexpression in E. coli: anvances and challenges. *Front Microbiol*, 5: 172.

Rug, M, Cyrklaff, M, Mikkonen, A, Kuelzern, S. (2014) Export of virulence proteins by malaria-infected erythrocytes involves remodeling of host actin cytoskeleton. *Blood*, 124: 3459- 3468.

Saibil, H. (2013) Chaperone machines for protein folding, unfolding and disaggregation. *Nat Rev Mol Cell Biol,* 14*: 630–642.*

Sargeant, T. J, Marti, M, Caler, E, Carlton, J. M, Simpson, K, Speed, T. P, and Cowman, A. F. (2006) Lineage-specific expansion of proteins exported to erythrocytes in malaria parasites. *Gen Bio*, 7: 654-676.

Scheufler, C, Brinker, A, Bourenkov, G, Pegoraro, S, Moroder, L, Bartunik, H, Hartl, F. U, Moarefi, I. (2000) Structure of Tpr domain-peptide complexes: critical elements in the assembly of the Hsp70-Hsp90 multi-chaperone machine. *Cell*, 101: 199–210.

Schmid, A. B, Lagleder, S, Grawert, M. A. (2012) The architecture of functional modules in the Hsp90 co-chaperone Sti1/Hop. *Embo J*, 31: 1506- 1517.

Senczuk, A. M, Reeder, J. C, Kosmala, M. M, Ho, M. (2001) *Plasmodium falciparum* erythrocyte membrane protein 1 functions as a ligand for P-selectin. *Blood*, 98: 3132-3135.

Shaner, L, Trott, A, Goeckeler, J. L, Brodsky, J. L, Morano, K. A. (2004) The function of the yeast molecular chaperone Sse1 is mechanistically distinct from the closely related Hsp70 family. *J Biol Chem*, 279: 21992–22001.

Sharma, Y. D. (1992) Structure and possible function of heat-shock proteins in *Plasmodium falciparum*. *Comp Biochem Physiol*, 102: 437–444.

Shonhai, A, Maier, A. G, Przyborski, J. M and Blatch G. L. (2011) Intracellular Protozoan Parasites of Humans: The Role of Molecular Chaperones in Development and Pathogenesis, *Prot Pept Lett*, 18: 143-157.

Shonhai, A. (2010) Plasmodial heat shock proteins: targets for chemotherapy, *FEMS Immunol Med Microbiol*, 589: 61- 67.

Shonhai, A. (2014) Role of Hsp70s in development and pathogenicity of plasmodium species: In Shonhai A, Blatch G, Editors. Heat Shock Proteins of Malaria, Springer New York; pp 47– 70.

Shonhai, A, Botha, M, de Beer, T. A. P, Boshoff, A, Blatch, G. L. (2008) Structure-function study of *Plasmodium falciparum* Hsp70 using three dimensional modelling and in-vitro analyses. *Protein Pept Lett*, 15: 1117-1125.

Shonhai, A., Boshoff, A., Blatch, G. L. (2007) The structural and functional diversity of Hsp70 proteins from *Plasmodium falciparum*. *Protein Sci*, 16: 1803-1818.

Siligardi, G, Hu, B, Panaretou B. (2004) Co- chaperone regulation of conformational switching in the ATPase cycle. *J Biol Chem*, 279: 51989- 51998.

Silva, M. D, Cooke, B. M, Guillotte, M, Buckingham, D. W, Sauzet, J. P, Le Scanf, C, Contamin, H, David, P, Mercereau-Puijalon, O and Bonnefoy, S. (2005) A role for the *Plasmodium*

falciparum RESA protein in resistance against heat shock demonstrated using gene disruption. *Mol Microbiol,* 56: 990–1003.

Singh, G. P, Chandra, B. R, Bhattacharya, A, Akhouri R. R, Singh, S. K, Sharma, A. (2004b) Hyper-expansion of asparagines correlates with an abundance of proteins with prion-like domains in *Plasmodium falciparum*. *Mol Biochem Parasitol,* 137: 307-319.

Song, Y, Wu, Y. X, Jung, G, Tutar, Y, Eisenberg, E., Greene, L. E, Masison, D. C. (2005) Role for Hsp70 chaperone in *Saccharomyces cerevisiae* prion seed replication. *Eukaryot Cel,* 4: 289-300.

Sreerama, N, Venyaminov, S. Y, Woody, R. W. (2000) Estimation of protein secondary structure from circular dichroism spectra: inclusion of denatured proteins with native proteins in the analysis. *Anal Biochem*, 287: 243–251.

Spielmann, T and Gilberger, T. (2015) Critical steps in protein export of *Plasmodium falciparum* Blood stages. *Trens in Parasitology,* 10: 514-525.

Street, T. O, Lavery, L. A, Agard, D. A. (2011) Substrate binding drives large-scale conformational changes in the hsp90 molecular chaperone, *Mol. Cell* 42: 96–105.

Swain, J.F, Dinler, G, Sivendran, R, Montgomery, D. L, Stotz, M, and Gierasch, L. M. (2007) Hsp70 chaperone ligands control domain association via an allosteric mechanism mediated by the interdomain linker. *Mol Cell*, 26: 27–39.

Szabo A, Langer, T, Schröder, H, Flanagan, J, Bukau, B. Hartl, F.U. (1994) The ATP hydrolysis-dependent reaction cycle of the *Escherichia coli* Hsp70 system—DnaK, DnaJ, and GrpE. *Proc Natl Acad Sci USA*, 91: 10345–10349.

Tarr, S. J. and Osborne, A. R. (2015) Experimental determination of the membrane topology of the *Plasmodium* protease Plasmepsin V. *PLoS ONE* 10, e0121786.

Tsai, J. And Douglas, M.D. (1996) A conserved HPD sequence of the J-domain is necessary for YDJ1 stimulation of Hsp70 ATPase activity at a site distinct from substrate-binding. *J Biochem*, 271: 9347-9354.

Vali, S, R. Pallavi, S, Tatu, U. 2010 Virtual prototyping study shows increased ATPase activity of Hsp90 to be the key determinant of cancer phenotype. *Syst Synthetic Biol*, 4: 25-33.

Vogel, M, Mayer, M. P, Bukau, B. (2006) Allosteric regulation of Hsp70 chaperones involves a conserved interdomain linker. *J Biol Chem*, 281: 38705–38711.

Walsh, P, Bursac, D, Law, Y. C, Cry, D and Lithgow, T. (2004) The J-protein family: modulating protein assembly, disassembly and translocation. *EMBO Rep,* 5: 567–571.
Wellems, T, Plowe, C, (2001) Chloroquine-resistant malaria. *J Infect Dis*, 184: 770–776.

Whitesell L, Lindquist S. L. (2005) HSP90 and the chaperoning of cancer. *Nat Rev Cancer*, 5:761–772.

Whitmore L, Wallace B. A. (2008) Protein secondary structure analyses from circular dichroism spectroscopy: methods and reference databases. *Biopolymers*, 89: 392–400.

World Health Organization (WHO). (2016) World Malaria Report. Available from http://www.who.int/malaria/publications/world-malaria-report-2016/report/en/. (Accessed 23 January 2017).

Yamamoto, S, Subedi, G. P, Hanashima, S. (2014) ATPase Activity and ATP-dependent conformational change in the co-chaperone HSP70/HSP90-organizing protein (HOP). *J Biol Chem*, 289: 9880–9886.

Zhang, P, Leu, J. I.-J, Murphy, M. E, George, D. L, Marmorstein, R. (2014) Crystal structure of the stress-inducible human heat shock protein 70 substrate-binding domain in complex with a peptide substrate. *PloS ONE*, 9: e103518.

Zhao, R, Davey, M, Hsu, Y. C, Kaplanek, P, Tong, A, Parsons, A. B. (2005) Navigating the chaperone network: An integrative map of physical and genetic interactions mediated by the Hsp90 chaperone. *Cell*, 120: 715-27.

Zhuravleva, A, and Gierasch, L.M. (2011) Allosteric signal transmission in the nucleotide -binding domain of 70-kDa heat shock protein (Hsp70) molecular chaperones. *Proc Natl Acad Sci U S A*, 108: 6987–6992.

Zininga, T, Achilonu, I, Hoppe, H, Prinsloo, E, Dirr, H. W, Shonhai, A. (2016) *Plasmodium falciparum* Hsp70-z, an Hsp110 homologue, exhibits independent chaperone activity and interacts with Hsp70-1 in a nucleotide-dependent fashion. *Cell Stress Chap*, 21: 499–513.

Zininga, T, Achilonu, I, Hoppe, H, Prinsloo, E, Dirr, H. W, Shonhai, A. (2015a) Overexpression, Purification and Characterization of the *Plasmodium falciparum* Hsp70-z (PfHsp70-z) Protein, *PLOS ONE*, 10: e0129445

Zininga, T, Makumire, S, Gitau, G. W, Njunge, J. M, Pooe, O. J, Klimek, H, Scheurr, R, Raifer, H, Prinsloo, E, Przyborski, J. M, Hoppe, H, Shonhai, A. (2015b) *Plasmodium falciparum* Hop (PfHop) interacts with the Hsp70 chaperone in a nucleotide-dependent fashion and exhibits ligand Selectivity. PloS ONE, 10: e0135326.

Zininga, T, Shonhai, A. (2014) Are heat shock proteins druggable candidates? *Am J Biochem Biotechnol*, 10: 211- 213.

APPENDIX A: SPECIAL REAGENTS

Table A: Special chemical reagents

Name of reagents	Supplier
Agarose	Merck
Ammonium persulphate	Sigma-Aldrich
Ampicillin	Calbiochem
Chemiluminescence Western blotting kit	Amersham
2-mercaptoethanol	Merck
Bovine serum albumin	Melford
Bromophenol blue	Merck
Calcium chloride	Merck
Coomassie brilliant blue R250	Merck
Ethidium bromide	Merck
Glacial acetic acid	Merck
Glycerol	Merck
Glycine	Merck
Imidazole	Merck
Lambda DNA	Fermantas Life sciences
Lysozyme	Merck
Methanol	Merck
Magnesium chloride	Merck
Monoclonal mouse anti-His antibody	Merck
Phenylmethylsulfonyl fluoride	Merck
Polyacrylamide	Merck

Ponceau S	Sigma-Aldrich
Restriction enzymes	Merck
Sodium chloride	Merck
Sodium dodecyl sulfate	Merck
Sodium hydroxide	Merck
TEMED	Sigma-Aldrich
Tris	Merck
Tryptone	Oxoid, England
Tween 20	Radchem
Yeast	Merck
Broth	Merck
Nutrient agar	Merck
Glucose	Merck
Protein ladder	Fermantas life sciences

APPENDIX B: GENERAL EXPERIMENTAL PROCEDURES

B1 Preparation of *E. coli* JM109/ *E. coli* XL1 Blue competent cells

Chemical competent cells were made for the purpose of transformation with a construct vector which would express the desired recombinant proteins. Glycerol stocks of *E. coli* JM109 cells and were streaked using the continuous streaking method under flame conditions to avoid aerobic microbial contamination. Streaking was done on (2 X YT agar). These cell lines were incubated for 16-24 hours at 37 ℃. Inoculation was done by picking a single colony from the plate and transferring into 5ml double strength yeast-tryptone broth (2 X YT broth) (1 % (w/v) yeast, 1.6 % (w/v) tryptone and 0.5 % (w/v) sodium chloride). The inoculum was incubated at 37 ℃ for 16-24 hours. The cells were diluted (1/10) in 2 X YT broth and allowed to grow to mid-log phase (A_{600} between 0.3 – 0.6). The cells were harvested and centrifuged at 5000 g for 10 minutes at 4 ℃. Chemical treatment of the cells followed by resuspension of the pellet in 0.1 M $MgCl_2$ and subsequent incubation ice for 30 minutes. Proceeding centrifugation as described before resuspension of the pellet fraction was done by adding 0.1 M $CaCl_2$ followed by incubation on ice for 8 hours. After incubation, centrifugation was repeated and resuspension of the pellet was done in a 3ml of each mixture of 0.1 M $CaCl_2$ and 30 % glycerol. Cells were stored in aliquots at -80 ℃. The procedure was repeated with the making of chemical competent *E. coli* XL1 Blue cells.

B2 Extraction of plasmid DNA

Plasmid DNA was extracted using Zyppy™ Plasmid Miniprep Kit following provided manufacturer's instructions.

B3 Agarose gel electrophoresis

A concentration of 0.8 % agarose gel was prepared by adding 1.2 g of agarose into 150 ml of 1X TAE (45 mM Tris pH 8, 45 mM acetic acid, 1 mM ethylenediaminetetraacetic acid [EDTA]). Microwaving was done to ensure complete dissolving. The solution was allowed to cool and 0.5 ug/ml ethidium bromide was added. The contents were slowly poured into the gel casting tray with

a pre-placed comb. The gel was solidified by cooling at room temperature for 20 minutes. After polymerization, the combs were removed and the casting tray was placed in the electrophoresis chamber prior filled by 1X TAE buffer. After addition of prepared samples (Appendix B4) into the wells, the gel was run at 100 volts for an hour and then visualized using UV light (GeneGenius Bioimaging System (Syngene), USA).

B4 Restriction digest of Plasmid DNA

Plasmid DNA was subjected to fast digest restriction enzymes *Bam* H1 and *Hind* III. The samples were incubated at 37 °C for 15 minutes. The samples were prepared as shown in the table below. The 2 µl DNA samples contained approximately (1 µg DNA). The digestion reaction was stopped by adding the loading dye (0.25 %) bromophenol blue and 30 % glycerol).

TABLE B1: Reaction mixture for restriction digest

Components	Tube 1 Control (uncut)	Tube 2 *Bam*HI	Tube 3 *Hind*III	Tube 4 *Bam*HI & *Hind*III
DNA	1 µg	1 µg	1 µg	1 µg
dH_2O	16 µl	14 µl	15 µl	13 µl
Buffer	2 µl	2 µl	2 µl	2 µl
R/Enzyme	--	2 units	1 unit	2 units& 1 unit
Loading dye	4 µl	4 µl	4 µl	4 µl
Total vol (µl)	20	20	20	20

B5 Transformation of competent cells

An aliquot of 100 µl of the competent cells was thawed and 2 µl (approximately 1 µg) of plasmid DNA was added prior incubation on ice for 30 minutes. Thereafter heat shocking at 42 °C for 50 seconds was done and subsequent incubation on ice for 10 minutes. A volume of 900 µl of fresh 2YT broth was added and incubation at 37 °C for one hour with gentle agitation followed. Thereafter the cells were streaked on 2YT plates containing 100 µg/ml of ampicillin which was to

act as a selection marker for successful transformants. These cells were incubated at 37 °C overnight.

B6 Sodium dodecyl sulphate-polyacrylamide gel electrophoresis (SDS-PAGE) analysis

Prior boiling at 100 °C on a heating blog for 10 minutes for the purpose of denaturing, the protein was mixed with SDS sample buffer (0.25 % coomassie brilliant blue (R250); 2 % SDS; 10 % glycerol (v/v); 100 mM Tris;1 % β-mercaptoethanol) in a ratio of 4:1 respectively. Proceeding the denaturing process, the samples were resolved on a 12 % SDS-PAGE gel prepared as shown in table A2. The gel was then transferred into the electrophoresis tank containing electrophoresis buffer (25 mM Tris, 250 mM glycine and 0.1 % (w/v) SDS, pH 8.3). The boiled samples were loaded in respective wells and pre-stained protein molecular weight markers (ThermoFisher Scientific, USA) were also loaded. The gel was run at 120 volts for 90 minutes utilizing the Bio-Rad Mini protein electrophoresis system (Biorad, U.S.A).

Table B3 Preparation of SDS PAGE

Reagent (ml)	5 % Stacking gel	12 % Separating gel
30 % Bis/acrylamide 2.08	0.235	2.08
1.0 M Tris (pH 6.8)	0.437	-
1.5 M Tris (pH 8.8)	-	1.25
10 % SDS	0.0175	0.05
Distilled water	1.05	1.58
10 % Ammonium persulphate	0.00875	0.025
TEMED	0.0020	0.0020

B7 Western blotting

Proteins are initially resolved by SDS-PAGE analysis (Appendix B6) and the unstained gel and the nitrocellulose membrane was incubated in Western transfer buffer (25 mM Tris, 192 mM and 20 % methanol) for 15 minutes. One of the pre-wetted Whatman filter papers were then put on the positive plate of the trans-blotter. The pre-wetted nitrocellulose membrane was then placed on the filter paper, followed by placement of the gel on the nitrocellulose membrane and lastly covering with another pre-wetted filter paper. The negative plate was placed on top of the filter to make a sandwich. The trans-blotter was run at 100 V, 3 A, for 10 minutes. After transfer, the blots were blocked with 5 % milk in TBS (20 mM Tris, pH 7.5, 500 mM NaCl) for an hour. Anti-PfHsp70-x primary antibodies were used to incubate the blot for 1hr with gentle shaking. Washing was done thrice with TBS-Tween for 10 minutes each time. Incubation was done with secondary rabbit raised antibodies for 1hour with gentle shaking. Proceeding washing as done with primary antibody visualization was done with chemiluminescence substrates (Thermoscientific) using the Chemidoc imager (Biorad, USA).

B8 Determination of protein concentration using Bradford's assay

Protein concentration was determined using Bradford's reagent (Sigma-Aldrich, USA). The principle of this process is based on the formation of a complex between the dye, Brilliant Blue G, and proteins in solution. The absorption of the solution at 595 nm is proportional to the amount of proteins present. Standards in the range 0.1- 1.4 mg/ml of bovine serum albumin (BSA) were prepared. The Bradford reagent in the bottle was mixed and brought to room temperature. 5ul of the buffer (PBS) (137 mM NaCl, 27 mM KCl, 4.3 mM Na_2HPO_4 and 1.4 mM KH_2PO_4) was added to the wells assigned as blanks. The addition of 5 µl of the protein standards to separate wells in the 96 well plates was done. The unknown sample(s) were prepared with an approximate concentration between 0.1 –1.4 mg/ml. To each well being used, 250 µl of the Bradford reagent was added and mixed on a shaker for approximately 30 seconds. Incubation was done at room temperature for 5 – 45 minutes. The absorbance was measured at 595 nm using a UV-Vis spectrophotometer. The concentrations of the proteins were determined by comparing the net absorbance at wavelength 595 nm values against the standard curve obtained.

B9 Determination of protein concentration

The protein concentration of the recombinant proteins was determined using an online website (http://christophleidig.de/tprot.html) which computes the following parameters to determine protein concentration.

A: Absorbance at 280 nm
c: concentration (mol/l)
d: cuvette length (cm)
ε: extinction coefficient (L/mol x cm)
M: molecular unit (g/mol)
m: mass (g)
n: quantity (mol)

These parameters used in the Christoph Leidig calculator are obtained from the web site (http://web.expasy.org) (Accessed 14 February 2016)

B10 Determination of molar residue ellipticity in CD spectroscopy

For the analysis of CD spectroscopy data CD spectrum ellipticity units from the CD spectrometer was converted to molar residue ellipticity using the following formulae:

$[\theta] = (100 \times \theta) / CMR \times l$ Equation 1

$CMR = c \times N$ Equation 2

Where $[\theta]$: molar residue ellipticity ($deg.cm^2/ dmol$)

100: constant converting path length in meters

θ: ellipticity (mdeg)

l: cuvette path length

CMR: mean residue concentration

Protein concentration (mol)

N: number of amino acids in the protein

B11 BioRad HTE chip activation and regeneration protocol

Conditioning of the HTE sensor chip, pre-concentration of ligand and immobilization of ligand (Appendix B6) and stabilization was done according to manufacturer's instructions BioRad bulletin 6414.

APPENDIX C: Supplementary data

C1 Bradford's Assay standard curve

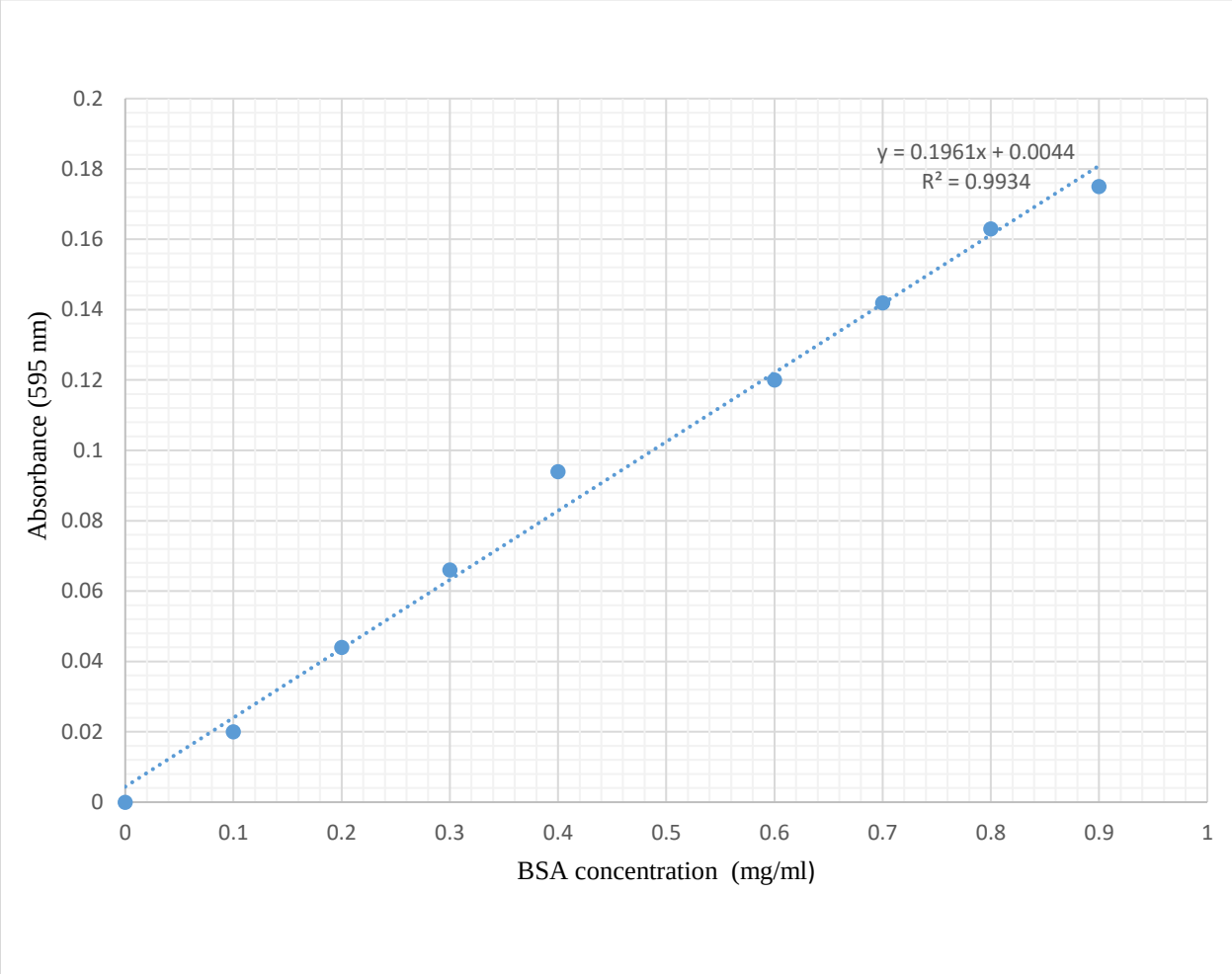

Fig C1 Bradford standard curve
Bovine serum albumin (BSA) standards of concentration varying from 0 to 0.9mg/ml were prepared and absorbance was read at 595 nm using Spectramax M3 spectrometer. The linear equation: y = 0.1961x + 0.0044, R^2 = 0.9934 was used to calculate the protein concentration. The protein concentrations determined using Bradford's were confirmed using the Christoph-Leidig assay Appendix B9.

C2: HTE sensor chip conditioning

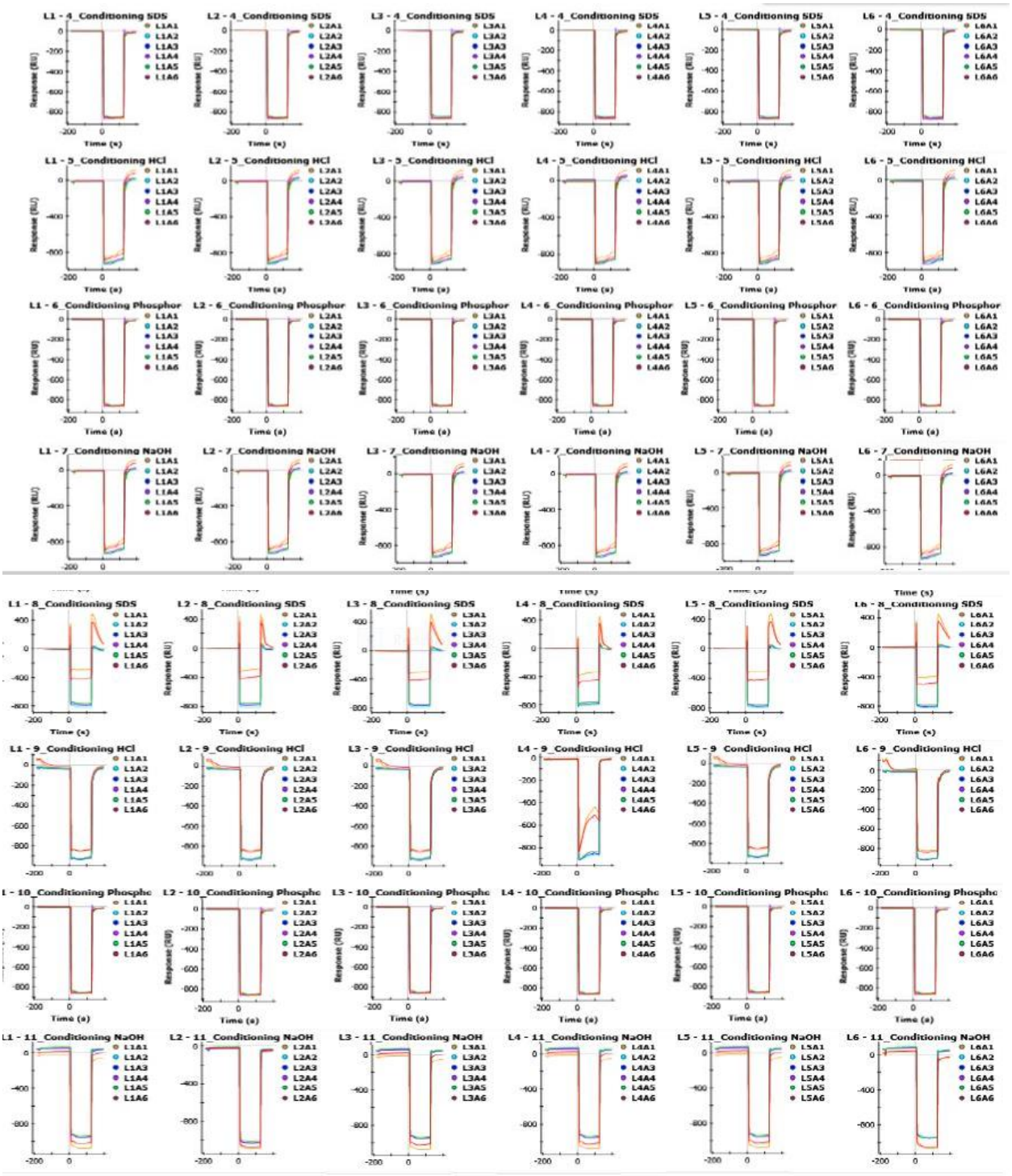

Figure C2. HTE sensor chip Conditioning

The HTE sensor chip was conditioned in a horizontal conformation with 50 mM NaOH 0.5 % (w/v) SDS, 100 mM HCl, and 0.85 % (v/v) Phosphoric acid. Conditioning vertically was performed with 50 mM NaOH, 0.5 % (w/v) SDS, , 0.85 % (v/v) Phosphoric acid and100 mM HCl Injections were done for all the 6 horizontal (L1-L6) X 6 vertical (A1-A6) channels on the HTE sensor chip.

C3 HTE sensor chip ligand pre-concentration

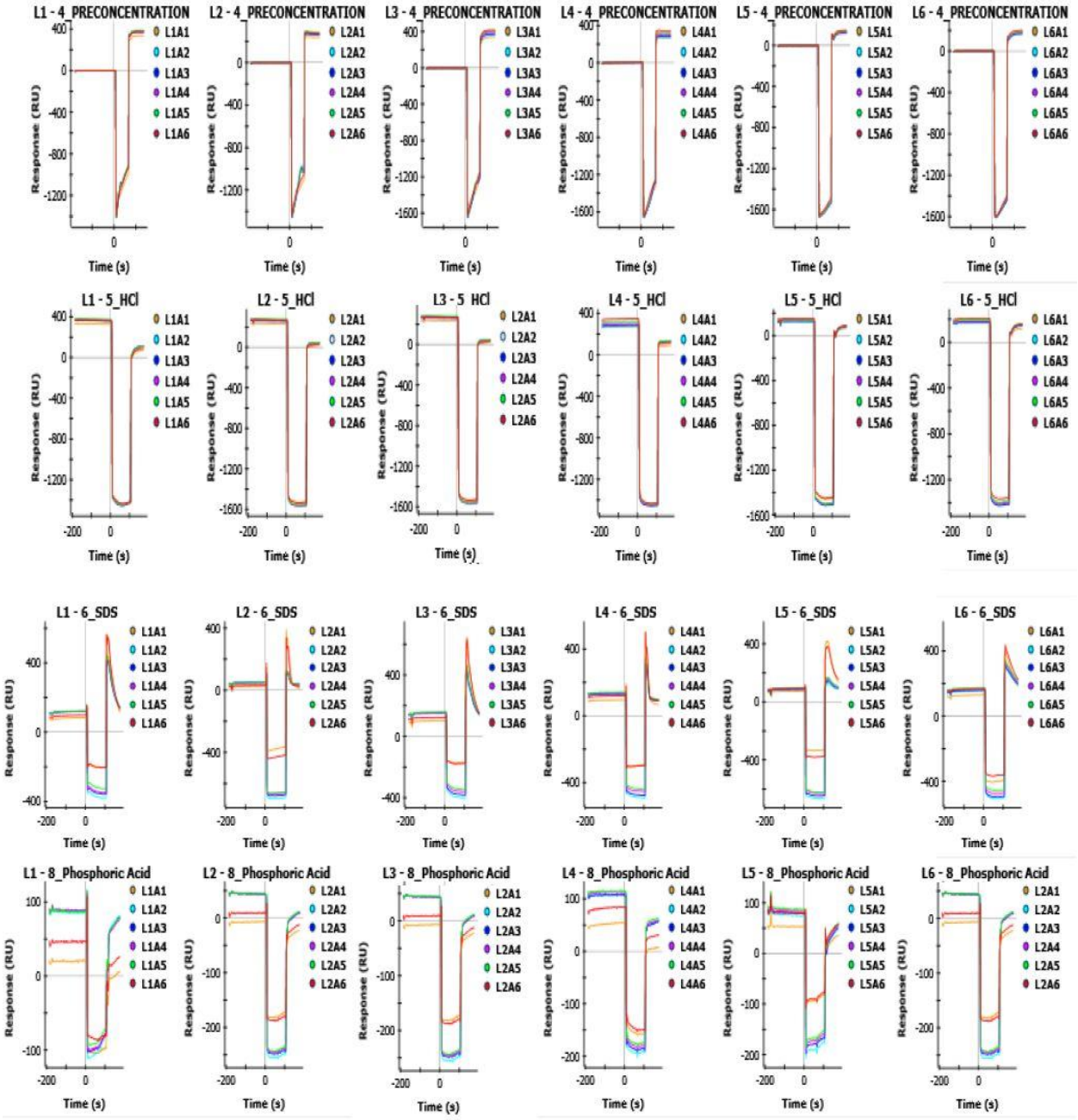

The ligand pre-concentration analysis was conducted using 10 mM Sodium Acetate buffers. to determine the optimum pH for immobilization. The pH values were varied between at pH 4.0 and pH 4.5. The chip was reconditioned using 0.85 % (v/v) Phosphoric acid and 100 mM HCl, 0.5 % (w/v) SDS

C4 Comparative thermal stability of PfHsp70-x and luciferase

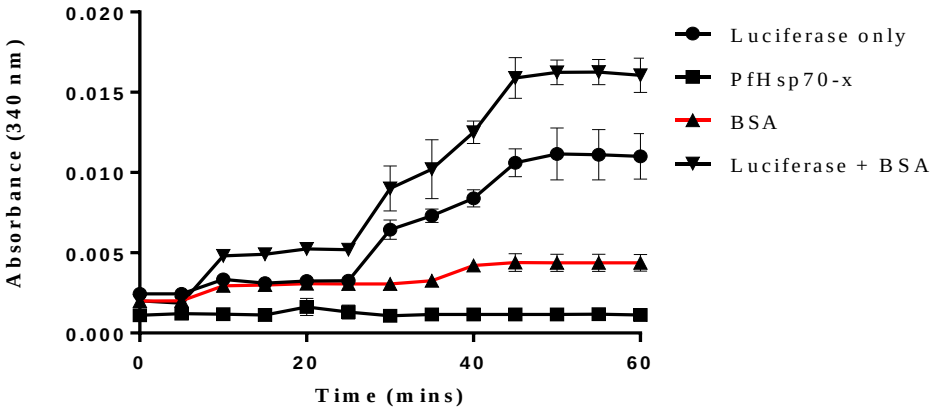

Fig C4: Comparative thermal stability of PfHsp70-x and luciferase
The thermal stability of the recombinant proteins was assessed by the presence of heat-induced aggregates measured by an increase in absorbance at 340 nm for luciferase using UV-vis spectrophotometer M3 Spectramax (Molecular Devices). The PfHsp70-x chaperone was also assessed for heat stability at the reaction temperature (48 ℃). BSA was included as a control. Error bars represent standard deviations about the mean obtained from three replicate assays.

C5 Comparative thermal stability of PfHsp70-x and MDH

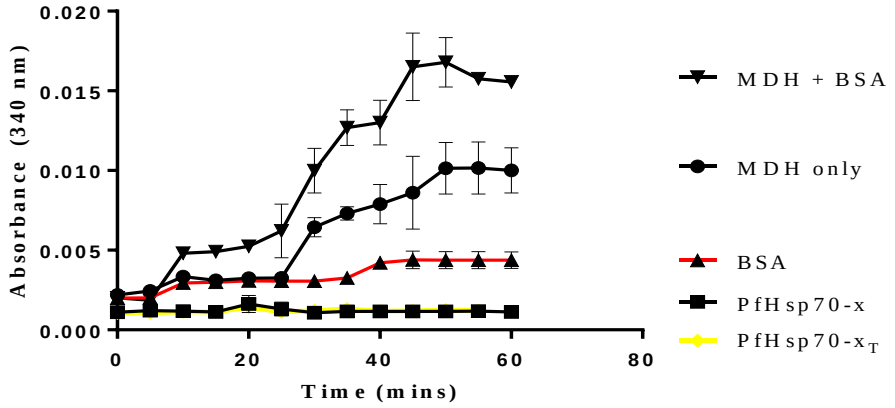

Fig C5 Thermal stability of PfHsp70-x in comparison to MDH
The thermal stability of the recombinant proteins was assessed by the presence of heat-induced aggregates measured by an increase in absorbance at 340 nm for luciferase using UV-vis spectrophotometer M3 Spectramax (Molecular Devices). The PfHsp70-x chaperone was also assessed for heat stability at the reaction temperature (48 ℃).. BSA was included as a control. Error bars represent standard deviations about the mean obtained from three replicates assays.

C6: Phosphate standard curve for ATPase assay

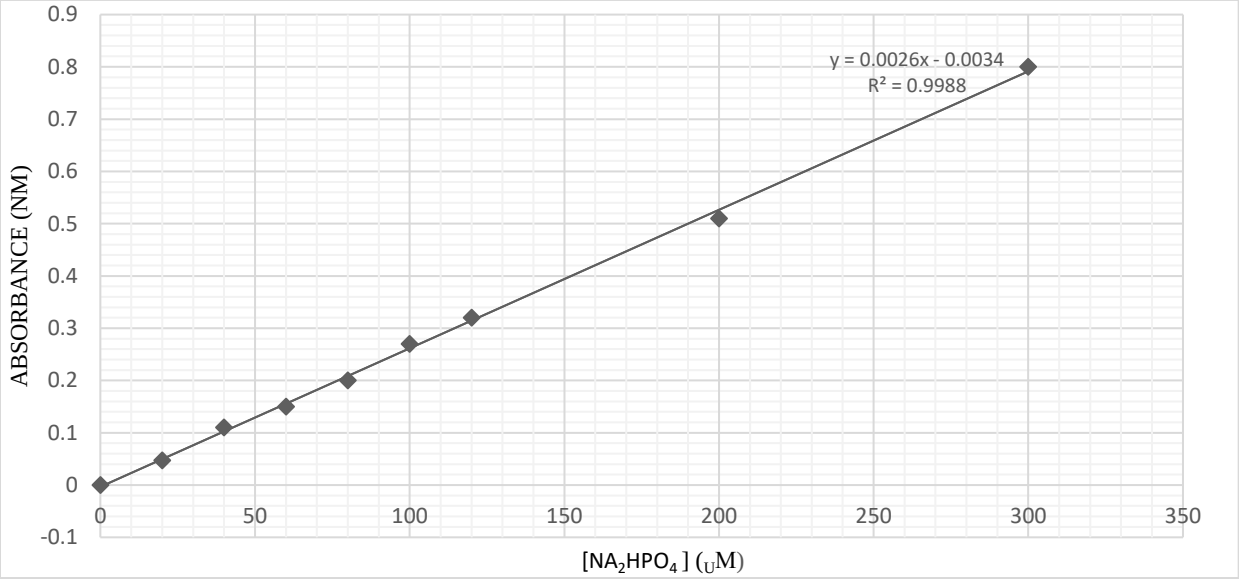

Fig C6 Phosphate standard curve

Phosphate standards curve showing [Na_2HPO_4] ranging from 0 to 300 µM and absorbance read at 660 nm using (SpectraMax M3, Molecular Devices, U.S.A). The linear equation: y = 0.0026x - 0.0034, R^2 = 0.9988 was used to calculate the inorganic phosphate released during ATP Hydrolysis.